Frameworks for Evaluating and Improving Simplified Hydrologic Models for Baseflow and Rainfall-Runoff Estimation Using Distributed Physical Models

Li Li

BEng, MEng

Thesis submitted in fulfilment of the requirements for the degree of Doctor of Philosophy

The University of Adelaide
Faculty of Engineering, Computer and Mathematical Sciences
School of Civil, Environmental and Mining Engineering

Table of Contents

Abstract

Hydrologic models are becoming increasingly important in the planning, design, operation and management of natural and engineered systems. However, development of such models is complicated by the fact that the underlying physical processes are extremely complex and that the observation and measurement of these processes are expensive and difficult. Consequently, simplified models are generally used in practice for purposes such as baseflow estimation and rainfall-runoff prediction. However, it is difficult to provide a rigorous assessment of how well such simplified models perform under a range of catchment characteristics (e.g. catchment area, soil type, slope) and hydrological inputs (e.g. rainfall, evaporation) and how well they are able to capture the underlying physical processes. In addition, without such assessments, it is difficult to change model structure and parameterization in order to improve the models' predictive capability and the ability to better represent physical processes.

In order to address these shortcomings, in this research, generic frameworks for (i) evaluating and improving recursive digital filters (RDFs) for baseflow estimation and (ii) evaluating the internal dynamic performance of conceptual rainfall runoff (CRR) models are developed and applied. The underlying premise of the frameworks is that fully integrated surface water/groundwater (SW/GW) models are able to provide the best possible approximation to the physical processes of water flow within catchments and can therefore be used as a benchmark against which the performance of these simplified models can be assessed for a variety of physical catchment characteristics and hydrological inputs.

The major research contributions are presented in three journal publications. These publications describe: 1) the development of frameworks to evaluate

and improve RDF performance for baseflow estimation based on catchment characteristics and hydrological inputs and their application to a single RDF under a limited number of catchment characteristics; 2) the application of the frameworks developed in the first paper to three RDFs under a larger range of catchment characteristics and hydrological inputs, as well as the development of regression equations for predicting RDF performance and optimal RDF parameters for improving RDF performance; and 3) the development and application of framework to evaluate the internal dynamic performance of one commonly used CRR model-Australian Water Balance Model (AWBM) under different calibration regimes under a larger range of catchment characteristics and hydrological inputs. Consequently, this research has developed a new way of evaluating and improving commonly used simplified hydrologic models for baseflow estimation and rainfall-runoff prediction.

Statement of Originality

I, *Li Li*, hereby declare that this work contains no material which has been accepted for the award of any other degree or diploma in any university or other tertiary institution to Li Li and, to the best of my knowledge and belief, contains no material previously published or written by another person, except where due reference has been made in the text.

I give consent to this copy of my thesis when deposited in the University Library, being made available for loan and photocopying, subject to the provisions of the Copyright Act 1968.

The author acknowledges that copyright of published works contained within this thesis resides with the copyright holder(s) of those works.

I also give permission for the digital version of my thesis being made available on the web, via the University's digital research repository, the Library catalogue, the Australian Digital Thesis Program (ADTP) and also through web search engines, unless permission has been granted by the University to restrict access for a period of time.

Signed:……………………………………………Date: ……………………

Acknowledgements

I gratefully acknowledge my principal supervisor Professor Holger Maier, co-supervisor Professor Martin Lambert and external supervisor Professor Craig Simmons, who have always supervised, supported and encouraged me during my candidature period. Professor Holger Maier kindly offered me this opportunity to study in the University of Adelaide as an international student and provided me much help initially from my application for my scholarship. He always gave me valuable advice and comments on research design and implementation and especially on my thesis and manuscript writing. Without his guidance, vision and passion for research, this thesis would not be possible.

I would like to sincerely thank the University of Adelaide, China Scholarship Council and Northwest A&F University for awarding me the scholarship. Professor Richard Russell, Ms Sandy McConachy and Ms Iris Liu at the University of Adelaide gave me much instruction and encouragement during my candidature. Professor Junmin Liu and Jinbu Yin, who were my supervisor and teacher at Northwest A&F University, gave me much support and trust throughout study.

I would like to thank Daniel Partington, the first person who introduced me HydroGeoSphere, the software directly related to my whole PhD research, and instructed me how to use this software step by step initially from the very beginning of my research. He also offered great help with model runs, data analysis and reviews of manuscript drafts.

I thank eResearch SA for proving server to run my programs. Special thank to Sean Reilly, Paul Coddington and Shunde Zhang from eResearch SA for their great help and advice with implementing the servers.

I would like to express my deep appreciation to Dr Stephen Carr for assistance with school server setting up and resolving modelling issues; Dr Michael Leonard for introducing FORTRAN and VB programming.

Many thanks go to my fellow postgraduate students within the School for sharing their research experience with me, and especially for their friendship. I am fortunate to have Ms Jaya Kashyap, Ms Mina Pazandeh and Ms Nora Abdullah as my "neighbours" in the office. Their encouragement, comfort, and the enjoyable discussions with them are an unforgettable part of my PhD study.

Finally, I would like to thank my parents, Mr Mingshan Li and Ms Xiulian Song, for supporting me emotionally during my PhD research. Last but not least, I would like to thank my husband Zhongyuan Fu for his selfless love and support.

List of Figures

List of Tables

Chapter 1

1 Introduction

1.1 Research background

A good understanding of surface water and groundwater hydrology is important for water resources management, such as low flow and rainfall-runoff prediction. Due to the difficulties associated with the observation and measurement of water movement processes within catchments, surface water and groundwater (SW/GW) have traditionally been studied and managed as isolated resources (Brodie and Hostetler, 2005). There is however an increasing recognition of the need to holistically study surface water and groundwater by using physically-based fully integrated SW/GW models, since the blueprint for such models suggested by Freeze and Harlan (1969) has been started to be realised in last decade. In the literature, many fully-integrated SW/GW models have been developed, including InHM (VanderKwaak and Loague, 2001), MODHMS (HydroGeoLogic, 2000), HydroGeoSphere (Therrien et al., 2009) [HGS] and ParFlow (Kollet and Maxwell, 2006). In general, these models can model the surface domain and the subsurface domain by using well-established physical laws that have mathematical representations. For example, the two-dimensional approximations of the St Venant equations are generally used to represent the surface flow component of overland flow, while the three-dimensional subsurface components, where there is variably saturated flow, can be represented by Richard’s equation (Freeze and Harlan, 1969; Sulis et al., 2010). A comprehensive description of the types of boundary conditions for fully coupling the surface and subsurface flow regimes is provided in Furman (2008). All of these governing equations are solved simultaneously for each time step, which results in realistic, physically-based simulation of the movement of water on and within catchments (Therrien et al., 2009). In addition, they can be used to simulate physical processes for catchments with different characteristics and hydrological inputs. Therefore, fully integrated SW/GW models are able to provide a rigorous representation of the underlying physical processes of hydrologic systems (Furman, 2008; Sulis et al., 2010), and have been widely used for different applications, including losing and gaining stream analysis (Partington et al., 2011), SW/GW disconnection problems (Banks et al., 2011; Brunner et al., 2009), solute transport analysis (Blessent et al., 2009; Weatherill et al., 2008), the assessment of impacts of climate change on groundwater (Goderniaux et al., 2009) and evaluation and improvement of simplified conceptual models (Partington et al., 2012).

However, firstly, development of such models is complicated by the fact that the underlying physical processes are extremely complex and that the observation and measurement of these processes, which are needed to develop such models, are expensive and difficult. In addition, fully integrated SW/GW models suffer from drawbacks due to large computational demands and potential over-parameterisation, all of which make them complex to calibrate and difficult to apply to real catchments. Consequently, simplified models are developed and generally used in practice.

One of the most important applications of these simplified models is baseflow estimation. During most of the year, streamflow can generally be considered to comprise two main components. Water that can enter the river rapidly is termed as quickflow and is sourced from direct rainfall onto the river surface and catchment surface runoff. In contrast, baseflow is sourced primarily from groundwater discharge, and normally takes a longer time to reach the river (Gilfedder et al., 2009; McCuen, 2005). Quantifying baseflow contributions to streamflow and understanding baseflow dynamics are of great interest in many applications, such as the analysis of event runoff, recharge estimation, low flow forecasting, hydrogeologic parameter estimation, hydrologic model calibration, and identification of source areas, in particular where baseflow supports important ecosystems and/or provides critical dry season water supply (Schwartz, 2007; Smakhtin, 2001; Werner et al., 2008).

However, due to the complex hydrological processes and interactions between baseflow and different catchment physical properties, there is no easy way to continuously and accurately measure baseflow in the field (Dukic, 2006; McCallum et al., 2010). As a result, baseflow separation methods have been developed for catchments without detailed field data, but for which streamflow hydrograph data are available, since the early twentieth century. Such baseflow separation methods include graphical separation methods (Linsley et al., 1988), recursive digital filters (RDFs) (Arnold et al., 1995; Lyne and Hollick, 1979; Nathan and McMahon, 1990) and recession analysis (Tallaksen, 1995). Among these, RDFs are the most commonly used, due to their relatively easy and efficient implementation. RDFs generally regard total streamflow as being composed of a high frequency quickflow signal and a low frequency baseflow signal. Through applying a filter to the total streamflow, the quickflow can be removed, leaving the baseflow component. However, there are many subjectivities/shortcomings in using RDFs. First of all, RDFs are a function of one or more user-defined filter parameters. These filter parameters are either fixed values for all catchments, or determined using subjective methods based on physical catchment characteristics. Secondly, the basic mathematical principle underpinning RDFs lacks any physical basis, e.g. they are not based on the underlying physical processes and do not consider catchment physical and hydrological properties. Finally, the relative performance of different RDFs cannot be assessed in absolute terms, as baseflow cannot be measured easily in the field, due to practical reasons, as mentioned above. Thus, no guidelines exist that enable suitable RDFs to be selected for particular catchments. Consequently, there is a need to evaluate and improve the performance of commonly used RDFs for baseflow estimation and to provide guidance on which RDFs are suitable for a particular catchment.

The ultimate goal of evaluating and improving commonly used RDFs is to obtain more accurate baseflow estimation for catchments with different catchment characteristics and hydrological properties that have an impact on baseflow generation and thus RDF performance. Firstly, catchment area has a significant impact on aquifer storage capacity, and thus the sustained baseflow contribution to the stream. Secondly, catchment slope may affect the infiltration capacity and overland flow towards to the stream (Partington et al., 2011), which will have an impact on how much groundwater discharges into a stream as baseflow. Thirdly, catchment aspect ratio, defined as the ratio of catchment width to length, is related to the distance between the catchment hillslope and the catchment outlet. As a result, the aspect ratio can also have a significant impact on baseflow generation by affecting travel time to the outlet. Fourthly, the amount of baseflow that a stream receives is closely linked to the permeability of the soil in the catchment (e.g. saturated hydraulic conductivity [K_s], van Genuchten parameters α and β). Finally, the hydrologic properties, such as rainfall and evapotranspiration (ET) (D'Odorico et al., 2005; Guttal and Jayaprakash, 2007, 2009), have direct impacts on seasonal and longer term trends of baseflow. Consequently, evaluating and improving RDF performance under a range of catchment characteristics and hydrological properties listed above becomes necessary.

The other significant application of simplified hydrological models is the estimation of rainfall-runoff. Conceptual rainfall runoff (CRR) models are the most widely utilized methods in practice for this purpose (Boughton, 2009; Ranatunga et al., 2008; Seibert, 1999). CRR models use a number of interconnected storages with associated empirical mathematical equations to conceptualise water movement processes. Similar to RDFs, most of the CRR model parameters have no physical interpretation or are not directly measurable (Delleur, 1982; Troutman, 1985), due to the fact that many complex catchment physical processes are lumped. Thus, CRR model parameters are generally obtained by calibration, as part of which a set of model parameters is determined that minimises an error measure between observed (measured) and predicted (modelled) total streamflow over a calibration period. Different optimisation methods can be implemented to obtain a well-defined optimal parameter set to get the best fit (Duan et al., 1992; Gupta and Sorooshian, 1985). Therefore, the predictions obtained using

CRR models depend on model structure, the quantity and quality of the input data (i.e. streamflow time series, rainfall and ET) and the quality of the parameter estimates (i.e. obtained by calibration) (Muleta and Nicklow, 2005). However, firstly, without detailed information about all of the physical processes from rainfall arrival to runoff generation, it is difficult to examine CRR model structure by assessing how well it captures the physical processes. In addition, there may be equifinality problems when using traditional calibration methods (i.e. by matching the total streamflow time series with observations by varying all model parameters simultaneously) to obtain the optimal set of CRR model parameters, which can result in different combinations of parameters values that give similar objective function values (Beven, 1993). Furthermore, as stated previously, total streamflow time series are composed of different components, i.e. baseflow and quickflow. However, even though total streamflow time series might be predicted well with the optimal set of CRR model parameters obtained using traditional calibration methods, due to the difficulty of measuring the component hydrographs, it is difficult to estimate CRR model internal dynamic performance, i.e. whether a good total streamflow prediction is composed of the correct baseflow and quickflow predictions. Consequently, it is crucial to evaluate the internal dynamic performance of CRR models under a range of catchment characteristics and hydrological inputs and to test the efficacy of different calibration methods in improving internal dynamic performance.

There are several considerations that need to be addressed in order to carry out this research. Firstly, in order to assess and improve commonly used RDF performance and CRR model internal dynamic performance under different catchment characteristics and hydrological inputs, generic approaches need to be developed. In addition, an appropriate benchmark for RDF performance and CRR model internal dynamic performance assessment must be selected, due to the lack of reliable physical processes measurement in the field (i.e. baseflow and quickflow). As stated previously, fully integrated SW/GW models can provide a rigorous representation of the underlying physical processes of hydrologic systems (Furman, 2008; Sulis et al., 2010), and have already been used successfully in the assessment of RDF performance

(Partington et al., 2012). While it is acknowledged that fully integrated SW/GW models are an approximation of the actual processes in real catchments, they are able to provide the first step towards being able to assess the performance of RDFs and the internal dynamic performance of CRR models under a range of physical conditions. Consequently, a fully integrated SW/GW model is used in this research to obtain estimates of streamflow, baseflow and quickflow time series for catchments with different characteristics and hydrological inputs as benchmarks, against which RDF performance and the internal dynamic performance of CRR models are assessed.

1.2 Research aims

The overall aim of this study is to evaluate and improve the predictive performance of simplified models, including RDFs for baseflow estimation and CRR models for rainfall runoff prediction, under the premise that fully integrated SW/GW models are able to provide the best possible approximation to the physical processes of water flow within catchments and can therefore be used as a benchmark against which the performance of these simplified models can be assessed for a variety of physical catchment characteristics and hydrological inputs. Ultimately, this research leads to a new way of evaluating and improving commonly used simplified models for baseflow estimation and rainfall-runoff prediction in real world practice. In order to fulfil the overall aim of this research, two main research aims have been developed, each with a number of sub-aims, as listed below. The linking of each of these objectives is shown in Figure 1.1.

Aim 1: To evaluate and improve the performance of commonly used RDFs for baseflow estimation (Journal Papers 1 and 2).

> *Aim 1.1:* To develop a framework for assessing and improving RDF performance by taking different catchment characteristics and hydrological inputs into account (Journal Paper 1).

Aim 1.2: To test the framework developed in 1.1 by applying it to one RDF and a synthetic catchment with different soil properties (Journal Paper 1).

Aim 1.3: To apply the framework developed in 1.1 to evaluate and improve the performance of three RDFs under a wider range of catchment characteristics and hydrological inputs (Journal Paper 2).

Aim 1.4: To develop regression equations for predicting RDF performance and optimal RDF parameters based on the catchment characteristics and hydrological inputs for the three RDFs investigated, which help to provide guidance on whether the use of a particular RDF is suitable for a particular catchment and if it is suitable, what the best filter parameter value is (Journal Paper 2).

Aim 2: To evaluate and improve the predictive ability and internal model dynamics of CRR models (Journal Paper 3).

Aim 2.1: To assess how well the Australian Water Balance Model (AWBM), which is a commonly used CRR model, is able to represent total-, base- and quick-flow under a wide range of catchment characteristics and hydrological inputs (Journal Paper 3).

Aim 2.2: To assess the impact of a number of calibration regimes that take internal model dynamics into account in different ways on the accuracy of total-, base- and quick-flow hydrograph prediction for the AWBM under a wide range of catchment characteristics and hydrological inputs (Journal Paper 3).

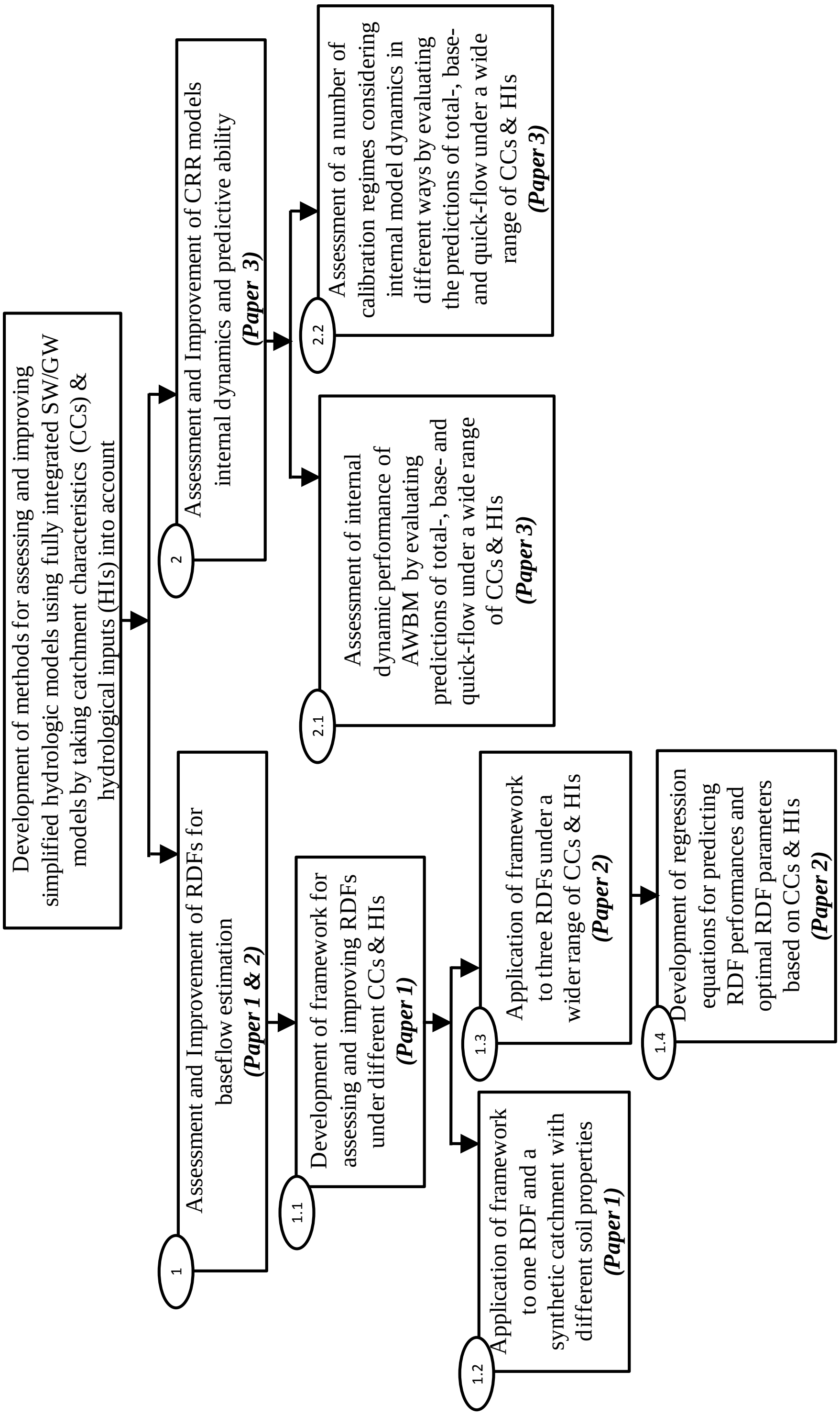

Figure 1.1 Specific research aims and their hierarchy, and linkage of research aims and publications

1.3 Organisation of thesis

This thesis is divided into 5 chapters. The main body of this thesis consists of Chapters 2 to 4, which correspond to three journal papers (Li et al. 2013a; Li et al., 2013b; Li et al., 2013c). Chapters 2 and 3 are related to the evaluation and improvement of the performance of commonly used RDFs for baseflow estimation (Aim 1).

Chapter 2 (Li et al., 2013a) presents the generic framework for assessing and improving RDF performance by taking different catchment characteristics and hydrological inputs into account (Aim 1.1). In Chapter 2, this framework is tested by applying it to one commonly used RDF (the Lyne and Hollick Filter) and a synthetic catchment with different soil properties (saturated hydraulic conductivity (K_s), porosity, residual water content (θ_r), and van Genuchten parameters α and $N(\beta)$) under a single hydrological regime (rainfall from Adelaide, without evapotranspiration (ET)) (Aim 1.2).

Chapter 3 (Li et al., 2013b) is an expansion of Chapter 2, which implements the framework developed in Chapter 2 to evaluate and improve the performance of three commonly used RDFs (the Lyne and Hollick, Boughton 2-parameter and Eckhart filters)under a wider range of catchment characteristics (catchment area, hill slope, channel slope, aspect ratio, K_s, and van Genuchten parameters α and β) and hydrological inputs (rainfall and ET values from Adelaide, Brisbane, Darwin, Melbourne and Sydney) (Aim 1.3). In addition, regression equations are developed to predict the performance and the optimal filter parameters based on these catchment characteristics and hydrological inputs for the three RDFs investigated, in order to provide guidance on the suitability of each of these RDFs for a particular catchment and if it is suitable, the optimal filter parameter that should be used (Aim 1.4).

Chapter 4 (Li et al., 2013c) is concerned with addressing research aim 2. It introduces a framework to evaluate the internal dynamic performance of AWBM, a commonly used CRR model, by assessing its ability to predict total-, base- and quick-flow under a wider range of catchment characteristics and hydrological inputs (Aim 2.1). In addition, the impact of a number of calibration regimes that take internal model dynamics into account in different ways on the accuracy of total-, base- and quick-flow hydrograph prediction for AWBM under a wider range of catchment characteristics and hydrological inputs is assessed (Aim 2.2).

The linking of each of the papers to the aims is depicted in Figure 1.1. Although the journal paper manuscripts have been reformatted in accordance with University guidelines, and sections renumbered for inclusion within this thesis, the material within this thesis is otherwise as in the published or submitted journal papers. Copies of the publications “as published” are provided in Appendix A

The final chapter, **Chapter 5**, summarises the major contributions of this research. In addition, the publications produced and the limitations and future directions of this research are summarised.

Chapter 2

2 Framework for assessing and improving the performance of recursive digital filters for baseflow estimation with application to the Lyne and Hollick filter (Paper 1)

Statement of Authorship

Title of Paper	Framework for Assessing and Improving the Performance of Recursive Digital Filters for Baseflow Estimation with Application to the Lyne and Hollick Filter
Publication Status	☑ Published ☐ Accepted for Publication ☐ Submitted for Publication ☐ Publication Style
Publication Details	Li, L., Maier, H.R., Lambert, M.F., Simmons, C.T., Partington, D., 2013. Framework for Assessing and Improving the Performance of Recursive Digital Filters for Baseflow Estimation with Application to the Lyne and Hollick Filter. Environmental Modelling & Software 41 163-175.

Author Contributions

By signing the Statement of Authorship, each author certifies that their stated contribution to the publication is accurate and that permission is granted for the publication to be included in the candidate's thesis.

Name of Principal Author (Candidate)	Li Li		
Contribution to the Paper	Developed and implemented the methodology, designed numerical experiments, interpreted and analysed results, prepared manuscript.		
Signature		Date	01/03/2013

Name of Co-Author	Holger Maier		
Contribution to the Paper	Supervised manuscript preparation and reviewed draft.		
Signature		Date	1/3/13

Name of Co-Author	Martin Lambert		
Contribution to the Paper	Supervised manuscript preparation and reviewed draft.		
Signature		Date	1/3/13

Name of Co-Author	Craig Simmons		
Contribution to the Paper	Supervised manuscript preparation and reviewed draft.		
Signature		Date	1/3/13

Name of Co-Author	Daniel Partington		
Contribution to the Paper	Assisted with running models and analysing results, reviewed draft and supervised manuscript preparation.		
Signature		Date	1/03/2013

Name of Co-Author			
Contribution to the Paper			
Signature		Date	

Name of Co-Author			
Contribution to the Paper			
Signature		Date	

Please cut and paste additional co-author panels here.

Abstract

Baseflow is often regarded as the streamflow component derived predominantly from groundwater discharge. The estimation of baseflow is important for water supply, water allocation, investigation of contamination impacts, low flow hydrology and flood hydrology. Baseflow is commonly estimated using graphical methods, recursive digital filters (RDFs), tracer based methods, and conceptual models. Of all of these methods, RDFs are the most commonly used, due to their relatively easy and efficient implementation. This paper presents a generic framework for assessing and improving the performance of RDFs for baseflow estimation for catchments with different characteristics and subject to different hydrological conditions. As part of the framework, a fully integrated surface water/groundwater (SW/GW) model is used to obtain estimates of streamflow and baseflow for catchments with different properties, such as soil types and rainfall patterns. A RDF is then applied to the simulated streamflow to assess how well the baseflow obtained using the filter matches the baseflow obtained using the fully integrated SW/GW model. In order to improve the performance of the filter, the user-defined parameter(s) controlling filter operation can be adjusted in order to obtain the best match between the baseflow obtained using the filter and that obtained using the fully integrated SW/GW model (i.e. through calibration). The proposed framework is tested by applying it to a common SW/GW benchmarking problem, the tilted V-catchment, for a range of soil properties. HydroGeoSphere (HGS) is used to develop the fully integrated SW/GW model and the Lyne and Hollick (LH) filter is used as the RDF. The performance of the LH filter is assessed using the commonly used value of the filter parameter of 0.925, as well as calibrated filter parameter values. The results obtained show that the performance of the LH filter is affected significantly by the saturated hydraulic conductivity (K_s) of the soil and that calibrated LH filter parameter can result in significant improvements in filter performance.

2.1 Introduction

Baseflow is often defined as the groundwater contribution to streamflow, however it is also referred to as slow flow, and sustained flow (Hall, 1968). Herein, the former definition of baseflow is adopted, i.e. the groundwater contribution to a stream. The estimation of baseflow can play a significant role in terms of understanding the interaction between surface water and groundwater (Evans and Neal, 2005; Gilfedder et al., 2009). In addition, baseflow estimation is important for a wide range of water and environmental management issues, such as water supply, water allocation, investigation of contamination impacts, low flow hydrology and flood hydrology (Linsley et al., 1988). One important application is the estimation of the baseflow index (BFI), which is the long term ratio of the volume of baseflow to total streamflow volume. This index was developed by the Institute of Hydrology (now CEH Wallingford), and was used in the UK Hydrometric Register, a comprehensive reference source to help assess the low flow characteristics of rivers and the catchment geology of the UK (Marsh and Hannaford, 2008).

There is no easy way to continuously and accurately measure baseflow in the field (Dukic, 2006; McCallum et al., 2010). In the early twentieth century, the focus of baseflow estimation methods was primarily on graphical separation methods, including the constant discharge, constant slope and concave methods (Linsley et al., 1988). Although these methods are able to capture the perceived understanding of the underlying physical processes (Bako and Hunt, 1988; Sloto and Crouse, 1996), their application is subjective in terms of the choice of appropriate starting and inflexion points. Since the 1980s, researchers have developed alternative baseflow separation algorithms by using automated techniques, such as recursive digital filters (RDFs) (Arnold et al., 1995; Nathan and McMahon, 1990). These methods regard total streamflow as being composed of both quickflow and baseflow and apply signal processing techniques to a streamflow time series in order to remove the high-frequency quickflow signal to obtain the low-frequency baseflow signal. These RDFs are computationally efficient, easily automated, and can be applied to long continuous streamflow records. However, RDFs do not take into consideration the physical processes responsible for baseflow generation as their inputs, but are simply based on streamflow records and user-defined filter parameters. In addition, filters are often constrained by the condition that baseflow must not exceed total streamflow or become negative (Furey and Gupta, 2001). Environmental isotopes and chemical tracers have also been utilised for streamflow separation by using end member mixing analysis (Chapman and Maxwell, 1996; McCallum et al., 2010; Murphy et al., 2009). These isotope and tracer approaches can be used to infer the various sources of streamflow, such as groundwater, interflow and direct rainfall. However, any uncertainty in the end member concentrations of these flow sources directly relates to the uncertainty of quantifying the groundwater component of streamflow (Jones et al., 2006; McCallum et al., 2010).

Recently, greater attention has been given to physically based approaches for analysing baseflow, including fully integrated surface water/ground water (SW/GW) flow models, such as InHM (VanderKwaak and Loague, 2001), MODHMS (HydroGeoLogic, 2000), HydroGeoSphere (HGS) (Therrien et al., 2009) and ParFlow (Kollet and Maxwell, 2006). With precipitation, evapotranspiration (ET) and parameters representing catchment characteristics as inputs, these complex, spatially distributed models can simulate both surface flow and baseflow and give a more detailed physical representation of the processes of SW/GW interaction (Khan et al., 2009; Partington et al., 2011; Ravazzani et al., 2011). In order to enable the baseflow component of streamflow to be extracted accurately from such models, Partington et al. (2011) developed a hydraulic mixing-cell (HMC) method, which accounts for stream losses and time lags within the catchment. Consequently, use of the HMC method in conjunction with fully integrated SW/GW models is likely to provide the most accurate means of estimating baseflow. However, the complexity of these models (e.g. the number of parameters that need to be obtained through calibration) requires increased data and computational resources, which make them exceedingly difficult to calibrate and apply to real catchments.

RDFs are currently the most widely used method for estimating baseflow around the world, due to their minimal input requirements and simple and efficient implementation. Such filters include the Lyne and Hollick (LH) filter (Lyne and Hollick, 1979; Nathan and McMahon, 1990), Chapman one-parameter algorithm (Chapman and Maxwell, 1996), Boughton two-parameter algorithm (Chapman, 1999), Eckhardt two-parameter algorithm (Eckhardt, 2005) and IHACRES three-parameter algorithm (Chapman, 1999). However, while there have been many studies comparing the performance of RDFs (Chapman, 1999; Eckhardt, 2005, 2008; Murphy et al., 2009; Nejadhashemi et al., 2003; Nejadhashemi et al., 2009; Partington et al., 2012), the relative performance of different RDFs cannot be assessed in absolute terms, as baseflow cannot be measured easily (Dukic, 2006; McCallum et al., 2010). This also makes it difficult to know which filters to select for particular applications.

This problem is compounded by the fact that RDFs operate solely on the total streamflow hydrograph, without considering potential impacts of physical catchment characteristics. However, by considering the hydrological processes driving baseflow, one might expect that physical catchment characteristics have a significant impact on baseflow. For example, if the rainfall rate over a dry catchment with sandy soils is smaller than the rate of infiltration, direct runoff from the surface will be very small, and the baseflow contribution to streamflow significant. On the other hand, if soils are clayey and the antecedent moisture content is high, most of the streamflow will consist of overland flow, with little contribution from baseflow. Consequently, it is likely that the performance of RDFs will vary, depending on physical catchment characteristics. However, at present, it is difficult to assess this.

The performance of RDFs is also affected by one or more user-defined parameters, which are used to change the amount of attenuation in the low/high-frequency domain of the flow spectrum, and therefore have an impact on the baseflow hydrograph obtained. However, determining appropriate values of these parameters is not straightforward and a range of values has been suggested in the literature. For example, in relation to the LH filter, Lyne and Hollick (1979) suggested that a filter parameter between 0.75 and 0.9 should be used. Arnold et.al. (1995) and Nathan and McMahon (1990) recommended using a filter parameter of 0.925. Mau and Winter (1997) found a value of 0.85 to be most appropriate and Tan et al. (2009a) suggested using the recession constant as the filter parameter value, which varies from catchment to catchment. Common to all of these studies was the goal of choosing ‘suitable’ filter parameters in order to obtain a better match between the baseflow obtained using the LH filter and that obtained using traditional methods of baseflow separation, such as manual graphical baseflow separation methods. However, as there is no objective way of assessing how well RDFs predict actual baseflow, it is difficult to know which of the suggested values should be used. In addition, even though many authors have attempted to find an optimal value of the LH filter parameter that can be applied to all catchments, adjusting filter parameter values for different types of catchments is particularly important, as even a modest change in the LH filter parameter can result in an almost 100% change in baseflow for more ephemeral streams, for example. While the need to adjust filter parameters for catchments with different physical properties has been recognized for some RDFs, such as the Boughton two-parameter algorithm (Chapman, 1999) and the Eckhardt filter method (Eckhardt, 2005), there is still a need to develop a generic approach for determining appropriate values of these filter parameters and to assess the impact these values have on filter performance for various catchments with different physical properties.

In order to address the shortcomings in filter based baseflow estimation outlined above, a generic framework for assessing and improving the performance of RDFs is introduced in this paper. The proposed framework enables the performance of different RDFs to be assessed systematically and the optimal values of filter parameters to be determined for a range of physical catchment characteristics. In order to demonstrate the usefulness of the proposed framework, it is applied to a hypothetical case study. The remainder of this paper is organised as follows. The proposed framework is introduced in Section 2.2, followed by a description of the case study in Section 2.3. The results obtained for the case study are presented and discussed in Section 2.4 and a summary and conclusions are given in Section 2.5.

2.2 Generic framework for assessing and improving the performance of RDFs for baseflow estimation

The underlying premise of the proposed framework for assessing and improving the performance of RDFs for baseflow estimation is that fully integrated SW/GW models can be used to obtain reasonably accurate estimates of actual baseflow, thereby providing a benchmark against which the performance of RDFs can be assessed. This is a reasonable assumption, as fully integrated SW/GW models provide a rigorous representation of the underlying physical processes of hydrologic systems (Brookfield et al., 2009; Furman, 2008; Partington et al., 2012; Sulis et al., 2010; Therrien and Sudicky, 1996). While it is acknowledged that fully integrated SW/GW models are in themselves an approximation of the actual processes in real catchments, they provide the best means of quantifying the absolute volume of baseflow currently available (Ferket et al., 2010). In addition, they can be used to obtain estimates of baseflow for catchments with different characteristics. Therefore they are able to provide the first step towards being able to assess the absolute performance of RDFs under a range of physical conditions. The generic frameworks for using fully integrated SW/GW models for assessing and improving the performance of RDFs used for baseflow estimation are given in Sections 2.2.1 and 2.2.2, respectively.

2.2.1 Performance assessment

The proposed framework for assessing the performance of RDFs under a range of physical catchment conditions is shown in Figure 2.1. As mentioned above, the underlying premise of the proposed approach is that a fully integrated SW/GW model provides the best possible approximation to the physical processes of water flow within catchments and can therefore be used as an approximation to such processes subject to a variety of physical characteristics and forcings. This is because rainfall is allowed to partition into overland flow, streamflow, evaporation, infiltration and recharge in a physically based fashion (Therrien et al., 2009), without prior definition of flow generation processes or storage discharge relationships. All of the governing flow equations implemented by the fully integrated SW/GW model are solved simultaneously to obtain the simulated streamflow (q) and baseflow (q_b^{sim}) as a function of user-defined catchment characteristics (e.g. soil types, catchment size, catchment shapes) and hydrological inputs (e.g. rainfall patterns, antecedent moisture, evaporation) (Figure 2.1).

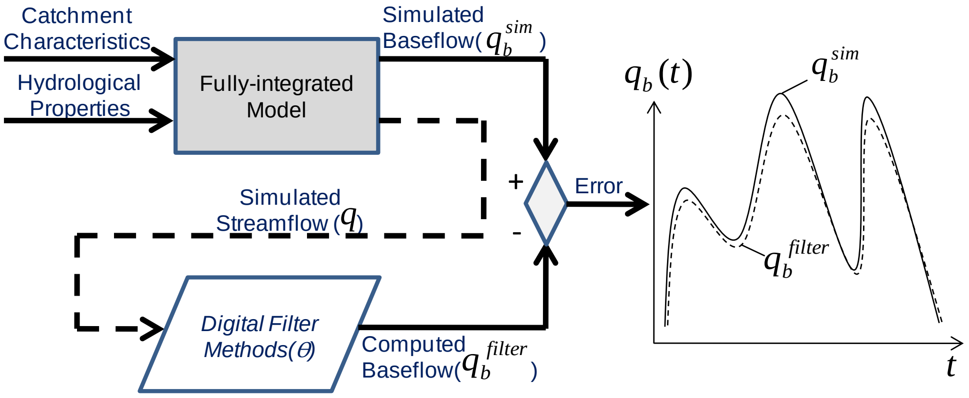

Figure 2.1 Schematic description of the framework for assessing the performance of RDFs for baseflow estimation

The simulated streamflow obtained from the fully integrated SW/GW model (q) is then used as the input to the RDF in order to compute the filtered baseflow hydrograph (q_b^{filter}) (Figure 2.1). The proposed framework can be used to assess the performance of any RDF. In order to assess RDF performance, the baseflow obtained with the aid of the RDF (q_b^{filter}) can be compared with the ’real’ baseflow estimated using the fully integrated SW/GW model (q_b^{sim}) (Figure 2.1). This comparison can be carried out using a number of different evaluation measures, such as the mean square error (MSE), Nash-Sutcliffe coefficient of efficiency (E_f) (Nash and Sutcliffe, 1970), percent bias (PBIAS) (Guttal and Jayaprakash, 2009) or the decompositions of MSE and E_f (Gupta and Kling, 2011; Gupta et al., 2009), among others. The choice of which measures are most appropriate is case study dependent (e.g. whether accurate estimation of the peak, timing or volume of the baseflow hydrograph is most important). The performance assessment of a particular filter can be repeated for different physical catchment conditions and hydrological inputs (Figure 2.1), providing insight into how filter performance is affected by these factors and determining the range of conditions under which filter performance is acceptable.

2.2.2 Performance improvement

As mentioned previously, the performance of RDFs is generally a function of the values of one or more user-defined parameters. Some filter parameters are simply used to alter the magnitude and shape of the resulting baseflow hydrograph, such as the parameter of the LH filter (Lyne and Hollick, 1979; Nathan and McMahon, 1990) and one of the parameters (C) of the Boughton two-parameter algorithm (Chapman, 1999), while others have some physical meaning through a relationship with the recession constant or being defined relative to some of the underlying physical processes.

In order to determine the best possible values of the filter parameters for a given catchment, the assessment framework introduced in the previous section can be extended, as shown in Figure 2.2. Based on the assumption that the simulated baseflow obtained using the fully integrated SW/GW model (q_b^{sim}) is representative of the ’real’ baseflow, the filter parameter(s) (θ) can be adjusted to minimize an error measure between the ’real’ baseflow (q_b^{sim}) and the baseflow computed using the RDF (q_b^{filter}). Any of the performance measures mentioned in Section 2.2.1 can be used for this purpose. Alternatively, a multi-objective approach can be adopted (e.g. (Gibbs et al., 2012)). This calibration process can be automated using various optimization methods, such as gradient based methods or evolutionary algorithms, depending on the complexity of the calibration problem (e.g. the number of parameters to be estimated).

By calibrating the RDFs, it is possible to determine whether filter performance can be improved by using optimal parameter values, rather than those commonly used in the literature. In addition, optimal filter parameters can be obtained for catchments with different physical characteristics, which will assist with providing an insight into the range of catchment properties for which different RDFs are applicable (i.e. perform adequately), provided the optimal filter parameters are used (referred to as the 'range of applicability' of different RDFs) and the sensitivity of optimal values of filter parameters to various catchment properties.

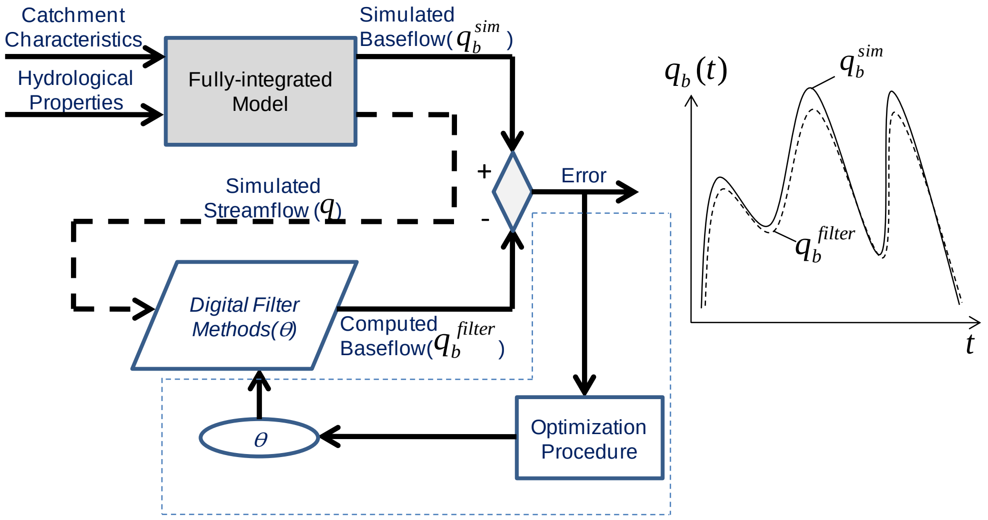

Figure 2.2 Schematic description of the framework for improving the performance of RDFs for baseflow estimation

2.3 Case study

In this section, a case study is used to illustrate the benefits of the proposed frameworks. The various components of the frameworks (Figure 2.1 and Figure 2.2) in relation to the case study are discussed in detail below.

2.3.1 Catchment characteristics and hydrological properties

The hypothetical catchment used in this study (shown in Figure 2.3) is loosely based on a common SW/GW benchmarking problem, the tilted V-catchment of Panday and Huyakorn (2004), which is based on DiGiammarco et al. (1996). Due to symmetry, the geometry of only half of the catchment is described here. The catchment is modified from the catchment given in Panday and Huyakorn (2004) in the following ways: The large slopes perpendicular and parallel to the channel have been reduced from 0.05m/m and 0.02m/m to 0.02m/m and 0.01m/m, respectively, in order to create a greater spatial distribution of the surface-subsurface exchanges throughout the catchment. The areal extent of the catchment has been increased from 810,000m^2 to 6,030,000m^2, by enlarging the original length (y direction) and width (x direction) of the catchment from 1000m and 810m to 3000m and 2010m, respectively. In order to obtain continuous baseflow contributions to the stream, the stream width was retained at 10m as in the original catchment, which can reduce the boundary effects and increase aquifer storage capacity.

The underlying aquifer extends to a depth of 20m below the stream outlet location, and is homogenous and isotropic. Five different homogeneous soil types are considered, which are characterized by different values of saturated hydraulic conductivity (K_s), porosity, residual water content (θ_r), and van Genuchten parameters α and N(β). The ranges and mean values of the soil parameters used are shown in Table 2.1, which were taken from Puhlmann et al. (2009). A typical ten year period of daily rainfall data from Adelaide, South Australia was used as hydrological input for illustration purposes, which is shown in Figure 2.4. In view of the small size of the catchment studied, rainfall intensities have been assumed to be spatially uniform. It should be noted that only the geometry of the catchment is based on the original test case presented in Panday and Huyakorn (2004), and that the other parameters, such as soil types and rainfall patterns, are described as above.

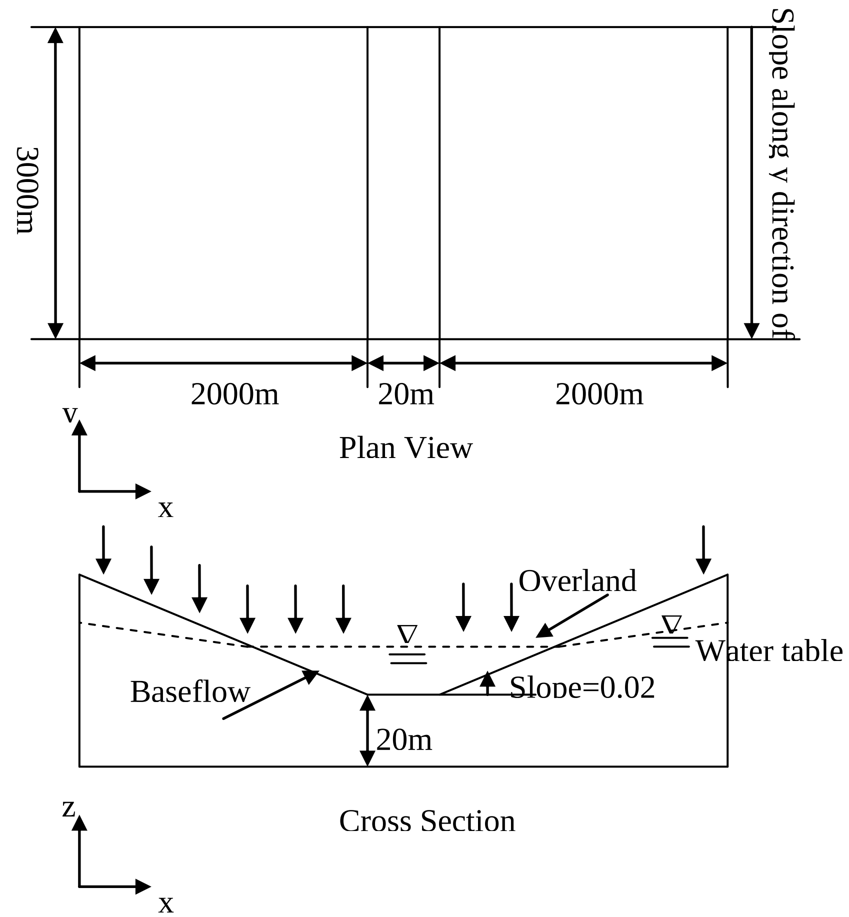

Figure 2.3 Schematic representation of tilted V-catchment flow problem (refer to Panday and Huyakorn (2004))

Table 2.1 Soil types and ranges and means (shown in brackets) of soil properties considered for model simulations (taken from Puhlmann et al. (2009))

Soil Type	Porosity	θ_r	K_s (m/s)	α (m^{-1})	N(β)
Sand	0.261-0.4578 (0.359)	0-0.0072 (0.004)	1.27E-6-9.66E-4 (1.6E-4)	0.572-16.412 (8.492)	1.32-8.52 (4.92)
Sandy loam	0.28-0.544 (0.412)	0-0.22 (0.108)	5.01E-7-1.26E-4 (2.44E-5)	0.47-11.75 (6.11)	1.2-5.16 (3.18)
Loam	0.29-0.818 (0.554)	0-0.456 (0.228)	6.31E-7-1.58E-4 (3.07E-5)	0.68-14.56 (7.418)	1.0822-2.252 (1.682)
Loamy sand	0.341-0.569 (0.455)	0-0.1584 (0.079)	1.42E-6-1.84E-4 (3.99E-5)	0.544-17.344 (8.944)	1.2821-2.266 (1.774)
Silt loam	0.35-0.65 (0.5)	0-0.3 (0.15)	1.51E-7-1.38E-5 (3.01E-6)	0.18-10.98 (5.58)	1.15-3.55 (2.35)

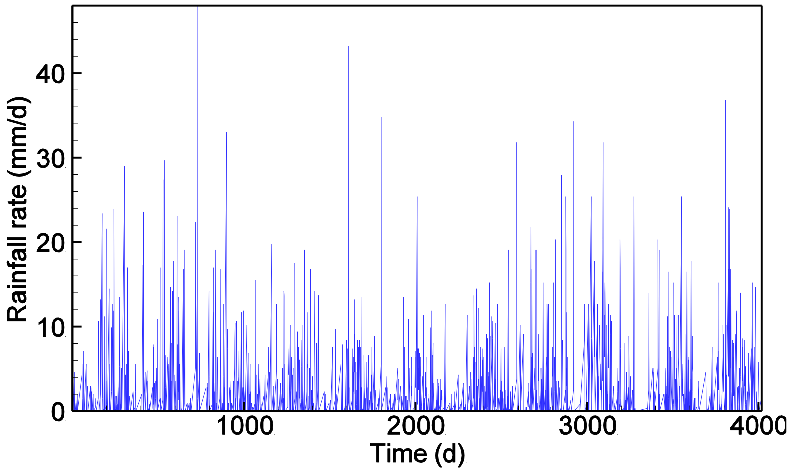

Figure 2.4 Ten year daily rainfall data for Adelaide, South Australia, gauge number 23000

2.3.2 Fully integrated SW/GW model

HydroGeoSphere (HGS) was used as the fully integrated SW/GW model. HGS was considered suitable for this application, as it represents the physical catchment processes explicitly. This is because HGS can solve the equations for both surface and variably-saturated subsurface flow regimes at each time step simultaneously, which results in realistic, physically-based simulation of the movement of water on and within catchments (Therrien et al., 2009). HGS has been applied successfully to losing/gaining stream analysis (Partington et al., 2011), SW/GW disconnection problems (Banks et al., 2011; Brunner et al., 2009), the dynamics of river bank storage processes (Doble et al., 2012) and dual permeability systems (Schwartz et al., 2010).

HGS uses the diffusion wave approximation to the 2D St. Venant equations to simulate surface flow (Therrien et al., 2009):

$$\frac{\partial \phi_0 h_0}{\partial t} - \frac{\partial}{\partial x}(d_0 K_{ox} \frac{\partial h_0}{\partial x}) - \frac{\partial}{\partial y}(d_0 K_{oy} \frac{\partial h_0}{\partial y}) + d_0 \Gamma_0 \pm Q_0 = 0 \qquad (2.1)$$

where ϕ_0 is the surface flow domain porosity; d_0 is the depth of water above the surface [L]; Γ_0 is the volumetric fluid exchange rate with the subsurface [LT^{-1}]; h_0 is the water surface elevation related to the datum [L]

($h_0 = d_0 + z_0$, where z_0 is the bed/land surface elevation [L]); Q_0 is a volumetric flow rate per unit area representing external sources and sinks [LT^{-1}]. All of the above symbols represent state variables, except for K_{ox} and K_{oy}, which are parameters representing surface conductance in the x- and y-directions [LT^{-1}] and can be calculated by Manning's equation or the Chezy equation.

The following modified Richard's equation is applied for subsurface flow (Therrien et al., 2009):

$$-\nabla \cdot (-\overline{K} \cdot k_r \nabla(\psi + z)) + \sum \Gamma_{ex} \pm Q = \frac{\partial}{\partial t}(\theta_s S_\omega) \tag{2.2}$$

where $\overline{K}$ is the hydraulic conductivity tensor [LT^{-1}]; k_r is the relative permeability; ψ is the pressure head [L]; z is the elevation head [L]; Γ_{ex} is the volumetric subsurface fluid exchange rate with the surface domain [L^{3}L^{-3}T^{-1}]; Q is a volumetric fluid flux per unit volume representing a subsurface source or sink [L^{3}L^{-3}T^{-1}]; θ_s is the saturated water content and S_ω is the degree of water saturation.

The degree of saturation can be determined by the Van Genuchten equations (van Genuchten, 1980):

$$S_\omega = S_{\omega r} + (1 - S_{\omega r})[1 + |\alpha\psi|^\beta]^{-v} \quad \mathit{for} \quad \psi < 0 \tag{2.3}$$

$$S_\omega = 1 \quad \mathit{for} \quad \psi > 0 \tag{2.4}$$

$$v = 1 - \frac{1}{\beta} \quad \mathit{for} \quad \beta > 1 \tag{2.5}$$

where $S_{\omega r}$ is the residual water saturation, and α , β and v are the van Genuchten parameters.

The surface and subsurface are coupled using either continuity of head or a conductance concept, with exchanges between the two domains. The latter concept was used in this study and is shown below (Therrien et al., 2009):

$$q_e = \frac{k_r K_{zz}}{l_e}(\psi - d_0) \tag{2.6}$$

where q_e is the exchange flux between the surface and subsurface domain [LT^{-1}]; K_{zz} is the vertical saturated hydraulic conductivity [LT^{-1}]; and l_e is the coupling length [L].

All of the equations above are solved simultaneously at each time step utilising either a finite difference, control volume finite difference or finite element approach (Therrien et al., 2009). For this study, the control volume finite difference method is used, due to its quick implementation on regular model grids and superior mass conservation (Partington et al., 2009).

A 3-D HGS model of the tilted V-catchment (Section 2.3.1) was developed in order to obtain the required simulated streamflow and baseflow. As shown in Figure 2.3, the catchment is symmetrical. As a result, all simulations were conducted for only half of the catchment, as shown in Figure 2.5. The simulated stream channel, which extends in the y direction, is 10m wide. In the x direction, perpendicular to the stream channel, the grid spacing is 50m from x=0-2000m and 10m from 2000-2010m. The grid spacing along the y axis is 50m. Therefore, the domain has 42 cells in the x direction and 61 cells in the y direction. In the z direction, there are 21 layers, with a discretisation of 0.5m for the first 10m below the surface and a single layer below this, with its thickness varying between 10 and 80m. Therefore, the maximum saturated thickness of the whole catchment is 90m. A critical depth boundary condition was utilized at the downstream end of the channel (nodes (2000,0,0) and (2010,0,0)) to allocate the surface head at these nodes to be at critical depth

(d_0). The discharge Q_0 per unit width at the critical depth boundary is then given by:

$$Q_0 = \sqrt{g d_0^3} \tag{2.7}$$

A no flow boundary condition was used for the bottom and lateral subsurface domain, meaning that water can only leave the catchment from the stream outlet (i.e. critical depth boundary). The surface friction was described using Manning's roughness coefficients of 0.015 and 0.15 for the slope and channel, respectively, as was the case in Panday and Huyakorn (2004). The rill storage and obstruction storage heights for this model implementation were also set to quite small values of 0.001m and 0.0m, respectively, to reduce their effects on baseflow generation. The coupling length used was 1x10^{-6}m, providing near continuity of pressure at the surface/subsurface interface.

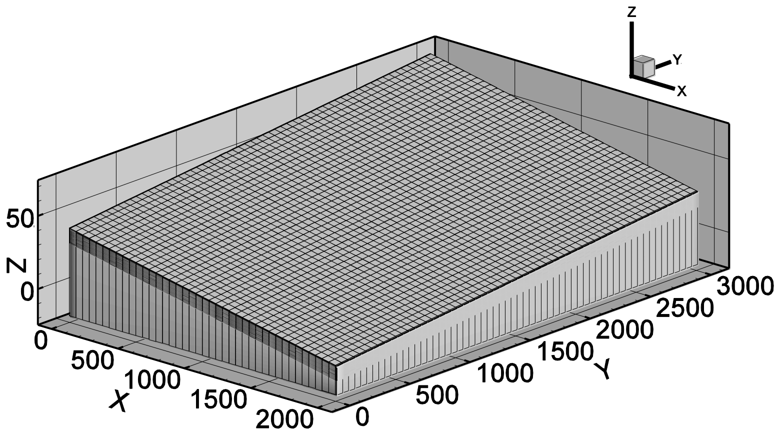

Figure 2.5 Catchment model for case study (modified version of the V-catchment in Panday and Huyakorn (2004))

The HGS model was used to simulate streamflow for catchments with different soil properties and the baseflow was calculated using the HMC method, details of which can be found in Partington et al. (2011). The two soil parameters that were varied include K_s and porosity (Table 2.1). For each soil type, each of the two parameters was varied over five values, the minimum, lower quartile, mean, upper quartile and maximum values of the ranges given in Table 2.1, while keeping the other soil parameter constant at its mean value. This resulted in 45 simulations in total; 9 for each of the five soil types in Table 2.1.

The simulations with different soil characteristics were conducted in three steps. Firstly, to determine steady initial conditions, a spatially and temporally uniform rainfall with a relatively high intensity (i.e. 10.8mm/hour) was applied to the catchment, with an initial water table parallel to the bottom of the channel across the whole catchment. This simulation was run for approximately one year until the total streamflow did not change with time, and was then allowed to drain under gravity in the next phase when the actual rainfall was applied.

Secondly, with the above initial conditions, the actual Adelaide rainfall record (see Section 2.3.1) was applied to the whole catchment and the model was run until a second equilibrium state based on the actual rainfall was reached, which required simulation periods between 2 and 35 years, depending on soil type. These simulations provided steady-state initial conditions for step three. It should be noted that, alternatively, initial conditions for different soil types can be obtained by directly applying the actual Adelaide rainfall to the catchment with a fully-saturated subsurface domain, and running the model until the catchment achieves a steady state. However, this method of deriving the initial condition takes much longer for some of the soil types considered, resulting in significantly diminished transient behaviour caused by the inconsistent boundary or initial conditions. Finally, based on these equilibrium states for the actual rainfall record, the simulation was run for a further ten years in order to obtain the data used for assessing and improving the performance of the RDF. For all of the simulations, adaptive time stepping with a maximum time step of 1000s was used to ensure that the maximum time step is significantly less than hourly.

2.3.3 Digital filter

In this study, the LH filter was used as the RDF. Although the LH filter has some limitations compared with other RDFs, such as the Chapman one-parameter algorithm (Chapman and Maxwell, 1996) and the Boughton two-parameter algorithm (Chapman, 1999) (e.g. it is unable to estimate baseflow when there is no direct runoff, as discussed by Chapman and Maxwell (1996)), it is used extensively in practice and has already been incorporated into a number of software tools, including BaseJumper (Murphy et al., 2009) and ABScan (Parker, 2006). The LH filter is a high-pass filter, which filters low frequency signals (i.e. baseflow) and transmits high-frequency input signals (i.e. quickflow). Consequently, baseflow has to be obtained by subtracting the filtered quickflow from the original streamflow. The corresponding equations are given by Nathan and McMahon (1990) as:

$$\begin{aligned} q_{f(i)} &= kq_{f(i-1)} + \frac{1+k}{2}(q_{(i)} - q_{(i-1)}) \quad \mathit{for} \quad q_{f(i)} \geq 0 \\ q_{b(i)} &= q_{(i)} - q_{f(i)} \end{aligned} \tag{2.8}$$

where i is the time step, in days [T]; $q_{(i)}$ is the original total streamflow at time step i, [LT^{-1}]; $q_{f(i)}$ and $q_{b(i)}$ are the filtered quickflow and corresponding baseflow at time step i, [LT^{-1}]; and k is the filter parameter, dimensionless, which is normally set in the range of 0.0-1.0.

Referring to equation (2.8), the initial condition is set as the total streamflow being equal to baseflow (i.e. $q_{b(1)} = q_{(1)}$). In order to better understand the impact of the values of the filter parameter on filter performance, it is useful to examine the outputs obtained from the LH filter for the extreme values of the filter parameter. If the LH filter parameter is set to its maximum value of 1.0, when $q_{(i)} > q_{(1)}$, the baseflow obtained using the LH filter at each time step is always equal to the first value of total streamflow ($q_{b(i)} = q_{(1)}$), even if there is a peak in the streamflow hydrograph. If $q_{(i)} \leq q_{(1)}$, the filtered baseflow is equal to the total streamflow ($q_{b(i)} = q_{(i)}$), due to the constrained condition that baseflow cannot exceed total streamflow or become negative. On the other hand, if the LH filter parameter is set to its minimum value of 0.0, for the rising limb of the total streamflow hydrograph, the baseflow obtained from the LH filter is attenuated by halving the sum of the values of the total streamflow at the current and previous time step ($q_{b(i)} = \frac{q_{(i-1)} + q_{(i)}}{2}$). As for the descending limb, the filtered baseflow is equal to the streamflow at the current time step ($q_{b(i)} = q_{(i)}$). Therefore, when the filter parameter is 0.0, the filtered baseflow hydrograph always has a peak right under the peak of the streamflow hydrograph. Baseflow hydrographs obtained from the LH filter with values of the filter parameter between 0.0 and 1.0 lie between the baseflow hydrographs derived using filter parameters of 0.0 and 1.0.

The filter can be passed forward and backward over a data set several times and the number of passes results in data smoothing and nullification of any phase distortion (Spongberg, 2000). Although some researchers have used a relatively large number of passes, such as Murphy et al. (2009), who implemented the LH filter with 9 passes across hourly data for eight case study catchments, most of the studies have used three passes (e.g. (Evans and Neal, 2005; Li et al., 2011; Spongberg, 2000; Tan et al., 2009a)), as suggested by Nathan and McMahon (1990). In this study, the filter was passed over the data three times in all of the analyses: forward, backward and then forward again. The time step ($i-1$) is replaced by ($i+1$) when conducting the "backward" pass, and after the first pass, $q_{(i)}$ is substituted by the computed baseflow calculated from the previous pass. During the calculation, if $q_{f(i)}$ is smaller than zero, the baseflow is equal to the current $q_{(i)}$.

The 45 simulated streamflow hydrographs obtained from the HGS model for the different combinations of soil properties were used as inputs to the LH filter in order to obtain the corresponding filtered baseflow. Two sets of 45 filtered baseflow hydrographs were obtained, one using optimal (calibrated) filter parameter values (see Section 2.3.4 for details) and one using a fixed filter parameter of 0.925, which is commonly used in the literature (Arnold and Allen, 1999; Murphy et al., 2009; Nathan and McMahon, 1990), in order to assess the potential benefits of obtaining calibrated filter parameter values.

2.3.4 Error measure and optimization procedure

The dimensionless coefficient of efficiency (E_f) was used as the error measure for evaluating the performance of filters with different parameters and applied to catchments with different soil conditions. This is because it is one of the most commonly used error measures in hydrology and provides a trade-off between objectives that emphasize different aspects of hydrographs (Gupta and Kling, 2011; Gupta et al., 2009). However, it should be noted that because of the nature of the LH filter, constrains are placed on the variability of the resulting baseflow hydrograph. For example, as discussed previously, the timing of the peak of the baseflow hydrograph always coincides with the timing of the peak of the total streamflow hydrograph and whenever baseflow is larger than the total streamflow, baseflow is forced to be equal to the total streamflow, thereby capturing the recession limb of the baseflow hydrograph. As a result, the only variability is in the magnitude of the baseflow hydrograph, which is controlled by the LH filter parameter, as discussed above (i.e. smaller values of the filter parameter result in larger peaks and vice versa).

The equation of E_f was given by Nash and Sutcliffe (1970) as:

$$E_f = 1 - \left[\frac{\sum_{i=1}^{n} (Y_i^{obs} - Y_i^{sim})^2}{\sum_{i=1}^{n} (Y_i^{obs} - Y^{mean})^2} \right] \tag{2.9}$$

where Y_i^{obs} is the ith observation of the flow rate being evaluated [LT^{-1}], Y_i^{sim} is the ith simulated value of the flow rate being evaluated [LT^{-1}], Y^{mean} is the mean of the observed data for the flow rate being evaluated [LT^{-1}], i is the time step [T], and n is the total number of observations.

When using E_f to evaluate the performance of RDFs, the observed data in equation (2.9) are given by the simulated baseflow results obtained from the fully integrated SW/GW model (q_b^{sim}), while the baseflow results derived from the RDFs (q_b^{filter}) correspond to the simulated values. Based on benchmark values available from other studies (Herron and Croke, 2009; Moriasi et al., 2007; Nejadhashemi et al., 2007), RDF performance can be judged as ‘perfect’ when E_f=1.0, while E_f values between 0.5 and 1.0 correspond to ‘good’ filter performance; E_f values between 0.0 and 0.5 show ‘acceptable’ filter performance and ‘unacceptable’ filter performance is represented by negative values of E_f.

In order to estimate the uncertainty associated with estimates of the optimal LH filter parameters, the following linear estimate of uncertainty was used (Vugrin et al., 2005):

$$\left\{ k : \frac{S(k) - S(\hat{k})}{S(\hat{k})} \le \frac{p}{n-p} F^{\alpha}_{p,n-p} \right\} \tag{2.10}$$

$$S(k) = \sum_{i=1}^{n} [q_{b(i)}^{filter}(k) - q_{b(i)}^{sim}]^2 \tag{2.11}$$

where $\hat{k}$ is the optimal LH filter parameter, obtained by minimizing the sum of squared errors between the baseflow obtained from the LH filter and that simulated using the HGS model (equation (2.11)); p is the number of parameters to be estimated, which is 1 in this case; n is the number of data points, which is 3650 days in this case; and $F^{\alpha}_{p,n-p}$ is the upper α percent point of the F-distribution, which was set to 0.05.

The optimization method used in order to obtain the optimal values of the filter parameters was the golden section search method (Press et al., 1992), as there was only one model parameter.

2.4 Results and discussion

2.4.1 Relationship between optimal filter parameters and soil properties

The optimal LH filter parameter values obtained for the different soil properties, as well as their linear estimates of uncertainty, are given in Table 2.2 and Figure 2.6. As can be seen, the uncertainty estimates are very small, indicating that the optimal values of the filter parameters are well defined and that the results obtained can be treated with confidence. In addition, it can be seen that there is a distinct inverse relationship between K_s and optimal values of the LH filter parameter, which vary between 0.0025 and 0.997, while the optimal values of the LH filter parameter do not vary significantly for soils with different values of porosity. This can be explained by examining the relationship between soil properties and the resulting baseflow, as well as the relationship between the values of the LH filter parameter and filter performance (see below).

2.4.1.1 Relationship between soil properties and resulting baseflow

Soils with different values of porosity were found to have similar baseflow components. Although soils with larger porosity can store more subsurface water before they become saturated and also allow more groundwater to discharge into the stream, for a given value of K_s, their rate of change in storage was similar to that of soils with smaller porosity, resulting in similar baseflow components.

In contrast, for soils with a given porosity, soils with larger values of K_s resulted in larger baseflow components. This is because there is a positive relationship between K_s and the ease with which water can infiltrate into the soil, which means that larger K_s values enable water to infiltrate into the soil more easily, resulting in increased soil saturation and groundwater exfiltration. This can be seen from the simulated streamflow and baseflow obtained from the HGS models (Figure 2.7). For catchments with sandy soil and mean values of K_s and porosity, most of the rain infiltrates into the ground, either percolating into the soil and staying in the catchment as groundwater or recharging the stream as baseflow. Consequently, compared with other soil types, the peak streamflow for sandy soils was smaller, with a high proportion of baseflow and a low proportion of quickflow (surface runoff). In contrast, for catchments with soil consisting of silt loam, rain cannot infiltrate easily, but is converted to direct runoff, rapidly feeding streamflow. Therefore, such catchments had streamflow with a higher peak, with almost no baseflow contribution.

This difference in the streamflow behaviour for the two different soil types can also be seen clearly by examining the corresponding flow duration curves, which are an estimate of the percentage of time a particular streamflow was equalled or exceeded, and therefore provide a graphical representation of the variability associated with streamflow (Vogel and Fennessey, 1994). As can be seen from Figure 2.8, the flow duration curve for the catchment with a sandy soil is very flat, indicating that streamflow is almost constant over time, which is representative of a stream that is fed primarily by baseflow. In contrast, the flow duration curve for the catchment consisting of silt loam indicates that flows are highly variable, with higher peak flows, but extended periods with little or no flow, which is indicative of a catchment that is dominated by surface flow.

Table 2.2 Optimal LH filter parameters and the linear estimates of uncertainty for sand, sandy loam, loam, loamy sand and silt loam with different soil properties

Soil Type	Min~Max	K_s & related optimal LH filter parameter				Porosity & related optimal LH filter parameter			
		K_s(m/s)	Filter Parameter	Lower Bound	Upper Bound	Porosity	Filter Parameter	Lower Bound	Upper Bound
Sand	Min	1.27E-06	0.997	0.9969	0.9976	0.261	0.415	0.4077	0.4241
	Lower Quartile	8.26E-05	0.787	0.7821	0.7937	0.31	0.465	0.458	0.4733
	Mean	1.60E-04	0.503	0.4956	0.5104	0.359	0.503	0.4956	0.5104
	Upper Quartile	5.65E-04	0.105	0.098	0.1142	0.409	0.537	0.5293	0.5474
	Max	9.66E-04	0.0025	0.0	0.01	0.4578	0.571	0.5635	0.5777
Sandy Loam	Min	5.01E-07	0.997	0.9969	0.9975	0.28	0.990	0.989	0.9907
	Lower Quartile	1.25E-05	0.997	0.9967	0.9982	0.346	0.991	0.9898	0.9916
	Mean	2.44E-05	0.992	0.9914	0.9938	0.412	0.992	0.9914	0.9938
	Upper Quartile	7.51E-05	0.837	0.833	0.8427	0.478	0.992	0.9913	0.9934
	Max	1.26E-04	0.612	0.605	0.6186	0.544	0.994	0.9929	0.995
Loam	Min	8.17E-06	0.997	0.9967	0.9978	0.29	0.983	0.9815	0.9836
	Lower Quartile	1.57E-05	0.997	0.9963	0.9979	0.422	0.986	0.9846	0.9864
	Mean	3.07E-05	0.987	0.9864	0.988	0.554	0.987	0.9864	0.988
	Upper Quartile	9.46E-05	0.719	0.7133	0.7257	0.686	0.988	0.9873	0.9891
	Max	1.58E-04	0.458	0.4501	0.4679	0.818	0.990	0.9885	0.9906
Loamy Sand	Min	1.10E-05	0.997	0.9966	0.9978	0.341	0.970	0.969	0.9713
	Lower Quartile	2.55E-05	0.996	0.9948	0.9967	0.398	0.973	0.9715	0.9738
	Mean	3.99E-05	0.974	0.9732	0.9753	0.455	0.974	0.9732	0.9753
	Upper Quartile	1.12E-04	0.665	0.6582	0.6713	0.512	0.976	0.975	0.9769
	Max	1.84E-04	0.438	0.4304	0.4477	0.569	0.978	0.9772	0.9794
Silt Loam	Min	1.51E-07	0.997	0.9968	0.9974	0.35	0.997	0.9968	0.9977
	Lower Quartile	1.58E-06	0.997	0.9969	0.9976	0.425	0.997	0.9968	0.9977
	Mean	3.01E-06	0.997	0.9968	0.9977	0.5	0.997	0.9968	0.9977
	Upper Quartile	8.41E-06	0.997	0.9967	0.9979	0.575	0.997	0.9968	0.9977
	Max	1.38E-05	0.997	0.9967	0.9982	0.65	0.997	0.997	0.9973

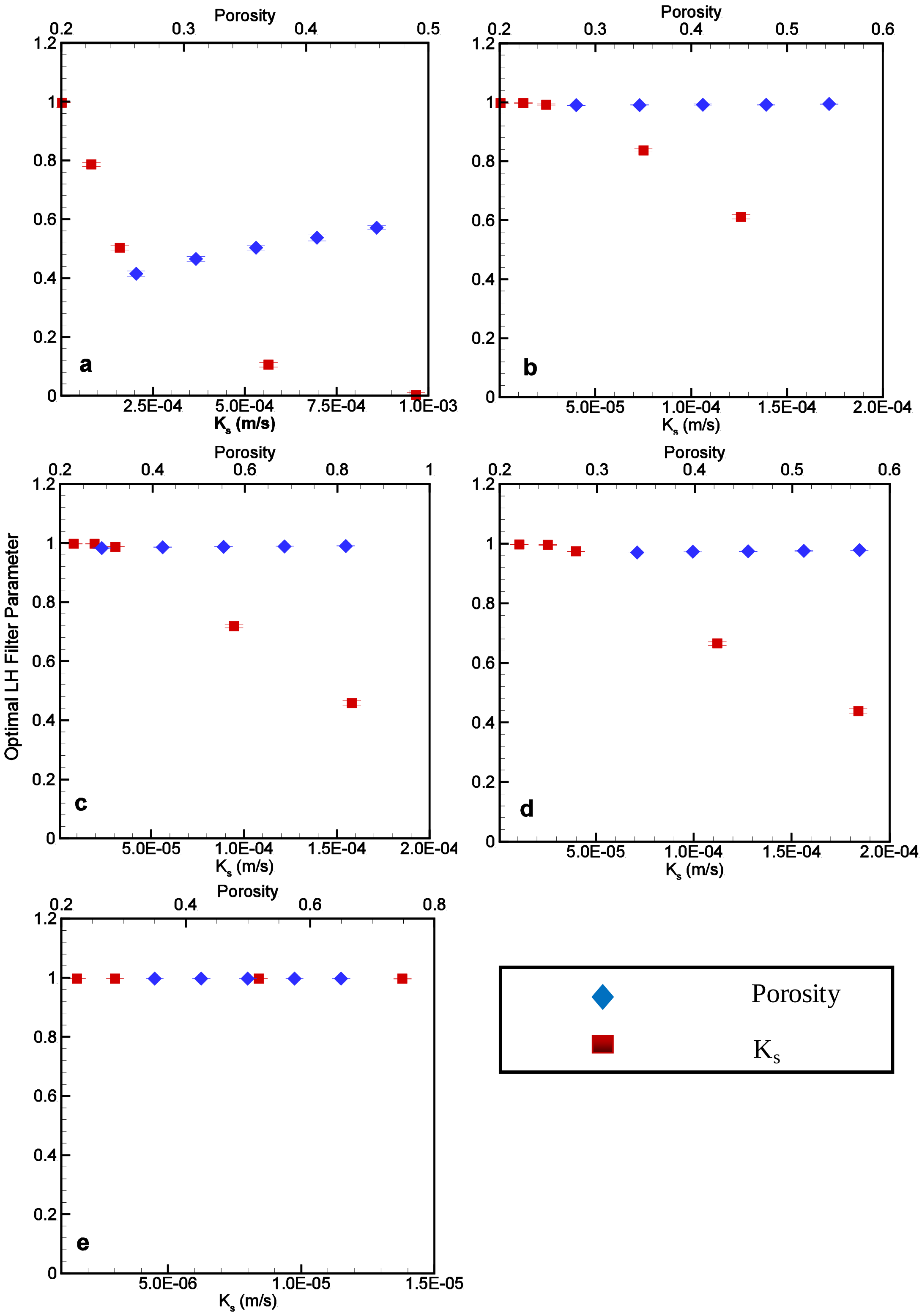

Figure 2.6 Values of the optimal LH filter parameter with the error bars obtained from the linear estimates of uncertainty for sand (a), sandy loam (b), loam (c), loamy sand (d) and silt loam (e) with different soil properties

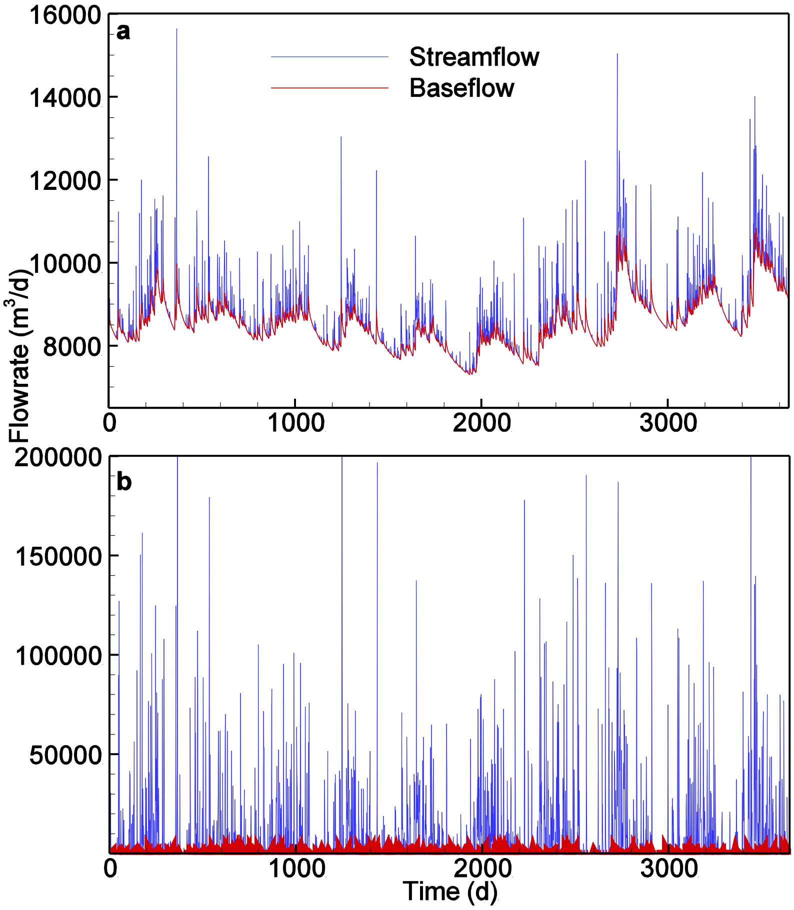

Figure 2.7 Simulated streamflow and baseflow for catchments with sand (a) and silt loam (b) with their mean values of K_s and porosity

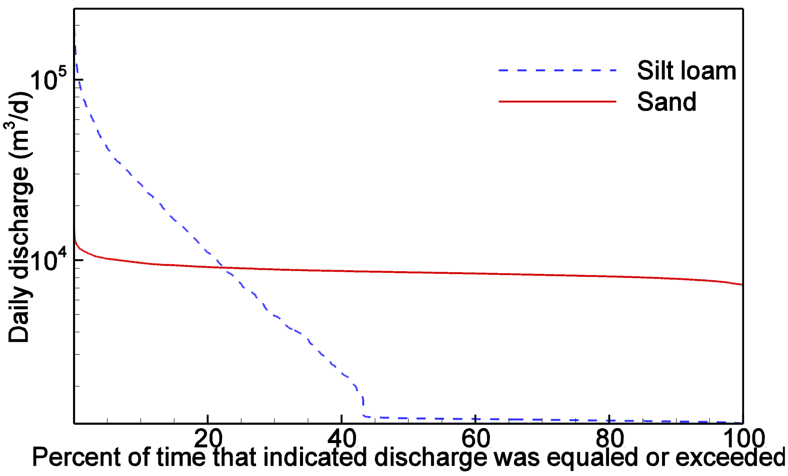

Figure 2.8 Flow duration curves for catchments with sand and silt loam with their mean values of K_s and porosity

2.4.1.2 Relationship between the values of the LH filter parameter and filter performance

As discussed above, larger values of K_s result in larger baseflow and vice versa, and as discussed in Section 2.3.3 and shown in Figure 2.9, for a catchment with sandy soil, smaller values of the LH filter parameter result in larger baseflow contributions and vice versa. Consequently, there exists an inverse relationship between K_s and the optimal LH filter parameter values, as shown in Figure 2.6.

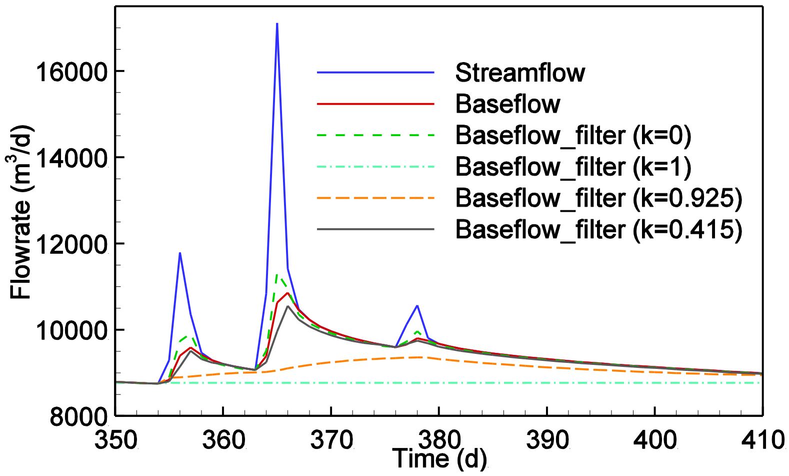

Figure 2.9 Impact of different values of LH filter parameter on baseflow for catchment with sand with minimum porosity

To further confirm the inverse relationship between K_s and the optimal value of the LH filter parameter, five additional simulations (i.e. generation of simulated streamflow and baseflow using HGS, optimization of the LH filter parameter and the determination of filtered baseflow) were conducted with K_s values between the mean and upper quartile values of K_s for sand. The results obtained for all of the simulations conducted are shown in Figure 2.10, including the linear estimates of uncertainty, which are very small, indicating that the results obtained can be treated with confidence. As can be seen, the additional results confirm the strong inverse relationship between the optimal value of the LH filter parameters and K_s, regardless of soil type, which is as expected, based on the discussion of the impact of K_s on baseflow and the way different filter parameter values affect the output from the LH filter given above. However, as can be seen from Figure 2.10, the optimal values of the LH filter parameter are almost constant very close to their maximum value of 1.0 for soils with small values of K_s, suggesting that for small values of K_s, baseflow estimates obtained using the LH filter might be inaccurate, as baseflow decreases with decreasing values of K_s, while the baseflow hydrographs obtained using the LH filter remain constant (also see Section 2.4.2). In addition, it can be seen that the optimal values of the filter parameter can be significantly different from the value of 0.925 most commonly used in the literature (Murphy et al., 2009; Nathan and McMahon, 1990).

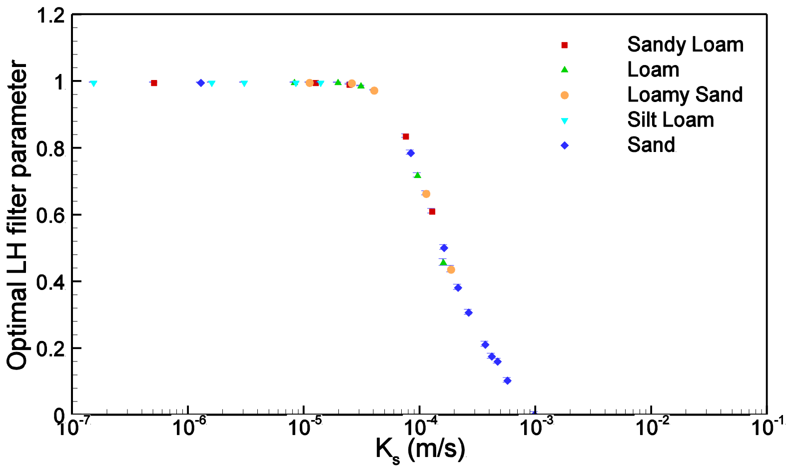

Figure 2.10 Relationship between the optimal LH filter parameter and K_s with the error bars obtained from the linear estimates of uncertainty for different soil properties

2.4.2 Relationship between filter performance and soil properties

Since K_s has the most significant impact on baseflow among the different soil parameters investigated, only baseflow results obtained for soils with different values of K_s are discussed in this section. The E_f values between the baseflow obtained using the LH filter with optimal filter parameters and the simulated baseflow from HGS are summarized in Table 2.3. As can be seen, in most cases, the filtered baseflow is similar to that obtained from the HGS model, especially for soils with larger values of K_s. For example, for sand with the maximum K_s value, the filtered baseflow obtained with the optimal filter parameter of 0.0025 is almost identical to the simulated baseflow obtained using HGS (Figure 2.11), with an E_f of 0.9998 (Table 2.3). In this case, the high K_s value results in most of the rain infiltrating into the ground and becoming groundwater, leading to increased exfiltration to the stream. As a result, surface runoff from the catchment is quite low, but the baseflow component of the streamflow is quite high. The same results can be observed from the flow duration curve for sand with maximum K_s (Figure 2.12). The flat slope of this curve throughout denotes the characteristics of a perennial stream, with continuous and significant baseflow discharge. Consequently, a very low value of the LH filter parameter is optimal, as discussed previously. Similar results were obtained for soils with K_s values greater than 2.44E-05m/s, provided the optimal LH filter parameter was used. Based on the results obtained, it is suggested that the baseflow obtained using the LH filter can provide a good approximation to the actual baseflow for perennial streams, in catchments with soils with relatively large values of K_s, as long as an appropriate value of the filter parameter is used.

Table 2.3 Comparison of LH filter performance for the case where the optimal filter parameter was used and a filter parameter of 0.925 was used for sand, sandy loam, loam, loamy sand and silt loam with different K_s

Soil type	K_s (m/s)		E_f between simulated baseflow and that obtained using LH filter with the optimal filter parameter	E_f between simulated baseflow and that obtained using LH filter with a filter parameter of 0.925
Sand	Min	1.27E-06	-2.266	-19.613
	Lower quartile	8.26E-05	0.960	0.900
	Mean	1.60E-04	0.989	0.903
	Upper quartile	5.65E-04	0.999	0.969
	Max	9.66E-04	0.9998	0.976
Sandy loam	Min	5.01E-07	-10.29	-73.56
	Lower quartile	1.25E-05	-0.044	-1.945
	Mean	2.44E-05	0.290	-0.679
	Upper quartile	7.51E-05	0.965	0.946
	Max	1.26E-04	0.981	0.900
Loam	Min	8.17E-06	-0.135	-2.704
	Lower quartile	1.57E-05	0.010	-1.613
	Mean	3.07E-05	0.517	-0.078
	Upper quartile	9.46E-05	0.958	0.888
	Max	1.58E-04	0.986	0.884
Loamy sand	Min	1.10E-05	-0.083	-2.136
	Lower quartile	2.55E-05	0.137	-1.125
	Mean	3.99E-05	0.825	0.698
	Upper quartile	1.12E-04	0.981	0.924
	Max	1.84E-04	0.991	0.906
Silt loam	Min	1.51E-07	-76.85	-489.41
	Lower quartile	1.58E-06	-1.603	-14.84
	Mean	3.01E-06	-0.589	-6.966
	Upper quartile	8.41E-06	-0.130	-2.651
	Max	1.38E-05	-0.029	-1.813

The performance of the LH filter is not as good for soils with small values of K_s, with small and even negative values of E_f (Table 2.3). For example, for silt loam with the minimum K_s value, the baseflow obtained using the filter with the optimal value of the filter parameter is much larger than the simulated baseflow obtained using HGS at almost all time steps (Figure 2.11), resulting in an E_f of -76.85. The reason for this is that K_s determines how much water infiltrates into the ground and how easily water moves through the subsurface of the catchment. Therefore, for a catchment with low K_s and high intensity rainfall, infiltration is low, which results in the generation of more surface runoff and the formation of sharp peaks in observed streamflow (Figure 2.11). Consequently, the simulated baseflow is quite small, with small fluctuations around the mean value at all time steps. This can be seen from the flow duration curve for silt loam with minimum K_s (Figure 2.12). This curve has a reasonably steep slope throughout, which intercepts the x-axis at around 53% of time, indicating that all of the discharges are less than or equal to the discharge that occurs 53% of the time. This flow duration curve is indicative of a highly variable ephemeral stream, the flow of which is largely from direct runoff with very small contributions from baseflow. Streams like this may cease to flow for relatively long periods without rainfall events. However, as discussed previously, the baseflow obtained using the LH filter is based solely on streamflow and the value of the filter parameter, so that the variations in filtered baseflow follow the sharp variations in streamflow, resulting in an over-prediction of baseflow whenever the filter parameter is between 0.0 and 1.0. Therefore, the LH filter does not appear to be suitable for catchments with K_s values smaller than 1.38E-05m/s that result in variable ephemeral streams with low baseflow contribution, even when the optimal filter parameter is used. This is an agreement with the discussion of Figure 2.10 in Section 2.4.1. It should be noted that, in practice, if the catchment has very little baseflow, there is generally no need to estimate it. However, the simulations for low baseflow contribution catchments (e.g. silt loam with minimum K_s) are shown here in order to illustrate the sorts of features, such as soil properties, that cause the catchment to have little baseflow contribution.

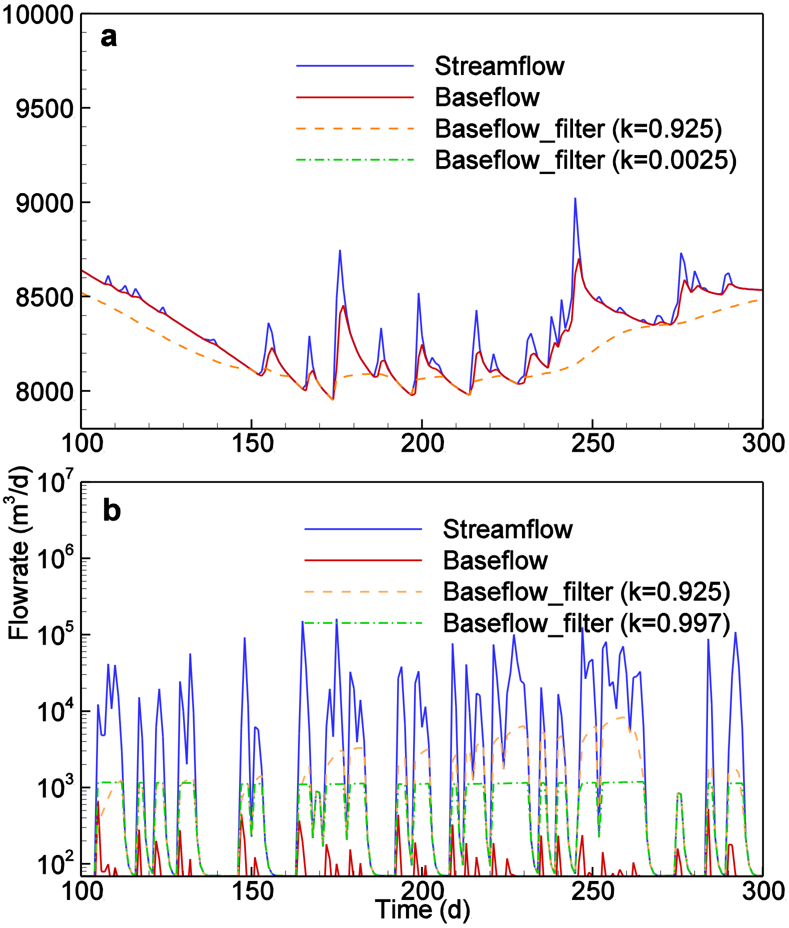

Figure 2.11 Comparison of baseflow calculated from the HGS model simulation and the LH filter with two different values of the filter parameter for sand with maximum K_s (a) and silt loam with minimum K_s (b)

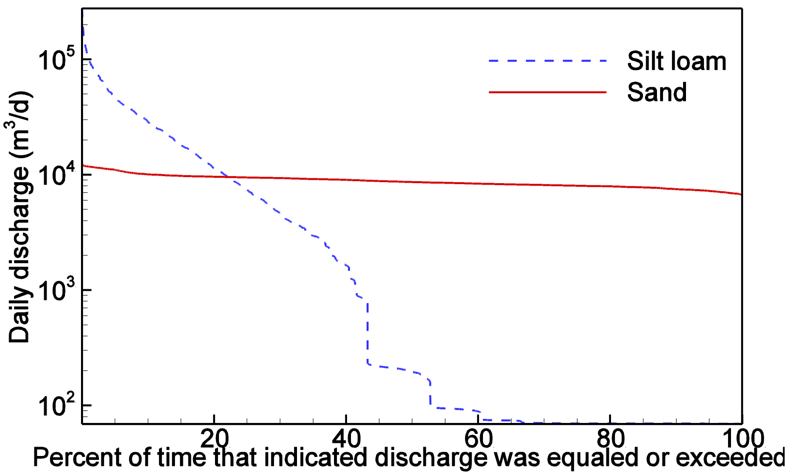

Figure 2.12 Flow duration curves for catchments with sand with maximum Ks, and silt loam with minimum K_s

The performance of the LH filter with the most commonly used filter parameter of 0.925 is also shown in Table 2.3 and Figure 2.11. As can be seen, by obtaining optimal values of the LH filter parameter for different soil properties, the performance of the LH filter can be improved significantly in certain situations. This is to be expected, given that the optimal values of the filter parameter for soils with different properties span such a large range, as discussed above. The results obtained indicate that the performance of the LH filter with a filter parameter of 0.925 is not adequate for most of the catchments with small values of K_s, but acceptable for catchments with K_s values greater than 3.99E-05m/s, with E_f values greater than 0.698. However, the range of soil types over which the LH filter performs well can be extended by using the filter parameter that is most appropriate for the soil conditions.

The results presented in this paper have utilized the simulations from the fully integrated SW/GW model as though they are the 'true' values. The results derived using this framework for this hypothetical case study illustrate the impacts of catchment soil properties on RDF parameters, and provide a clearer understanding that among catchment soil properties, K_s is likely to play a key role in determining the appropriate values of optimal filter parameters for catchments with different physical properties. Physical processes in real catchments are more complicated than those represented in the hypothetical case study, due to catchment heterogeneity, macropores, and vegetation; however, the dominant physical processes are captured by the fully integrated SW/GW model, which clearly identifies the need for a variable filter parameter, and to carefully consider the application of digital filtering approaches to determining baseflow.

2.5 Summary and conclusions

In this study, a generic framework for assessing and improving currently used RDFs for quantifying baseflow has been developed. This framework provides a procedure that enables research studies to be conducted in order to test the accuracy and improve the performance of various baseflow filter methods.

The framework makes use of fully integrated surface water and groundwater (SW/GW) models to obtain estimates of streamflow and baseflow for catchments with different properties (e.g. soil types and rainfall patterns). A recursive digital filter (RDF) is then applied to the simulated streamflow to estimate baseflow, which can be compared with the simulated baseflow obtained from the fully integrated SW/GW model in order to assess filter performance. Filter performance can be improved by adjusting the filter parameter(s) until the best match between the filtered baseflow hydrograph and the simulated baseflow hydrograph from the fully integrated SW/GW model is obtained. If a sufficient number of studies of this nature are conducted (i.e. using different RDFs, different fully integrated SW/GW models, different catchment hydrogeological properties, etc.), general guidelines for the applicability and improvement of RDFs can be developed.

In order to demonstrate the usefulness of the proposed framework, it was applied to a commonly used hypothetical case study. A fully integrated SW/GW model of a hypothetical catchment was developed using HGS, which was used to generate streamflow and baseflow hydrographs for 45 different soil properties. The generated streamflow hydrographs were used as inputs to the LH filter, which was applied using two sets of filter parameters; a constant value of 0.925, which is the value most commonly used in the literature, and values that were calibrated in order to minimize the difference between the baseflow hydrograph obtained using the LH filter and that obtained using the HGS model for each of the soil types. The results obtained show that the optimal value of the LH filter parameter is sensitive to the saturated hydraulic conductivity (K_s), and should therefore be adjusted accordingly, thus better reflecting the actual physical processes producing the baseflow. The results obtained also show that the baseflow obtained using the LH filter can represent the baseflow simulated using the HGS model reasonably well for catchments with relatively large K_s. However, for catchments with small values of K_s, the LH filter does not appear to be suitable. Furthermore, when a fixed filter parameter of 0.925 is used, the range of soil properties over which the LH filter is applicable is reduced significantly.

It should be noted that the generalisability of the results is restricted by the range of factors considered in the analysis. For example, consideration of the impact of vegetation and thus transpiration is likely to affect seasonal and longer term trends in baseflow as a result of vegetation growth, which could result in significantly more complex interactions (D'Odorico et al., 2005; Guttal and Jayaprakash, 2007, 2009). One must also be aware of the fact that no calibration-evaluation was undertaken to independently assess the calibrated LH filter parameters. Also, it should be noted that repetition of the analysis conducted in this paper with different climate records would possibly lead to other optimal LH filter parameters for the same soil type. Consequently, this should be the focus of future studies. Furthermore, it should be noted that the optimal values of the LH filter parameter are likely to be influenced by a number of other factors, such as catchment size, slope and aspect ratio, streamflow routing, soil heterogeneity, maximum saturated thickness and depth to water table. The impact of these factors on the optimal LH filter parameter should be investigated in future studies.

2.6 Acknowledgements

This research was supported by the Chinese Scholarship Council (CSC) and the University of Adelaide. The authors also gratefully thank Dr. Philip Brunner, Dr. Tim Peterson and the other anonymous reviewer for their detailed comments, which have greatly improved the quality of the paper.

Chapter 3

3 Performance assessment and improvement of recursive digital baseflow filters for catchments with different physical characteristics and hydrological inputs (Paper 2)

Statement of Authorship

Title of Paper	Prediction of Accuracy and Optimal Parameter Values of Recursive Digital Baseflow Filters Based on Physical Catchment Characteristics and Hydrological Inputs
Publication Status	○ Published ○ Accepted for Publication ◉ Submitted for Publication ○ Publication Style
Publication Details	Li, L., Maier, H.R., Partington, D., Lambert, M.F., Simmons, C.T., 2013. Prediction of Accuracy and Optimal Parameter Values of Recursive Digital Baseflow Filters Based on Physical Catchment Characteristics and Hydrological Inputs. Environmental Modelling & Software Submitted.

Author Contributions

By signing the Statement of Authorship, each author certifies that their stated contribution to the publication is accurate and that permission is granted for the publication to be included in the candidate's thesis.

Name of Principal Author (Candidate)	Li Li		
Contribution to the Paper	Developed and implemented the methodology, designed numerical experiments, interpreted and analysed results, prepared manuscript.		
Signature		Date	01/03/2013

Name of Co-Author	Holger Maier		
Contribution to the Paper	Supervised manuscript preparation and reviewed draft.		
Signature		Date	1/3/13

Name of Co-Author	Daniel Partington		
Contribution to the Paper	Assisted with running models and analysing results, reviewed draft and supervised manuscript preparation.		
Signature		Date	1/03/2013

Name of Co-Author	Martin Lambert		
Contribution to the Paper	Supervised manuscript preparation and reviewed draft.		
Signature		Date	1/3/2013

Name of Co-Author	Craig Simmons		
Contribution to the Paper	Supervised research and reviewed draft.		
Signature		Date	1/3/13

Name of Co-Author			
Contribution to the Paper			
Signature		Date	

Name of Co-Author			
Contribution to the Paper			
Signature		Date	

Please cut and paste additional co-author panels here.

Abstract

Recursive digital filters (RDFs) are one of the most commonly used methods of baseflow separation in practice. However, how accurately they estimate baseflow and how to select appropriate values of filter parameters is generally unknown, as it is extremely difficult to obtain accurate measurements of baseflow in the field. In this paper, a previously developed framework for calibrating and assessing the accuracy of RDFs based on the output of fully integrated surface water/groundwater (SW/GW) models is used to obtain optimal parameters for, and assess the accuracy of, three commonly used RDFs, including the Lyne and Hollick (LH), Boughton two-parameter and Eckhardt filters, under a range of physical catchment characteristics and hydrological inputs. In addition, regression relationships are developed that enable the suitability of these RDFs, as well as the optimal values of the filter parameters, to be determined based on these catchment characteristics and hydrological inputs. The results obtained indicate that the LH filter performs better than the Boughton and Eckhardt filters, which are mathematically equivalent but with different parameters, over a larger range of conditions and that the optimal values of the filter parameters vary considerably for all three filters, depending on catchment characteristics and hydrological inputs. In addition, optimal values of the filter parameters for the LH and Eckhardt filters, as well as the accuracy of all three filters, can be predicted very well based on physical catchment characteristics and hydrological inputs by using the developed regression models.

3.1 Introduction

The estimation of baseflow plays an important role in the management of many environmental systems, including water supply (Linsley et al., 1988), low flow hydrology (Nathan and McMahon, 1992; Smakhtin, 2001), flood hydrology (Murphy et al., 2009), contamination investigation (Smakhtin, 2001) and stream ecology (Price, 2011). There are various definitions of baseflow, including groundwater discharge (Chapman, 1999; Freeze, 1972), slow flow and sustained flow (Hall, 1968). In this study, groundwater discharge from aquifers represents the baseflow contribution to streamflow.

Due to the difficulties associated with the estimation of baseflow in the field (Li et al., 2013a; Partington et al., 2012), various graphical and automated techniques have been developed for baseflow estimation from gauged streamflow data since the early twentieth century. Among these, recursive digital filters (RDFs) are one of the most commonly used methods for estimating baseflow in practice, due to their simplicity and ease of implementation (Arnold et al., 1995; Nathan and McMahon, 1990). The basic principle underpinning these RDFs is that streamflow hydrographs consist of a high frequency signal (i.e. quickflow) and a low frequency signal (i.e. baseflow) and that by applying a filter to the total streamflow hydrograph, the quickflow component can be removed, leaving the baseflow component. Many different RDF configurations have been proposed in the literature in order to achieve this, including the Lyne and Hollick (LH) filter (Nathan and McMahon, 1990), the Chapman one parameter algorithm (Chapman and Maxwell, 1996), the Boughton two-parameter filter (Boughton, 1993; Chapman, 1999) and the Eckhardt filter (Eckhardt, 2005). A common feature of all of these RDFs is that the baseflow hydrographs obtained are a function of one or more user-defined filter parameters. For some RDFs (Eckhardt, 2005; Nathan and McMahon, 1990), fixed values of the filter parameters are used, while for others (Chapman, 1999; Eckhardt, 2005), values of some of the filter parameters are selected based on various catchment and/or streamflow characteristics.

A number of studies have compared the performance of different RDFs (Chapman, 1999; Eckhardt, 2008; Evans and Neal, 2005; Murphy et al., 2009; Tan et al., 2009b). However, determining the relative performance of different filters in terms of their ability to estimate baseflow accurately is not easy, primarily because it is extremely difficult to measure baseflow in the field (Dukic, 2006; McCallum et al., 2010), thereby making it almost impossible to determine an appropriate benchmark against which filter performance can be assessed. In order to overcome this problem, a number of different approaches have been used. Nathan and McMahon (1990), Chapman (1999), Eckhardt (2008) and Schwartz (2007) subjectively used the physical plausibility of the resulting baseflow hydrographs to evaluate RDF performance. Szilagyi (2004) and Ferket et al. (2010) applied the outputs of lumped and semi-distributed catchment models as a basis of comparison. Other authors have used process-based models as a performance benchmark. For example, Furey and Gupta (2003) used a process-based model of a hill-slope to evaluate the physically-based baseflow separation method developed by Furey and Gupta (2001). Most recently, Partington et al. (2012) used the baseflow simulated from a fully integrated surface water and groundwater (SW/GW) model at the catchment scale in order to evaluate the performance of simple automated baseflow estimation methods. While significant research efforts have been devoted to the assessment of the overall performance of different RDFs with commonly used values of filter parameters, there has been limited research on the impact of the values of the filter parameters on RDF performance.

In order to address this shortcoming, Li et al. (2013a) developed a calibration framework for RDFs. As part of this framework, optimal values of filter parameters can be obtained by minimising the difference between the baseflow hydrograph predicted by the RDF under consideration and the baseflow hydrograph obtained from a fully integrated SW/GW model. This assumes that fully integrated SW/GW models can provide reasonably accurate estimates of actual baseflow. They also tested this framework on a synthetic catchment with different soil properties in order to determine appropriate values of these filter parameters and to assess the impact these values have on filter performance for various catchments with different soil properties. They found that there was a strong relationship between the optimal filter parameter value and saturated hydraulic conductivity (K_s). Also, the optimal values of the filter parameter obtained using the framework for various catchments with different soil types were quite different from the commonly used constant value suggested by other researchers. Their findings showed that the proposed framework has promise in terms of enabling optimal filter parameter values to be selected *a priori* based on physical catchment characteristics. However, Li et al. (2013a) only tested their calibration framework on a single RDF, the most commonly used LH filter, and did not consider a range of catchment characteristics that are likely to have an impact on optimal filter parameter values, such as catchment size, slopes, aspect ratio and van Genuchten parameters α and β. In addition, Li et al. (2013a) only tested their approach on a single hydrological record and did not consider the impact of evapotranspiration (ET), which could affect the seasonal and longer term trends in baseflow (D'Odorico et al., 2005). While other studies have attempt to predict certain baseflow properties as a function of catchment characteristics (e.g. (Lacey and Grayson, 1998; Longobardi and Villani, 2008; Mazvimavi et al., 2005; Mwakalila et al., 2002)), they have focused on summary statistics, such as the baseflow index (BFI), rather than the optimal parameters of RDFs.

In order to overcome the shortcomings of previous studies outlined above and to test the generality of the results obtained by Li et al. (2013a), the objectives of this paper are (i) to determine optimal values of the filter parameters for, and assess the overall performance of, different RDFs under a wider range of physical catchment characteristics (e.g. catchment slopes, area, aspect ratio and soil properties) and hydrological inputs (e.g. rainfall and ET) using the frameworks developed by Li et al. (2013a), and (ii) to develop regression relationships that will enable the suitability of different RDFs and the optimal values of filter parameters to be determined based on physical catchment characteristics and hydrological inputs. The remainder of this paper is organised as follows: the methodology is presented in Section 3.2, followed by the results and discussion of the study in Section 3.3. A summary and conclusions are given in Section 3.4.

3.2 Methodology

As stated in the introduction, in order to obtain optimal values of the filter parameters and assess overall RDF performance under a range of physical catchment characteristics and hydrological inputs, the calibration and assessment framework introduced by Li et al. (2013a) is used, as shown in Figure 3.1. As part of the framework, a fully integrated SW/GW model is used to generate streamflow and baseflow hydrographs for a catchment with particular physical properties, given a particular hydrological input. Both of these hydrographs are assumed to provide the best possible representation of the actual streamflow and baseflow hydrographs, as discussed in Li et al. (2013a). It should be noted that in order to obtain the most accurate estimate of the baseflow hydrographs, the hydraulic mixing cell (HMC) method developed by Partington et al. (2011) is used.

The streamflow hydrograph obtained from the fully integrated SW/GW model (q) is used as the input to the RDF and the baseflow hydrograph obtained from the fully integrated SW/GW model using the HMC method (q_b^{sim}) is used as the benchmark for the calibration of the filter parameters and the assessment of overall RDF performance. As part of the calibration of the RDF filter parameters, an appropriate error measure between the baseflow hydrograph obtained using the fully integrated SW/GW model (q_b^{sim}) and that obtained using the RDF (q_b^{filter}) is minimised by adjusting the RDF filter parameter(s) using a suitable optimization algorithm. This minimised error measure is also used to assess the overall performance of the calibrated RDF.

As part of this study, the above process is repeated for different combinations of (i) physical catchment characteristics, including the saturated hydraulic conductivity (K_s) and van Genuchten parameters α and β (van Genuchten, 1980) of the soils, the area and aspect ratio of the catchment and the slopes along and perpendicular to the channel, and (ii) hydrological inputs, including rainfall and ET. Given the large number of possible combinations of the different catchment characteristics and hydrological inputs investigated and the long computer run times associated with each simulation of the fully integrated SW/GW model, a suitable sampling strategy (Figure 3.1) is used in order to obtain representative combinations of the catchment characteristics and hydrological inputs considered, while keeping the total computational effort to a manageable level. After obtaining optimal filter parameter values and corresponding RDF performances (i.e. error measures), regression models are developed for predicting optimal filter parameter values and filter performance based on catchment characteristics and hydrological inputs. The calibration, assessment and regression model development procedure is repeated for three different RDFs, including the LH filter considered by Li et al. (2013a), as well as the Boughton two-parameter and the Eckhardt filters. Details of the various steps in the methodology are given in the subsequent sections.

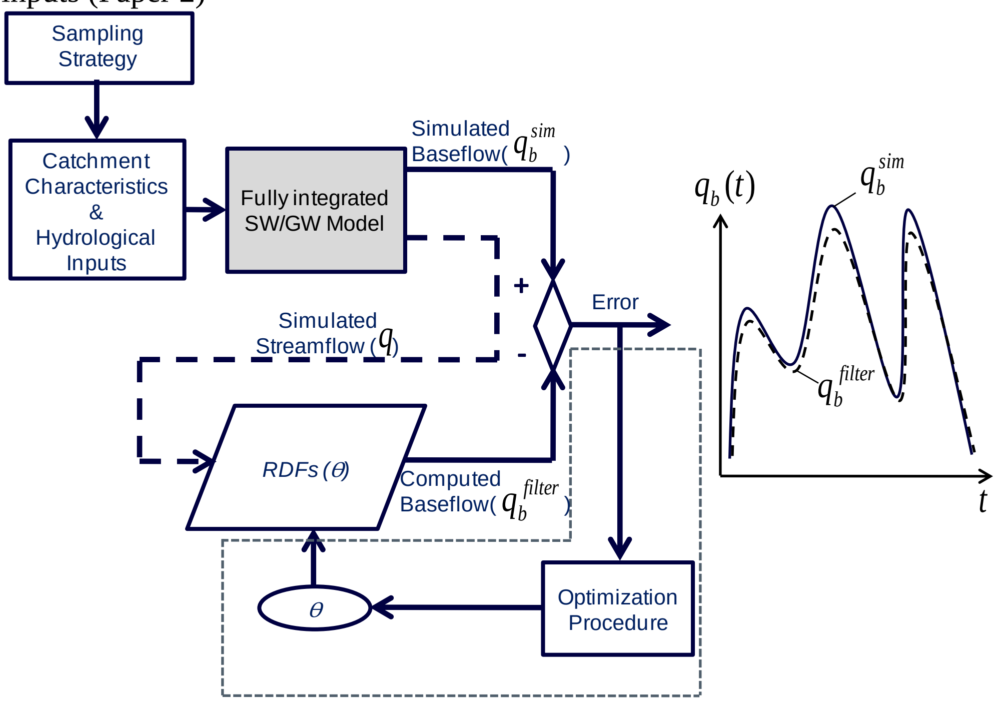

Figure 3.1 Schematic representation of the adopted methodology

3.2.1 Selection of catchment characteristics and hydrological inputs

3.2.1.1 Synthetic catchment description

In this study, a synthetic catchment, which is loosely based on a benchmarked integrated surface-subsurface hydrology problem, the tilted V-catchment test case (Figure 3.2), is used (Panday and Huyakorn, 2004) (P&H). The P&H case has the same surface geometry features as diGiammarco et al. (1996). In this study, modifications are made to the P&H case as follows: The original roughness coefficients used for the hill-slope and channel domains cause overland flow to be preponderant parallel and adjacent to the stream, rather than in the stream (Gaukroger and Werner, 2011), which was also mentioned as unrealistic by Panday and Huyakorn (2004). Thus, the same roughness coefficient (0.015 s/m$^{1/3}$) is used for both the overland flow and channel domains. Furthermore, the horizontal water table used in the P&H case represents an unrealistic (overly dry) initial condition (Partington et al., 2012). To start the model from more realistic initial conditions, the catchment is fully saturated and allowed to drain with a long time series of representative rainfall and ET events until the average annual discharge is stable (Partington et al., 2012). In order to reduce the influence of the coarse discretisation on the surface and subsurface flow, the unsaturated subsurface domain should have a finer discretisation. As a result, the original discretisation of the subsurface domain of the P&H catchment model is changed from 11 layers to 41 layers, with the top 20m being formed with 40 uniform permeable layers of soil. Similar P&H case problems and the corresponding modifications are discussed in Gaukroger and Werner (2011), Partington et al. (2012) and Li et al. (2013a). Below the 40 permeable soil layers is a single impermeable layer with variable thickness due to the different catchment slopes used, as detailed in Section 3.2.1.2. Details of the different catchment areas and aspect ratios investigated are also given in Section 3.2.1.2.

The top 20 m permeable soil layer is homogeneous and isotropic, and is underlain by a single impermeable layer.

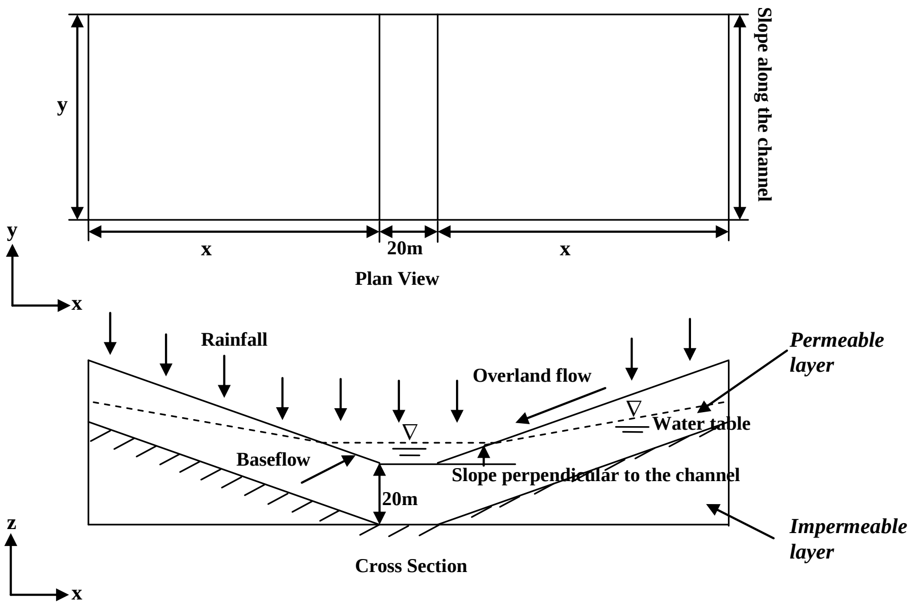

Figure 3.2 Schematic representation of tilted V-catchment flow problem (refer to Panday and Huyakorn (2004))

3.2.1.2 Physical catchment characteristics and hydrological inputs

Baseflow is a function of a large number of variables, including topographic, geological, soil and climatic factors, as well as vegetation. In this study, physical catchment characteristics are represented by seven variables: catchment area (A), catchment hill slope (S1, which is perpendicular to the channel), catchment channel slope (S2, which is parallel to the channel), catchment aspect ratio (AR), and soil type, which includes K_s and van Genuchten parameters α and β. Details of the different values of these physical catchment characteristics and hydrological inputs considered in this study are given in Table 3.1 and Table 3.2.

The impact of different catchment areas on optimal filter parameter values and filter performance is assessed as larger catchment areas increase aquifer storage capacity, and therefore promote sustained baseflow contribution to the channel, when exposed to spatially uniform rainfall patterns. Five discrete catchment areas are included in this study, including: 6km^2, 48km^2, 80km^2, 120km^2 and 192km^2. These catchment areas are selected in order to test the generality of the results obtained by Li et al. (2013a) for catchments with different areas. In addition, there are limits on the range of applicability of some of the filters when their commonly used filter parameters are used. These limits are used to select the extreme values of the areas investigated. For example, Chapman (1991) indicated that the LH filter with its commonly used filter parameter of 0.925 gives satisfactory baseflow separation for catchments ranging in area from 4.2 to 210km^2.

The impact of different hill slopes (S1) and channel slopes (S2) on optimal filter parameter values and filter performance is assessed, as these slopes affect infiltration capacity and control the rate at which soil water moves downslope. Consequently, they have an impact on the proportion of precipitation entering the channel as direct runoff and the proportion infiltrating into the ground and discharging into the channel as baseflow. In this study, five discrete values are considered for each slope, including 0.005, 0.008, 0.012, 0.016, 0.02 for S1, and 0.0025, 0.004, 0.006, 0.008, 0.01 for S2. All of these values are smaller than those used in the original P&H case study in order to avoid groundwater discharge being concentrated around the channel outlet.

The impact of different catchment aspect ratios (i.e. ratios of catchment widths to lengths (x/y, as shown in Figure 3.2)) on optimal filter parameter values and filter performance is evaluated as these values are related to the length of the channel and the distance between the hill slope and the channel, and therefore affect the travel time of baseflow to the channel outlet. Five discrete aspect ratio values are investigated, including 0.5, 0.75, 1.0, 1.25 and 1.5, as they cover conditions ranging from a rectangular shape for which the width (x) is smaller than the length (y), to a rectangular shape for which the width (x) is greater than length (y), including a square catchment.

The impact of different soil types, including K_s and van Genuchten parameters α and β, on optimal filter parameter values and filter performance is also considered. The previous study by Li et al. (2013a) on the sensitivity of baseflow to soil properties showed that K_s has a significant impact on baseflow and is a key parameter. The van Genuchten parameters, α and β, are included in this study as they affect the relative permeability of the soil and are therefore also likely to have an impact on baseflow response. In addition, their effect on baseflow was not investigated in Li et al. (2013a). Five values of K_s are considered, including 2.44E-05m/s, 3.99E-05m/s, 1.12E-04m/s, 2.11E-04m/s and 9.66E-04m/s, which represent sand, sandy loam and loamy sand. These values are chosen in order to cover all regions of the plot of K_s versus the optimal LH filter parameter given by Li et al. (2013a). Based on the ranges of α for sand (0.572-16.412), sandy loam (0.47-11.75) and loamy sand (0.544-17.344), five discrete values, including the minimum, lower quartile, mean, upper quartile and maximum values of the range of overlapping values for these soil types (i.e. 0.572-11.75), are considered for α (see Table 3.1). The same method is used for obtaining the five discrete values for β (see Table 3.1). It should be noted that all of the values used for K_s, α and β are obtained from the values originally given in Puhlmann et al. (2009), to be consistent with Li et al. (2013a).

Table 3.1 Different physical catchment characteristics considered

Catchment Characteristic	Unit	Explanation	Values Considered
K_s	m/s	Saturated hydraulic conductivity	2.44E-05, 3.99E-05, 1.12E-04, 2.11E-04, 9.66E-04
α	-	van Genuchten parameter	0.572, 3.366, 6.161, 8.955, 11.75
β	-	van Genuchten parameter	1.32, 1.556, 1.793, 2.029, 2.266
A	km^2	Catchment area	6, 48, 80, 120, 192
S1	-	Hill slope (perpendicular to the channel)	0.005, 0.008, 0.012, 0.016, 0.02
S2	-	Channel slope (along the channel)	0.0025, 0.004, 0.006, 0.008, 0.01
AR	-	Ratio of catchment width to length (x/y)	0.5, 0.75, 1.0, 1.25, 1.5

Five discrete patterns of the hydrological inputs are represented in terms of the ratio of the actual rainfall and potential ET (R/ET) from five Australian cities, including Adelaide, Melbourne, Sydney, Brisbane and Darwin, as they represent the full range of the climate classification groups for Australian capital cities (i.e. temperate, sub-tropical, tropical) (Table 3.2). Areal rainfall and ET for each city are derived from the same gauges, and no attempt is made to assess the sensitivity of the optimal filter parameter and optimal filter performance to spatial variability in rainfall and ET patterns. A typical ten year period of daily rainfall data is obtained for these five cities from the Australian Bureau of Meteorology National Climate Centre and the corresponding daily potential ET data are obtained based on the average seasonal daily potential ET for these five cities. Details of the gauges from which the data are obtained, as well as the average annual rainfall and potential ET for each of these five cities, are given in Table 3.2.

Table 3.2 Different hydrological inputs considered

City	Climate [1]	Gauge No.	Average annual rainfall (mm/a)	Average annual potential ET (mm/a)	R/ET (average annual rainfall/average annual potential ET)
Adelaide	Temperate	023011	510.16	1470.97	0.347
Melbourne	Temperate	086071	525.33	911.33	0.576
Sydney	Temperate	066062	1095.85	920.90	1.190
Brisbane	Sub-Tropical	031011	2238.22	2077	1.078
Darwin	Tropical	014015	1667.16	2056.37	0.811

1) Based on the Köppen classification of the major classification groups of Australian climate zones (http://www.bom.gov.au/climate/environ/other/kpn_group.shtml)

3.2.1.3 Sampling strategy

In order to cover all possible combinations of physical catchment characteristics and hydrological inputs detailed in Table 3.1 and Table 3.2, 5^8 simulations using the fully integrated SW/GW model would be required, where 8 is the number of inputs considered (i.e. the hydrological input and the 7 different catchment characteristics considered) and 5 is the number of options available for each input. Given that the runtime of the simulation model varies between 7,200 and 43,200 minutes, depending on model inputs, the total runtime required to perform all of these simulations would be approximately 168,750,000 hours (19,263 years). Consequently, as stated previously, it is necessary to sample the space of possible catchment characteristics and hydrological inputs in order to reduce computational effort to an acceptable level, while still obtaining a set of representative combinations of different catchment characteristics and hydrological inputs.

Several sampling strategies are suitable for this purpose, including random sampling, the Sobol' method (Sobol, 1993), the Morris method (Morris, 1991) and Latin Hypercube Sampling (LHS) (McKay et al., 1979; Stein, 1987). Among these approaches, LHS is very popular for use with computationally demanding models, as is the case here, due to its efficient stratification properties, which enable a large amount of sensitivity information to be extracted with a relatively small sample size (Helton et al., 2006). Consequently, LHS is used as the sampling strategy in this study.

When LHS is used, each input is divided into N equi-probable, non-overlapping intervals, with N representing the number of necessary parameter combinations. One parameter value is taken from each interval, and combined randomly with the values of the other investigated parameters to obtain N parameter sets, which can guarantee that the complete input space (i.e. all different combinations of catchment characteristics and hydrological inputs in this case) can be explored using as few samples as possible. Yu et al. (2001) found that LHS produces similar results to random sampling methods with only 10% of the samples. LHS has also been used successfully for the sensitivity analyses of hydrological and environmental models by Sieber and Uhlenbrook (2005), Wagener and Kollat (2007) and Manache and Melching (2008). Further details about LHS are given in McKay et al. (1979), Stein (1987), Iman and Shortencarier (1984) and Isukapalli and Georgopoulos (1999).

The LHS design involves sampling without replacement; therefore, if there are K uncertain parameters, the lower limit of the value of N (where N equals the number of necessary parameter combinations) should be at least K+1. An exact formula for calculating N does not exist in the literature, although various empirical guidelines are given in relation to the number of samples required when implementing LHS. Janssen et al. (1992) recommended that a sample size of 4/3 times the number of inputs should be used, Iman and Helton (1985) suggested that this figure should be two to five times the number of inputs and SIMLAB (2010) recommended a range for the sample size between 1.5 and 10 times the number of inputs. In this study, a sample size of 70 (i.e. 8.75 times the number of inputs) is adopted, which is near the upper end of the sample sizes recommended in the literature, to ensure that a good coverage of the input space is obtained, while keeping computational effort to reasonable levels.

3.2.2 Fully integrated SW/GW model

HydroGeoSphere (HGS) is used as the fully integrated SW/GW model in order to simulate the 3D synthetic V-catchment's response to rainfall and ET inputs for different catchment characteristics, as it can be used to simulate the hydrological processes within the catchment in a physically based manner (Therrien et al., 2009). HGS has been used successfully in previous research for the comparison of baseflow estimation methods (Partington et al., 2011; Partington et al., 2012), SW/GW disconnection problems (Banks et al., 2011; Brunner et al., 2009), bank storage dynamic processes analysis (Doble et al., 2012) and the study of dual permeability systems (Schwartz et al., 2010).

In HGS, surface flow is simulated using the diffusion wave approximation to the 2D St. Venant equations, and the modified 3D Richard's equation is applied for variably-saturated subsurface flow. The surface and subsurface flow are coupled using a conductance concept with exchanges between the two domains. By using a finite difference method to solve all of the equations for both surface and subsurface flow regimes at each time step simultaneously, HGS can represent the physical catchment processes explicitly. Actual ET is considered as a function of leaf area index, soil moisture and root depth. Further description of the code and its numerical formulation can be found in Therrien et al. (2009) and Brunner and Simmons (2012).

As shown in Figure 3.2, the catchment used in this study is symmetrical. As a result, all simulations are conducted for only half of the catchment, as shown for one example of the catchment configurations considered in Figure 3.3. The reported fluxes are correspondingly half of those expected when accounting for both sides of the stream. The grid spacing along the x and y axes is different for the different catchment areas and aspect ratios investigated. For instance, the grid spacings along the x and y axes for the catchment with an area of $6km^2$ range from 40m and 50m to 50 and 100m, respectively, while for the catchment with an area of 192km^2, the grid spacings along the x and y axis range from 150m and 200m to 200m and 300m, respectively. However, the width for the channel is constant at 10m. As discussed in Section 3.2.1.1, the bottom layer of the catchment is impermeable, therefore, all of the simulations for the 70 models developed for catchments with different combinations of catchment characteristics and hydrological inputs are conducted for the first 20m of permeable soil below the catchment surface, which has 40 horizontal layers, with a spacing of 0.5m for each layer to provide discretisation in the unsaturated zone, as shown in Figure 3.3. Grid convergence checks have been undertaken and indicated that there is less than 1% difference compared with the finer discretisation for the total streamflow and baseflow outputs.

The time steps used in the model vary in accordance with an adaptive time-stepping approach (HydroGeoLogic, 2000). A maximum step of 3,600 seconds is used to ensure that the maximum time step is significantly less than daily. A critical depth boundary condition is utilised at the downstream end of the channel to allocate the surface head at these nodes to be at critical depth. A no flow boundary condition is used for the bottom and lateral subsurface domain, meaning that water can only leave the catchment from the stream outlet. Relatively small values of rill storage and obstruction height are used in order to reduce their effects on baseflow generation, and a reasonably small coupling length is used to provide near continuity of pressure at the surface/subsurface interface (Table 3.3). Properties for ET inputs for this model are also included in Table 3.3, which are obtained from Partington et al. (2012).

Initially, the whole catchment is fully saturated, as discussed in Section 3.2.1.1. The fully saturated catchments are then drained by repeatedly applying a representative ten year pattern of rainfall and potential ET for each of the five cities. This pattern is applied over a period ranging from 10 to 50 years, until the average annual discharge is stable in the simulated hydrographs. With these initial conditions, the simulation is then run for a further ten years with the same ten year record in order to obtain the data used for calibrating and assessing the performance of the RDFs.

Table 3.3 Surface and subsurface parameters for the synthetic catchment model (refer to Partington et al. (2012))

Parameter	Value
Surface	
Manning's roughness	0.015 s/m$^{1/3}$
Rill storage height	0.001 m
Obstruction storage height	0.0 m
Transpiration fitting parameter c1	0.3
Transpiration fitting parameter c2	0.2
Transpiration fitting parameter c3	10
Leaf area index	2.08
Wilting point	0.1
Field capacity	0.15
Oxic limit	0.9
Anoxic limit	1.0
Limiting saturation (minimum)	0.2
Limiting saturation (maximum)	0.32
Canopy storage parameter	0.0 m
Initial interception storage	0.0 m
Subsurface	
Evaporation depth (quadratic decay function)	3 m
Root depth (quadratic decay function)	6 m
Surface/Subsurface coupling	
Coupling length	0.001m

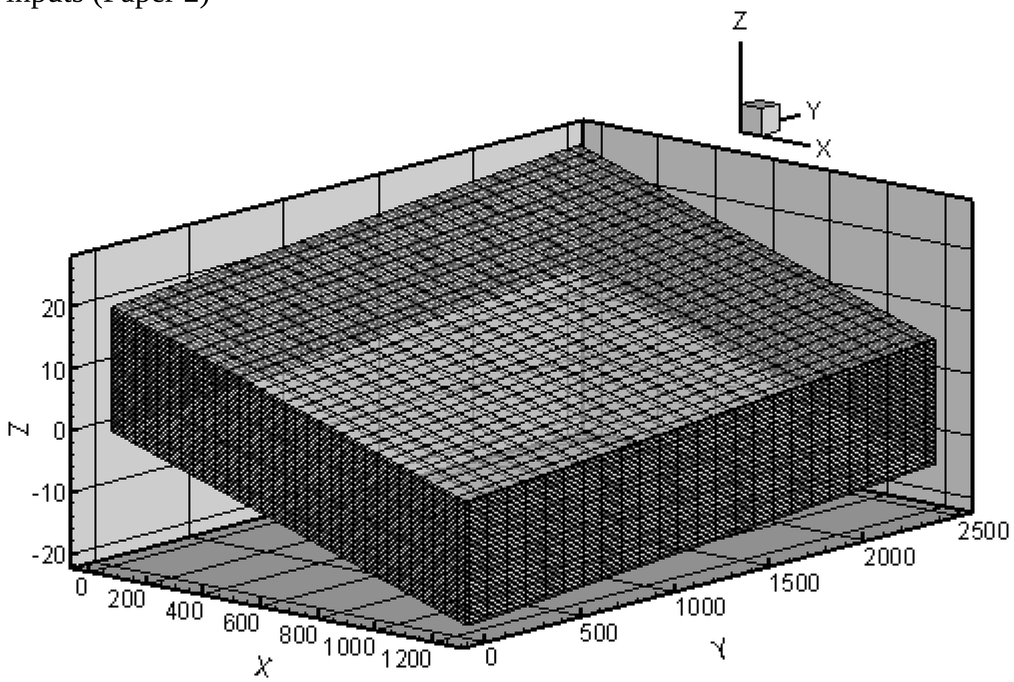

Figure 3.3 3D Catchment model (modified version of the V-catchment in Panday and Huyakorn (2004))

The HGS model is used to obtain the simulated streamflow (q) hydrographs for the catchments with the 70 sets of different catchment characteristics and hydrological inputs generated using LHS, as described above. These simulated streamflow hydrographs are then used as the inputs to the RDFs in order to estimate the filtered baseflow hydrographs (q_b^{filter}). The simulated baseflow hydrograph (q_b^{sim}) is extracted from the HGS model using the HMC method (Partington et al., 2011), based on the nodal fluid mass balance obtained from the model simulations. The HMC method is able to account for storage effects and time lags within catchments, which provides a means of estimating baseflow from fully integrated SW/GW models. Details of the HMC method can be found in Partington et al. (2011).

3.2.3 RDFs

In this study, three commonly used RDFs are calibrated and evaluated by comparing the baseflow extracted from these RDFs (q_b^{filter}) with that obtained from the HGS simulations (q_b^{sim}) with the different combinations of catchment characteristics (see Table 3.1) and hydrological inputs (see Table 3.2) obtained using LHS (see Section 3.2.1.3) as inputs. The RDFs considered include the LH filter (Nathan and McMahon, 1990), the Boughton two-parameter filter (Boughton, 2004; Chapman, 1999) and the Eckhardt filter (Eckhardt, 2005). These RDFs are selected as they are readily available and commonly used. In addition, there is some subjectivity in determining appropriate values of the parameters for these filters, making them suitable candidates for calibration. Detailed descriptions of the RDFs can be found in the references given above, thus only a brief overview of these methods is provided below.

3.2.3.1 Lyne and Hollick (LH) filter

The LH filter applies signal processing techniques to a streamflow time series in order to remove the high-frequency quickflow signal so as to obtain the low-frequency baseflow signal. The corresponding equations are given by Nathan and McMahon (1990) as:

$$\begin{aligned} q_{f(i)} &= a q_{f(i-1)} + \frac{1+a}{2}(q_{(i)} - q_{(i-1)}) \quad \textit{subject to} \quad q_{f(i)} \geq 0 \\ q_{b(i)} &= q_{(i)} - q_{f(i)} \end{aligned} \tag{3.1}$$

where i [T] is the time step; $q_{(i)}$ [L^3T^{-1}] is the original total streamflow at time step i; $q_{f(i)}$ and $q_{b(i)}$ [L^3T^{-1}] are the filtered quickflow and corresponding baseflow at time step i; and a is the filter parameter to be calibrated, dimensionless, which is normally set within the range 0.0-1.0. As can be seen from equation (3.1), larger values of the filter parameter result in smaller values of baseflow and vice versa. An additional property of the LH filter is that the peak of the resulting baseflow hydrograph generally coincides with that of the streamflow hydrograph. The LH filter can be passed forward and backward over the data set several times resulting in data smoothing and nullification of any phase distortion (Spongberg, 2000). Three passes are used in this study: forward, backward and forward, as suggested by Nathan and McMahon (1990).

3.2.3.2 Boughton two-parameter filter

The Boughton two-parameter filter (Boughton, 2004) is based on the Chapman one parameter algorithm (Chapman and Maxwell, 1996), but has an additional parameter (C) so that the algorithm can be used more flexibly for hydrograph separation. The resulting equation is as follows (Chapman, 1999):

$$q_{b(i)} = \frac{k}{1+C} q_{b(i-1)} + \frac{C}{1+C} q_{(i)} \qquad subject \quad to \qquad q_{b(i)} \leq q_{(i)} \tag{3.2}$$

where k is the recession constant, which is determined using the method outlined in Eckhardt (2008) in this study, and C is the filter parameter to be calibrated. It should be noted that k could also be considered as a parameter to be calibrated, which would result in a multi-objective calibration problem. However, in this study, only C is calibrated. As can be seen from equation (3.2), larger values of the filter parameter result in larger values of baseflow and vice versa. However, unlike the parameter in the LH filter, for adequately sampled long time series, the parameter of this filter not only affects the magnitude of the peak of the baseflow hydrograph, but also its timing, with larger values of C resulting in more rapid increases in the rising limb of the filtered baseflow hydrograph and vice versa. Consequently, the peak of the filtered baseflow hydrograph does not necessarily coincide with that of the streamflow hydrograph from which it is derived. This filter is passed over the data only once.

3.2.3.3 Eckhardt filter

Eckhardt (2005) developed a two-parameter algorithm based on the assumption that outflow from an aquifer is linearly proportional to its storage. The resulting equation is given by:

$$q_{b(i)} = \frac{k(1-BFI_{\max})q_{b(i-1)} + (1-k)BFI_{\max} q_{(i)}}{1-kBFI_{\max}} \qquad subject \quad to \qquad q_{b(i)} \leq q_{(i)} \tag{3.3}$$

where k is the recession constant, which is determined using the method outlined in Eckhardt (2008) in this study, and BFI_{max} is the maximum value of the baseflow index (BFI is the ratio of the volume of baseflow to the volume of total streamflow), which is the parameter obtained by calibration in this study, as the BFI is generally not known with certainty due to the difficulties associated with measuring baseflow. It should be noted that k could also be considered as a parameter to be calibrated, which would result in a multi-objective calibration problem. However, in this study, only *BFImax* is calibrated.

It is interesting to note that the Eckhardt filter is mathematically equivalent to the Boughton two-parameter filter (Eckhardt, 2005). However, as a result of the reformulation of the filter equation, the BFI_{max} parameter in the Eckhardt filter has a physical interpretation, whereas the C parameter in the Boughton filter does not. As can be seen from equation (3.3), larger values of BFI_{max} result in larger values of baseflow and vice versa. As is the case with the Boughton filter parameter, values of BFI_{max} not only affect the magnitude of the filtered baseflow hydrograph, but also its timing. The Eckhardt filter is passed over the data once.

3.2.4 Calibration and performance assessment

Various measures can be used for assessing model performance, such as the Nash-Sutcliffe coefficient of efficiency (CoE) (Nash and Sutcliffe, 1970), percent bias (*PBIAS*) (Gupta et al., 1999), least squares (Stigler, 1986) and mean square error (MSE). The CoE is one of the most widely used dimensionless metrics and has been implemented successfully in hydrologic model calibration and evaluation (Gupta and Kling, 2011; Li et al., 2013a; Moriasi et al., 2007; Partington et al., 2012). However, there have been concerns regarding the use of the CoE as a metric in the literature (Gupta et al., 2009; Legates and McCabe, 1999; McCuen et al., 2006). One of the main concerns is its use of the observed mean as a baseline, which can lead to overestimation of model skill for highly seasonal variables (Legates and McCabe, 1999). In addition, the CoE has often been criticized for varying over an unbounded range, in particular becoming negative and potentially approaching -∞ under extreme circumstances. In order to address this issue, Gupta and Kling (2011) introduced a normalized CoE (E_f) to constrain its range within [-1,1]. Detailed information of the derivation of E_f can be found in Gupta et al. (2009) and Gupta and Kling (2011). In this study, E_f is used as the error measure during the filter parameter optimization (calibration) process by adjusting the RDF parameters to be calibrated (i.e. *a* (LH), *C* (Boughton) and BFI_{max} (Eckhardt)) until the best match between the filtered baseflow hydrograph (q_b^{filter}) and the simulated baseflow hydrograph from the fully integrated SW/GW (q_b^{sim}) model is obtained. In addition, E_f is used to assess the performance of the calibrated RDFs. The equation for E_f is as follows (Gupta and Kling, 2011):

$$
\begin{aligned}
E_f &= 2 * \rho_{so} - 1 \\
\rho_{so} &= \frac{1}{n-1}\sum_{i=1}^{n}\left(\frac{q_{b(i)}^{obs} - \overline{q_b^{obs}}}{\sigma_{obs}}\right)\left(\frac{q_{b(i)}^{sim} - \overline{q_b^{sim}}}{\sigma_{sim}}\right) \qquad (3.4) \\
\sigma^2 &= \frac{1}{n}\sum_{i=1}^{n}(q_{b(i)} - \overline{q_b})^2
\end{aligned}
$$

where $q_{b(i)}^{obs}$ [L^3T^{-1}] is the simulated baseflow obtained from the HGS model using the HMC method at time step *i* [T], $q_{b(i)}^{sim}$ [L^3T^{-1}] is the baseflow derived from the RDFs at time step *i*, $\overline{q_b^{obs}}$ and $\overline{q_b^{sim}}$ [L^3T^{-1}] are the mean values of $q_{b(i)}^{obs}$ and $q_{b(i)}^{sim}$ over the *n* observations, respectively. It should be noted that in this study, only data during rainfall periods are used in the calculation of E_f, as suggested by Partington et al. (2012), as comparison between simulated and filtered baseflow is not meaningful in recession periods because the baseflow obtained using RDFs matches the simulated baseflow perfectly, due to the constraints that are part of the formulation of the RDFs. Consequently, the value of *n* varies from 1846 to 3650 in this study.

During the calibration process, the error measure is minimised by optimising the value of the filter parameter to be obtained by calibration (i.e. *a* (LH), *C*

(Boughton) and BFI_{max} (Eckhardt)) using the golden section search method (Press et al., 1992). This method is used as there is only a single parameter that requires calibration. In addition, it has been used successfully for this purpose previously (Li et al., 2013a). The E_f values of the calibrated RDFs are used to assess filter performance. As suggested by Moriasi et al. (2007), RDF performance can be judged as 'perfect' when E_f =1.0, while E_f values between 0.5 and 1.0 correspond to 'good' filter performance; E_f values between 0.0 and 0.5 show 'acceptable' filter performance and 'poor' filter performance is represented by negative values of E_f. In order to account for any uncertainties associated with the estimates of the optimal filter parameters, linear estimates of uncertainty are obtained using the procedure outlined in Li et al. (2013a). However, as the resulting errors are very small, as was the case for the analysis conducted by Li et al. (2013a), the bounds are not presented in the Results and Discussion section of this paper. In addition, multiple calibration runs from different random starting positions in parameter space are conducted in order to ensure the globally optimal solution is found. As expected for such a simple calibration problem with a single parameter, the results suggest that the error surface is smooth with a single global optimum.

It should be noted that of the 70, 10-year streamflow time series obtained by running HGS with the 70 different combinations of catchment characteristics and hydrological inputs generated by LHS, 4 result in zero flow, and are therefore excluded from the model calibration and evaluation process. Consequently, the RDF calibration and evaluation process is carried out 198 times, 66 times for each of the three RDFs investigated.

3.2.5 Development of regression models

Regression models are developed in order to predict (i) values of the optimal (calibrated) filter parameters and (ii) the performance of the calibrated RDFs (see Section 3.2.4) as a function of the catchment characteristics (Table 3.1) and ratios of R/ET (Table 3.2) considered. Individual models for optimal filter parameter prediction are developed for the three RDFs. However, only two models are developed for predicting filter performance, one for the LH filter and one for the Boughton and Eckhardt filters, as the performance of the Boughton and Eckhardt filters is the same, due to their identical mathematical formulations, as discussed previously.

Initial trials are conducted with different functional forms of regression models. Based on the results of these trials, the following underlying regression equation is adopted:

$$Y = \theta_1 lnX_1 + \theta_2 lnX_2 + ... + \theta_n lnX_n + \theta_{n+1} \quad (3.5)$$

where Y is the predicted model output (i.e. optimal values of a, C and BFI_{max} in the case of the models predicting optimal filter parameter values and E_f (LH) and E_f (Boughton/Eckhardt) for the models predicting filter performance), θ_i are the regression coefficients (model parameters), which are obtained by calibration, and X_i are the independent variables/model inputs (e.g. (R/ET), K_s, S1, S2, A). It should be noted that more flexible model structures, such as artificial neural networks (Maier et al., 2010), could not be considered in this instance as a result of the limited set of available data (i.e. 66 data points).

Two different sets of model inputs are considered. Firstly, all eight independent variables, including the seven catchment characteristics in Table 3.1 and the ratio of R/ET, are used. Secondly, a reduced number of inputs is used, as some independent variables might not have a significant impact. In addition, from a practical perspective, it might be difficult to obtain data on all eight inputs and having a smaller number of inputs might make the regression equations more easily applicable.

In order to identify the most important of the 8 potential model inputs, the partial mutual information (PMI) algorithm introduced by Sharma (2000) is used. This is because it has been found to perform well in a number of studies (Bowden et al., 2005; May et al., 2008a; May et al., 2008b). In order to strike an appropriate balance between model performance and complexity, the

Akaike Information Criterion (AIC) based stopping criterion introduced by May et al. (2008a) is used.

The results of the PMI analysis indicate that K_s and (R/ET) are the only significant inputs for all models, including the models predicting model performance and those predicting optimal filter parameter values for all RDFs. As the ratio of R/ET is a significant input for all models, two additional input sets that include Rainfall and ET as separate inputs are included, as shown in Table 3.4. This is done to check whether the inclusion of Rainfall and ET as separate inputs, rather than as a ratio, improves model performance. Consequently, four different inputs sets are used (Table 3.4). As a result, 12 regression models are developed for the prediction of the optimal filter parameters (i.e. 4 models with different inputs for each of the three RDFs) and 8 regression models are developed for the prediction of filter performance (i.e. 4 models with different inputs for the LH filter and 4 models for the Boughton/Eckhardt filters).

Table 3.4 Different input sets considered for the development of all regression models

Input Set	Number of Inputs	Inputs
1	2	(R/ET), K_s
2	3	Rainfall, ET, K_s
3	8	(R/ET), K_s, S1, S2, A, AR, α, β
4	9	Rainfall, ET, K_s, S1, S2, A, AR, α, β

All regression models are calibrated using the generalised reduced gradient algorithm implemented in Excel Solver, with E_f as the objective function.

3.3 Results and discussion

3.3.1 Simulated streamflow and baseflow

As mentioned in Section 3.2.4, of the 70, 10-year streamflow time series generated using HGS for the different catchment characteristics and hydrological inputs, 4 streamflow time series are zero, and are therefore excluded from further analysis. The maximum, median and minimum values of daily streamflow, daily baseflow and BFI for the 66 records, as well as the percentage of these records containing periods of zero flow, are shown in Table 3.5, categorised by city (i.e. hydrological inputs).

As can be seen, among these five cities, the hydrological response obtained using the Adelaide climate inputs has the lowest maximum and minimum daily streamflow and baseflow, but with the highest maximum and minimum baseflow index (BFI). Also, only the Adelaide response has some percentage of hydrographs with periods of zero streamflow (49.04%, 39.32% and 0.14% of the time). This is because the Adelaide climate data have the smallest average annual rainfall, but relatively large average annual potential ET, with a ratio of R/ET of 0.347. In addition, Adelaide has cool, rainy winters and hot, dry summers. Consequently, for simulations during periods without rainfall in summer, most of the streams have zero streamflow. However, during periods without rainfall in winter, most of the streams are fed by baseflow. Simulations subject to the Brisbane climate drivers have the highest maximum daily streamflow and baseflow, but with the smallest maximum and minimum BFI values. This is because Brisbane has the largest average annual rainfall and a ratio of R/ET of 1.078. Due to Brisbane's humid subtropical climate, more rainfall becomes direct runoff and streams have less baseflow contribution relative to total streamflow. The Sydney climate response has the second highest maximum total daily streamflow, but the largest minimum total daily streamflow and baseflow. The reason for this is that Sydney has the highest ratio of R/ET of 1.190. However, rainfall in Sydney is evenly distributed throughout the year, so that more water infiltrates into the soil and flows into the stream as baseflow, compared with other cities. Consequently, although Sydney has the highest minimum baseflow, the BFI value is relatively small.

As the results in Table 3.5 can be physically and reasonably explained based on the climate data, it is assumed that the 66 streamflow time series obtained using HGS for catchments with different catchment characteristics and hydrological inputs provide a rigorous and robust platform for determining the optimal filter parameters and assessing the overall performance of the RDFs over a wide range of conditions. In addition, HGS has been successfully used for simulating a variety of physical catchment processes by a number of researchers, as mentioned in Section 3.2.2, and has been used successfully in previous studies to simulate realistic hydrographs that cover a wide range of catchment characteristics and hydrological inputs (Li et al., 2013a; Panday and Huyakorn, 2004; Partington et al., 2012; VanderKwaak, 1999).

Table 3.5 Maximum, median and minimum daily streamflow, daily baseflow and BFI for the 66 records

City	Average Annual Rainfall (mm/a)	Average Annual Potential ET (mm/a)	R/ET	Percentage of hydrographs with periods of zero streamflow	HGS daily streamflow (q) (m^3/d)			HGS daily baseflow (q_b^{sim}) (m^3/d)			Baseflow Index (BFI)		
					Max	Median	Min	Max	Median	Min	Max	Median	Min
Adelaide*	510.2	1471	0.347	25%	33343.8	424.3	0	23712.7	357.1	0	0.9972	0.8152	0.4619
Melbourne*	525.3	911.3	0.576	0%	6042600.5	3548.2	34.2	46206.1	3286.3	34.2	0.9929	0.9171	0.1236
Darwin	1667.2	2053.4	0.811	0%	5628043.9	7713.8	0.13	148237.2	5854.9	0.13	0.9891	0.427	0.0306
Brisbane	2238.2	2077	1.078	0%	21062142.3	18569.6	11.6	374606.8	10362.6	11.6	0.9634	0.1188	0.0055
Sydney	1095.9	920.9	1.190	0%	11147679.4	18406.2	340.3	113374.8	7015.3	340.3	0.9763	0.1227	0.014

* Does not include zero streamflow time series cases

3.3.2 Optimal filter parameters

3.3.2.1 Values of optimal filter parameters

The maximum and minimum values of the calibrated filter parameters, which correspond to the low and high baseflow contributions obtained for the five different cities, as well as the corresponding values of BFI (shown in brackets), are summarised in Table 3.6. As can be seen, higher values of the calibrated LH filter parameter correspond to lower baseflow contributions and vice versa, which is as expected, based on the way the LH filter works (see Section 3.2.3). Conversely, higher values of the calibrated Boughton and Eckhardt filter parameters correspond to higher baseflow contributions and vice versa, which is also expected, based on the way the filters work (see Section 3.2.3).

It can also be seen from Table 3.6 that there is generally considerable difference between the minimum and maximum optimal filter parameter values, suggesting that use of a constant filter parameter value is inappropriate and that the optimal value of the filter parameters is a function of catchment characteristics and hydrological inputs. It should be noted that in some instances for the Boughton and LH filters, the same optimal filter parameter values are obtained for a range of BFI values (as indicated by the ranges in BFI values in Table 3.6), suggesting that the parameters might not be as well defined at the extreme ranges. However, the same does not apply to the Eckhardt filter. Actually, the fact that the value of the Eckhardt filter parameter (*BFImax*) is better defined for different values of BFI is not surprising, given that the Eckhardt filter was designed so that there is a close correspondence between the value of the filter parameter, which corresponds to BFImax, and BFI. The strong relationship between the Eckhardt BFImax filter parameter and BFI can be observed from the values in Table 3.6 and Figure 3.4.

Table 3.6 Maximum and minimum optimal values of filter parameters corresponding to high and low flows and the corresponding value of BFI (shown in brackets)

City	Baseflow	LH	Boughton	Eckhardt
		a	C	BFI_{max}
Adelaide	Low	0.945 (0.462)	0.024 (0.462)	0.549 (0.462)
	High	0.0001 (0.981-0.997)	3.97 (0.982)	0.999 (0.997)
Melbourne	Low	0.997 (0.124)	0.0006 (0.124)	0.126 (0.124)
	High	0.0001 (0.946-0.977)	1.302 (0.947)	0.994 (0.993)
Sydney	Low	0.996 (0.014)	0.0001 (0.014-0.046)	0.015 (0.014)
	High	0.555 (0.973)	0.158 (0.973)	0.979 (0.973)
Brisbane	Low	0.997 (0.002)	0.0001 (0.002-0.013)	0.0013 (0.002)
	High	0.419 (0.963)	0.190 (0.963)	0.968 (0.963)
Darwin	Low	0.998 (0.031)	0.0002 (0.031)	0.028 (0.031)
	High	0.0001 (0989)	0.581 (0.989)	0.993 (0.989)

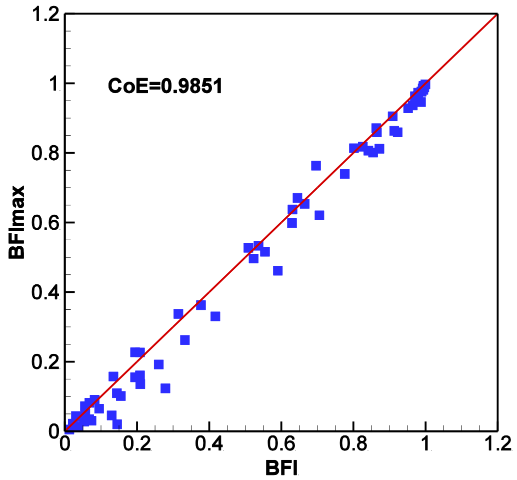

Figure 3.4 Scatter plot of BFI and Eckhart *BFImax* filter parameter

3.3.2.2 Prediction of optimal filter parameter values

The predictive performance of the 12 regression models for the prediction of optimal filter parameters in terms of CoE is summarised in Table 3.7 and the resulting equations and scatter plots of actual versus predicted values of optimal filter parameters for the best models with the lower (i.e. 2 or 3) and higher (i.e. 8 or 9) number of inputs are given in Figure 3.5.

As can be seen from Table 3.7, the optimal parameters of both the LH and Eckhardt filters can be predicted very well, with CoE values ranging from 0.65 to 0.78 and 0.77 to 0.91, respectively, for the four models with different inputs. In contrast, the predictability of the optimal Boughton filter parameter is significantly worse, with CoE values ranging from 0.24 to 0.38. The marked difference in the predictability of the optimal Boughton and Eckhardt filter parameters is interesting, given that both filters are equivalent from a mathematical perspective. However, it appears as though the Eckhardt formulation, in which the filter parameter has an explicit physical meaning (i.e. BFI_{max}), makes it much easier to be predicted based on catchment characteristics and hydrological inputs. While both the optimal LH and Eckhardt filter parameters can be predicted very well, the predictability of the Eckhardt filter is consistently better for all four models with different inputs, which is likely to be due to the physical meaning that can be attributed to the Eckhardt filter parameter, as discussed previously.

Table 3.7 Predictive performance (CoE) of regression models for the prediction of optimal filter parameter values

Input Set	LH	Boughton	Eckhardt
1	0.65	0.24	0.772
2	0.67	0.25	0.81
3	0.76	0.37	0.87
4	0.78	0.38	0.91

The results in Table 3.7 also show that using rainfall and ET as separate inputs, rather than a ratio (i.e. R/ET), improves model performance, both for the models with the small number of inputs selected using the PMI algorithm (i.e. Input Sets 1 and 2) and the models with all inputs (i.e. Input Sets 3 and 4). Consequently, the regression equations and scatter plots for the models using Input Sets 2 and 4 are given in Figure 3.5.

The scatter plots in Figure 3.5 confirm that the optimal Eckhardt filter parameter (BFI_{max}) can be predicted very well, that the optimal LH filter parameter can be predicted reasonably well and that the optimal Boughton filter parameter (C) is difficult to predict. In general, lower values of the optimal values of all three filter parameters are over-predicted, while larger values are under-predicted. The under-prediction of larger filter parameter values is particularly pronounced for the Boughton filter. The scatter plots and CoE values also indicate that while the majority of the variance in the data is captured by the three inputs identified as significant by the PMI algorithm, there is a reasonable improvement in predictive ability when all inputs are included. However, this increased accuracy is at the expense of increased model complexity, and a balance between the two has to be struck, which is what the AIC stopping criterion used as part of the PMI algorithm is trying to achieve. In practice, the more complex model is likely to be more difficult to apply, as some of the required input information (e.g. catchment slopes and values of van Genuchten parameters) might be difficult to obtain and is generally not uniform over the catchment.

As can be seen from the regression equations in Figure 3.5, the signs of the coefficients of the majority of the input variables are in opposite directions for the LH and Boughton/Eckhardt filters. This is as expected, as large values of the filter parameters for the LH and Boughton/Eckhardt filters have the opposite effect on baseflow magnitude (i.e. for the LH filter, large values of the filter parameter result in small baseflow contributions, while the opposite applies to the Boughton and Eckhardt filters) (see Section 3.2.3). In general, the signs (i.e. positive and negative) of the coefficients are in agreement with the underlying physics. The two exceptions are the signs of the coefficients for β and S2 for the Eckhardt filter, which are the same as those for the LH filter and opposite to those for the Boughton filter.

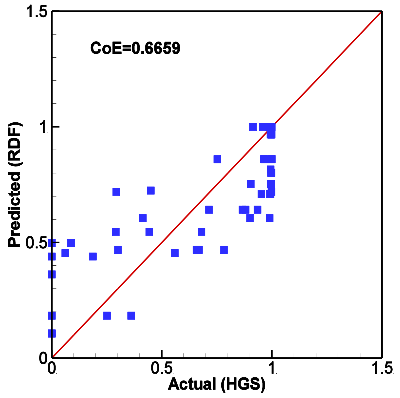

a=-0.168ln(K_s)+0.37ln(rainfall)-0.139ln(ET)-2.353

(a) LH *a* Parameter (Input Set 2)

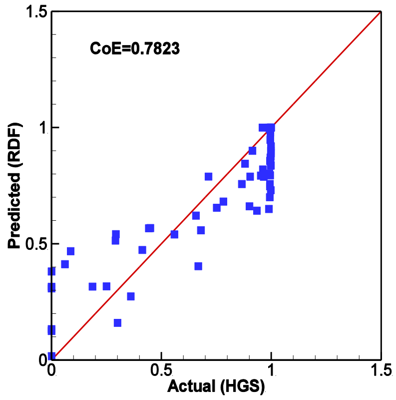

a=-0.178ln(K_s)+0.033ln(α)-0.049ln(β)+0.062ln(A)-0.105ln(S1)+0.107ln(S2)+0.138ln(AR)+0.331ln(rainfall)-0.0791ln(ET)-2.783

(b) LH *a* Parameter (Input Set 4)

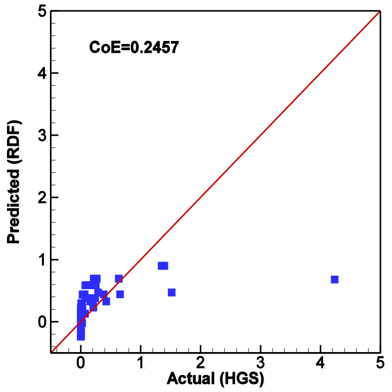

C=0.145ln(K_s)-0.502ln(rainfall)+0.404ln(ET)+2.09

(c) Boughton *C* Parameter (Input Set 2)

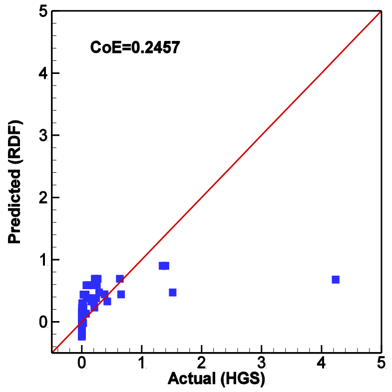

C=0.148ln(K_s)-0.208ln(α)+0.324ln(β)+0.002ln(A)+0.027ln(S1)-0.209ln(S2)-0.027ln(AR)-0.545ln(rainfall)+0.488ln(ET)+0.958

(d) Boughton *C* Parameter (Input Set 4)

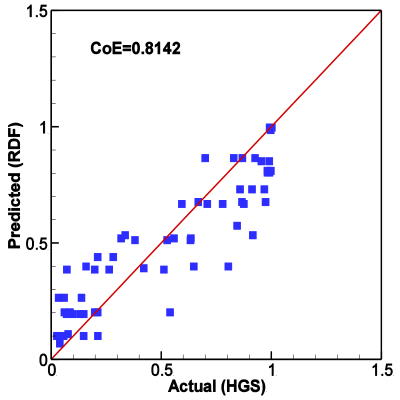

BFI_{max}=0.191ln(K_s)-0.465ln(rainfall)+0.252ln(ET)+3.662

(e) Eckhardt BFI_{max} Parameter (Input Set 2)

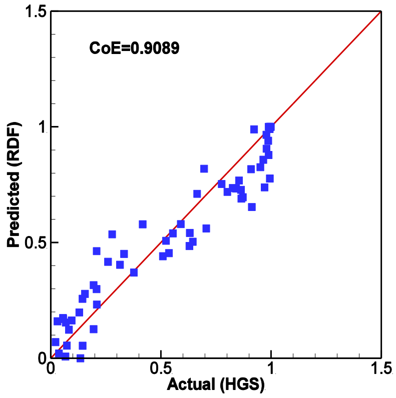

BFI_{max}=0.175ln(K_s)-0.002ln(α)-0.054ln(β)-0.048ln(A)+0.19ln(S1)+0.114ln(S2)-0.129ln(AR)-0.408ln(rainfall)+0.179ln(ET)+5.33

(f) Eckhardt BFI_{max} Parameter (Input Set 4)

Figure 3.5 Regression models for the prediction of optimal filter parameter values using input sets 2 and 4

3.3.3 Filter performance

3.3.3.1 Assessment of filter performance

The performance of the three filters in terms of their ability to match the baseflow hydrograph obtained using HGS for the 66 cases investigated is given in Table 3.8 and Figure 3.6 in terms of E_f. The results are split into three categories, including good filter performance (i.e. $E_f \geq 0.5$), acceptable filter performance (i.e. $0 < E_f < 0.5$) and poor filter performance (i.e. $E_f \leq 0$). It should be noted that the same performance was obtained for the Boughton and Eckhardt filters, as they are mathematically equivalent. Consequently, combined results are presented for these two filters. As can be seen from Table 3.8 and Figure 3.6, the overall performance of the LH filter is better than that of the Boughton and Eckhart filters. It results in good performance in 77.3% of cases, compared with 53.0% of cases for the Boughton and Eckhart filters, and in poor performance in 10.6% of cases, compared with 16.7% for the Boughton and Eckhart filters.

In general, the performance of both filters deteriorates for smaller values of simulated HGS baseflow (see Section 3.1.3.2). However, the performance of the Boughton and Eckhardt filters deteriorates more quickly as baseflow decreases. This is because of the different way in which the filter parameters affect the magnitude and shape of the resulting baseflow hydrographs. When the LH filter is used, the timing of the peak of the baseflow hydrograph generally coincides with that of the streamflow hydrograph. However, this is not the case for the Boughton and Eckhardt filters, where the value of the filter parameter affects both the magnitude and timing of the baseflow hydrograph. As can be seen from equations (3.2) and (3.3), the filter parameters affect the rate of rise of the rising limb of the baseflow hydrograph. Consequently, if the magnitude of the peak of the HGS simulated baseflow is small, the values of the filter parameters also have to be small in order to match the peak as best as possible. However, small values of the filter parameters also result in a small rate of rise in the rising limb of the baseflow hydrograph, resulting in a mismatch in the timing of the HGS simulated peak of the baseflow hydrograph and that obtained using the Boughton and

Eckhardt filters in some instances. However, if the value of the filter parameter is increased in order to ensure the timing of the peak is correct, the peak will be overpredicted. Consequently, there appears to be a tradeoff between being able to match the timing and magnitude of the baseflow hydrograph when using the Boughton and Eckhardt filters for catchments with small baseflow contribution. The same problem does not appear to exist with the LH filter.

Table 3.8 Performance of LH and Eckhardt/Boughton filters

Filter Performance	E_f	LH	Bougthon & Eckhardt
Good	≥0.5	77.3%	53.0%
Acceptable	>0&<0.5	12.1%	30.3%
Poor	≤0	10.6%	16.7%

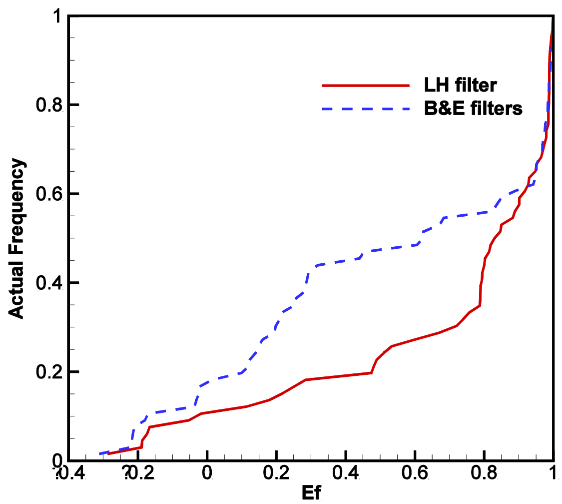

Figure 3.6 Plot of cumulative distribution functions of E_f values for the different RDFs investigated

3.3.3.2 Prediction of filter performance

The predictive performance of the 8 regression models for the prediction of model performance is summarised in Table 3.9 and the resulting equations and scatter plots of actual versus predicted values of optimal filter parameters for the best models with the lower (i.e. 2 or 3) or higher (i.e. 8 or 9) number of inputs are given in Figure 3.7.

As can be seen from Table 3.9, the performance of all RDFs can be predicted quite well, with all CoE values ranging from 0.70 to 0.82 for the LH filter and from 0.60 to 0.76 for the Boughton and Eckhart filters. The results in Table 3.9 show that using rainfall and ET as separate inputs, rather than a ratio, improves model performance, both for the models with the small number of inputs selected using the PMI algorithm (i.e. Input Sets 1 and 2) and the models with all inputs (i.e. Input Sets 3 and 4). Consequently, the regression equations and scatter plots for the models using Input Sets 2 and 4 are given in Figure 3.7.

Table 3.9 Predictive performance (CoE) of regression models for the prediction of optimal filter performance (in terms of E_f)

Input Set	LH	Boughton & Eckhardt
1	0.70	0.60
2	0.71	0.69
3	0.81	0.73
4	0.82	0.76

The scatter plots shown in Figure 3.7 confirm that the performance of all three filters can be predicted quite well and that model performance can be improved by the inclusion of all inputs, which is confirmed by the CoE values. However, as was the case for the models for the prediction of the optimal filter parameters, this increased accuracy is at the expense of increased model complexity, and a balance between the two must be arrived at, depending on input data availability and required model accuracy.

It should be noted that from a practical perspective, the primary purpose of the models predicting filter performance would most likely be an assessment of the suitability of a particular filter for the catchment characteristics and hydrological inputs under consideration. Consequently, it is not so much the actual performance value that is of interest, but whether filter performance is likely to be good (i.e. $E_f \geq 0.5$) or not (i.e. $E_f < 0.5$). Such an assessment for the models with Input Sets 2 and 4 is provided for the different filters in

Table 3.10. As can be seen, when the models with all inputs are used, the performance of the LH and Boughton/Eckhardt filters are classified correctly

as either good or not in 96.1% and 94.3% of cases, respectively. The value of 96.1% drops to 94.1% for the LH filter when only 3 inputs are used. However, the drop in performance when only 3 inputs are used, compared with 9 inputs, is more marked for the Boughton/Eckhardt filters, where the percentage of correct classification drops from 94.1% to 85.7%.

As can be seen from the regression equations in Figure 3.7, all of the signs of the coefficients of the input variables are in the same directions for the LH and Boughton/Eckhardt filters. This is as expected, as large values of E_f have the same effect on the overall performance for the LH and Boughton/Eckhardt filters (i.e. large values of E_f result in better performance for the LH and Boughton/Eckhardt filters), as discussed above. Therefore, the signs of the coefficients are in agreement with the underlying physics. For catchments with high baseflow contribution, all three RDFs can estimate baseflow quite well, with higher values of E_f.

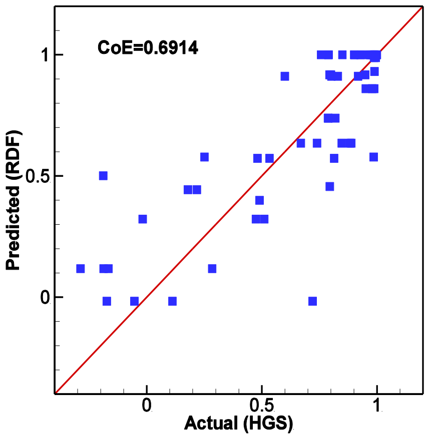

E_f_LH=0.273ln(K_s)-0.64ln(rainfall)+0.979ln(ET)+0.685

(a) LH Filter Performance (Input Set 2)

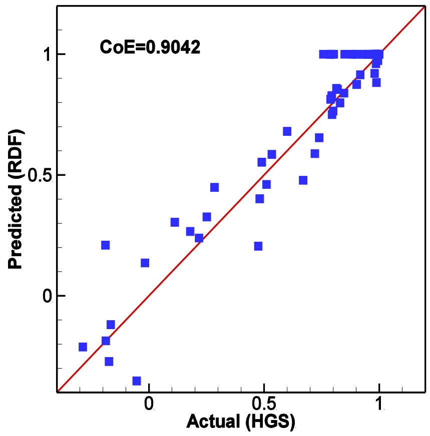

E_f_LH=0.303ln(K_s)-0.129ln(α)-0.202ln(β)-0.17ln(A)+0.015ln(S1)+0.173ln(S2)-0.0004ln(AR)-0.699ln(rainfall)+1.118ln(ET)+2.409

(b) LH Filter Performance (Input Set 4)

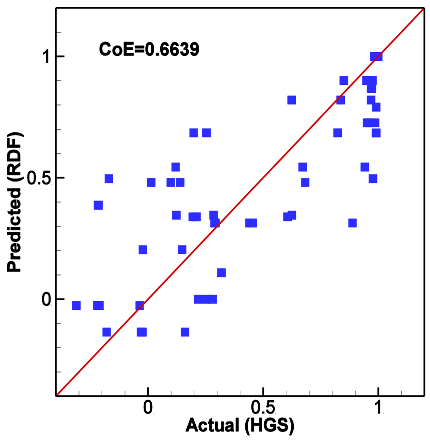

E_f_B&E=0.223ln(K_s)-0.722ln(rainfall)+0.8ln(ET)+1.827

(c) Boughton and Eckhardt Filter Performance (Input Set 2)

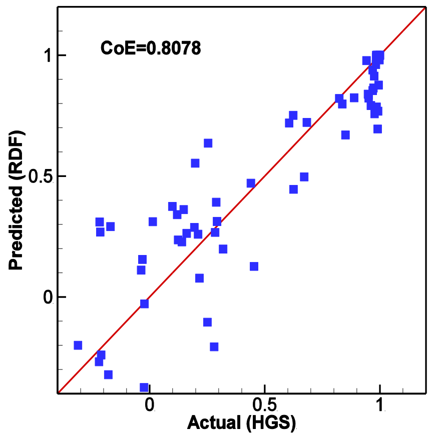

E_f_B&E=0.226ln(K_s)-0.064ln(α)-0.121ln(β)-0.125ln(A)+0.11ln(S1)+0.145ln(S2)-0.089ln(AR)-0.687ln(rainfall)+0.744*ln(ET)+3.943

(d) Boughton and Eckhardt Filter Performance (Input Set 4)

Figure 3.7 Regression models for the prediction of optimal filter performance (in terms of E_f) using input sets 2 and 4

Table 3.10 Percentage of correct prediction of good filter performance (i.e. Ef ⩾0.5) using the regression models

Input Set	LH	Boughton & Eckhardt
2	94.1	85.7
4	96.1	94.3

3.3.4 Practical implications

From a practical perspective, the regression models developed in this research might be able to be used to assess whether use of a particular RDF is suitable for the catchment characteristics and hydrological inputs under consideration and if so, to determine what filter parameter value should be used. The procedure for achieving this is given in Figure 3.8 and described below.

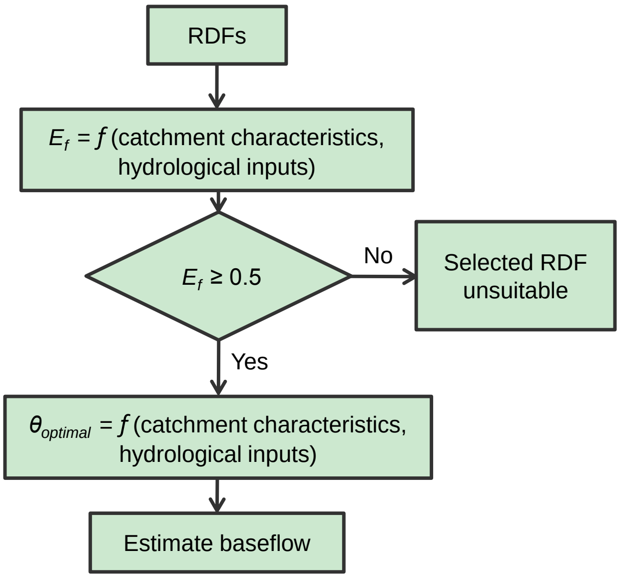

Figure 3.8 Procedure for checking filter suitability and estimation of optimal filter parameter values

Procedure:

Use the appropriate regression model to determine whether a particular RDF will be a good predictor of baseflow or not (i.e. if $E_f \geq 0.5$ or not). Two different models can be used for this purpose, depending on the amount of information available and the desired level of accuracy. The simpler model only requires rainfall, ET and K_s as inputs, whereas the more complex model also requires information on catchment area, hillslope, channel slope, aspect ratio and van Genuchten parameters α and β.

If E_f <0.5, the selected RDF is not suitable to be used, as the filtered baseflow obtained is likely to provide a poor estimate of actual baseflow. Other RDFs or baseflow estimation methods should be tried.

If $E_f \geq 0.5$, the selected RDF can be used, as the filtered baseflow obtained is likely to provide a good estimate of actual baseflow.

If the RDF can be used, the optimal value of the filter parameter can be estimated using the corresponding regression equation and the RDF used for baseflow estimation.

Given that the predictive performance of the Eckhardt and Boughton filters is equivalent and that the optimal filter parameter can be estimated much more easily for the former, the Boughton filter is least preferred. Consequently, of the RDFs considered in this research, the choice will be between the LH and Eckhardt filters. In addition, compared with the Eckhardt filter, the LH filter is likely to be suitable for a wider range of conditions. However, if both filters are found to be suitable, the Eckhardt filter should probably be used, as its optimal filter parameter value can be estimated with greater accuracy. In addition, given the strong correlation between BFI and the optimal values of the *BFImax* parameter in the Eckhart filter (Figure 3.4), the regional relationships between catchment characteristics and BFI developed in other studies (e.g. Lacey and Grayson, 1998; Longobardi and Villani, 2008; Mazvimavi et al., 2005; Mwakalila et al., 2002) can also be used to obtain the optimal filter parameter for the Eckhart filter, making it more widely applicable.

However, it should be noted that the results obtained are a function of the adopted error measure, the conceptualisation of the underlying physical processes used in HGS, as well as the range of conditions tested. While the number of physical catchment characteristics and hydrological inputs investigated is larger than that used in Li et al. (2013a), it is by no means exhaustive. Consequently, there is a need to test the robustness of the results obtained under a wider range of conditions, such as such as heterogeneity of catchment properties and hydrological inputs, more complex catchment geometries, non-uniform slopes, different climates etc., before they can be applied with any degree of confidence.

3.4 Summary and conclusions

The estimation of baseflow is important in many environmental and water resources settings. Recursive Digital Filters (RDFs) are a commonly used method for achieving this, as they are quick and simple to implement. However, due to the difficulties in measuring baseflow in the field, it is not possible to assess the accuracy of these RDFs, nor is it possible to determine the most appropriate values of the parameters that control RDF output, based on measured data. In order to overcome this shortcoming, the baseflow extracted from the outputs of a fully integrated surface water/groundwater (SW/GW) model using the HMC method are used to obtain optimal filter parameter values by calibration and as a benchmark against which to assess RDF performance. This is done for a synthetic catchment with 70 combinations of different catchment characteristics (e.g. saturated hydraulic conductivity (K_s), catchment area, aspect ratio, slopes, van Genuchten parameters) and hydrologic inputs (e.g. rainfall and evapotranspiration (ET)) obtained using Latin hypercube sampling (LHS). HydroGeoSphere (HGS) is used as the fully integrated SW/GW model and the calibration and assessment procedure is applied to three different RDFs, including the Lyne and Hollick (LH), Boughton two-parameter and Eckhardt filters. It is recognised that the baseflow generated using HGS is only an approximation to reality, but given that HGS represents physical processes explicitly, this is very likely to be the best approximation to reality that we have at present.

The outputs from the RDF calibration and performance assessment procedures are used to develop regression models predicting RDF performance (i.e. how well each RDF can predict the HGS generated baseflow) and optimal values of the filter parameters (i.e. the calibrated values of the filter parameters that result in the best match between RDF and HGS generated baseflow) as a function of the different catchment characteristics and hydrological inputs investigated. Models are developed that use all, as well as a subset, of the catchment characteristics and hydrological values considered as inputs. The subset of the most significant inputs is obtained using a partial mutual information (PMI) input selection procedure and results in the selection of only two inputs, including the ratio of rainfall/ET and K_s, indicating that these factors have the biggest influence on both filter performance and the optimal values of the filter parameters.

The results obtained show that the values of the optimal filter parameters vary significantly as a function of catchment characteristics and hydrological input, with rainfall, K_s and ET having the largest influence, as mentioned above. This variation is able to be predicted very well for the LH (CoE=0.78) and Eckhardt (CoE=0.94) filters using the regression models. However, the models are less successful in predicting optimal values of the Boughton filter parameter, with CoE=0.38. The difference in the predictability of the Boughton and Eckhardt filter parameters is despite the fact that both filters produce equivalent outputs. The likely reason for this is that the filter parameter in the Eckhardt formulation has a physical meaning (i.e. BFI_{max}), and is therefore more likely to be a function of physical catchment characteristics and hydrological inputs than the filter parameter in the Boughton formulation, which does not have any physical meaning.

The results also indicate that the LH filter is able to better match the HGS derived baseflow than the other two filters, the performance of which is equivalent. Over the 66 trials included in the analysis, the LH filter performs well (i.e. E_f >0.5) 77.3% of the time and poorly (i.e. $E_f \leq 0$) 10.6% of the time. In contrast, the Boughton/Eckhardt filters result in good and poor performance 53.0% and 16.7% of the time, respectively. The regression models are able to predict the performance (in terms of E_f) of all three RDFs very well, with CoE values of 0.82 and 0.76 for the models predicting the performance of the LH and Boughton/Eckhardt filters, respectively. Again, the ratio of rainfall/ET and K_s have the largest influence, as mentioned above.

The ability of the regression models to provide good predictions of filter performance and optimal filter parameters has potential practical applications. For example, the models predicting model performance can be used to assess whether the use of a particular filter is suitable, given the catchment characteristics and hydrological inputs considered. If use of a particular filter is considered adequate (e.g. if the value of E_f predicted using the regression model >0.5), then the optimal value of the filter parameter can be predicted using the appropriate regression model. Given that the output, and hence performance, of the Boughton and Eckhardt filters is equivalent and that the optimum Eckhardt filter parameter can be predicted with more accuracy, the Eckhardt filter should be used in preference to the Boughton two-parameter filter in practice. In addition, the Eckhart filter is likely to be more widely applicable than the other two filters, as regional relationships between catchment characteristics and BFI, which is strongly related to optimal values of the optimal filter parameters for the Eckhart filter, have been developed in previous studies (e.g. Lacey and Grayson, 1998; Longobardi and Villani, 2008; Mazvimavi et al., 2005; Mwakalila et al., 2002).

One limitation of using the regression models for determining whether use of a particular filter is appropriate or not, and for determining values of the optimal filter parameters, is that they require input information on the seven catchment characteristics, as well as rainfall and ET, some of which might be difficult to obtain, especially representative values of parameters that are spatially heterogeneous. However, the models that only use rainfall, ET and K_s as inputs perform only marginally worse than the models using all 9 input variables and might therefore be easier to use in practice.

The performance of the Boughton/Eckhardt filter could possibly be improved further by also considering the recession constant as a parameter to be calibrated. However, this might make estimation of the optimal filter parameters more complicated. It would also be interesting to assess the impact of spatial variability in catchment characteristics and hydrological input on the performance of the regression relationships developed in this research. However, given that RDFs are currently applied without any knowledge of their likely accuracy, nor any knowledge of how to select appropriate values of the filter parameters, the predictive relationships presented in this paper provide a first step towards maximising filter performance and increasing confidence in the accuracy of the baseflow obtained using RDFs. Consequently, it would be useful to develop such relationships for other RDFs.

Finally, it must be acknowledged that results and conclusions are based on the outputs from a model that was run under a limited number of catchment and hydrological conditions. Consequently, the robustness and generality of the results need to be tested under a wider range of model conceptualisations, catchment characteristics and hydrological inputs and, where possible, using actual data.

3.5 Acknowledgement

This research was supported by the Chinese Scholarship Council (CSC) and the University of Adelaide. The authors also gratefully thank the three anonymous reviewers for their detailed comments, which have greatly improved the quality of the paper.

Chapter 4

4 Assessment of the internal dynamics of the Australian Water Balance Model under different calibration regimes (Paper 3)

Statement of Authorship

Title of Paper	Assessment of the Internal Dynamics of the Australian Water Balance Model under Different Calibration Regimes
Publication Status	○ Published ○ Accepted for Publication ● Submitted for Publication ○ Publication Style
Publication Details	Li, L., Lambert, M.F., Maier, H.R., Partington, D., Simmons, C.T., 2013. Assessment of the Internal Dynamics of the Australian Water Balance Model under Different Calibration Regimes. Environmental Modelling & Software Submitted.

Author Contributions

By signing the Statement of Authorship, each author certifies that their stated contribution to the publication is accurate and that permission is granted for the publication to be included in the candidate's thesis.

Name of Principal Author (Candidate)	Li Li		
Contribution to the Paper	Developed and implemented the methodology, designed numerical experiments, interpreted and analysed results, prepared manuscript.		
Signature		Date	01/03/2013

Name of Co-Author	Martin Lambert		
Contribution to the Paper	Supervised manuscript preparation and reviewed draft.		
Signature		Date	1/3/13

Name of Co-Author	Holger Maier		
Contribution to the Paper	Supervised manuscript preparation and reviewed draft.		
Signature		Date	1/3/13

Name of Co-Author	Daniel Partington		
Contribution to the Paper	Assisted with running models and analysing results, reviewed draft and supervised manuscript preparation.		
Signature		Date	1/03/2013

Name of Co-Author	Craig Simmons		
Contribution to the Paper	Supervised research and reviewed draft.		
Signature		Date	1/3/13

Name of Co-Author			
Contribution to the Paper			
Signature		Date	

Name of Co-Author			
Contribution to the Paper			
Signature		Date	

Please cut and paste additional co-author panels here.

Abstract

Conceptual rainfall runoff models (CRRs) are used extensively in practice, as they provide a good balance between transparency on one hand and computational and data requirements on the other. However, even though such models are based on a conceptual representation of the principal physical processes affecting rainfall and runoff, the degree to which these processes are captured by the model structure and calibrated model parameters is not well understood. This is because the performance of such models is generally assessed based on their ability to match total streamflow hydrographs, rather than how well they match component processes, such as baseflow and quickflow. In this paper, the ability of the Australian Water Balance Model (AWBM), which is a commonly used CRR, to represent baseflow and quickflow is assessed for 66 synthetic catchments with different physical characteristics and hydrological inputs under seven calibration regimes that consider internal model dynamics during the calibration process in different ways . The "observed" total-, base- and quick-flow hydrographs for these catchments are generated using the fully integrated surface water/groundwater (SW/GW) model Hydrogeosphere (HGS) under the assumption that such models provide a realistic representation of the underlying physical processes. The results obtained indicate that while AWBM is generally able to match total streamflow hydrographs very well, the same does not apply to baseflow and quickflow, hydrographs, suggesting that these processes are not represented particularly well by AWBM. Consideration of the internal model dynamics during the calibration process results in some improvements in the representation of baseflow and quickflow.

4.1 Introduction

Modelling approaches for estimating runoff from rainfall and evapotranspiration (ET) can be broadly classified into three types: black box models, physical process based models and conceptual rainfall runoff (CRR) models (Beven, 2005). While all of these approaches have been shown to be able to predict total streamflow successfully, the degree to which they are able to represent underlying streamflow generating mechanisms is highly variable.

Black box modelling approaches, such as artificial neural networks (Maier et al., 2010), are at one end of the spectrum while physically based approaches are at the other end. Black box models produce streamflow outputs solely as a function of their inputs and transfer characteristics without any knowledge or understanding of the underlying physical processes, but they are generally computationally efficient and can be developed using limited data. Physically based approaches attempt to simulate the detailed mechanisms of the component physical processes within the hydrologic cycle using well-established physical laws, with numerical solutions of the mathematical representation of these processes (Jayatilaka et al., 1998). Such approaches include fully integrated surface water/ground water (SW/GW) models, such as InHM (VanderKwaak and Loague, 2001), MODHMS (HydroGeoLogic, 2000), HydroGeoSphere (HGS) (Therrien et al., 2009) and SHE (Abbott et al., 1986). However, there are problems with the application of these models in practice due to the difficulties and expense associated with obtaining the data required (e.g. due to limitations of existing instrumentation and intrinsic uncertainty in the measurements), their high computational demands, as well as the inability to derive the formation from first principles.

CRR models represent a compromise between the high data and computational requirements of physical process based models and the lack of transparency of black-box models. They are more computationally efficient and less data intensive than process based models, as they do not attempt to represent all physical processes explicitly. However, they are more transparent than black-box models, as they represent the underlying physical processes in a conceptual manner, generally in the form of a number of interconnected storages that are linked with empirical mathematical equations to conceptualise the movement of water into, between and out of a catchment. Many different CRR models have been proposed in the literature, such as the Australian Water Balance Model (AWBM) (Boughton, 1993, 2004), the Soil Moisture and Accounting Model (SMAR) (Tuteja and Cunnane, 1999), SIMHYD (Chiew et al., 2002) and GR4J (Oudin et al., 2005), for example.

Among the different rainfall-runoff modelling approaches mentioned above, CRR models are the most widely utilized in practice, due to their relatively simple structure, small number of parameters and production of reasonable results. A common feature of CRR models is that most of their model parameters have no direct physical interpretation and are not directly measurable (Delleur, 1982; Troutman, 1985), due to the fact that many complex catchment physical processes are lumped together. Therefore, CRR model parameters are generally estimated by calibration, by comparing the modelled total streamflow time series to the corresponding observed data until a good fit has been obtained. Most of the time, this fit is measured using a single objective function, which generally aggregates the time-series residuals over the whole calibration period. Significant research effort has been directed towards obtaining a well-defined optimal parameter set, including local-type direct search optimisation methods and globally based optimisation methods (Duan et al., 1992). However, because CRR models are usually calibrated using only observed total streamflow time series, while internally they calculate a number of additional states and fluxes, such as baseflow and quickflow, there may be many combinations of parameter values that give similar objective function values. This phenomenon is called 'equifinality' (Beven, 1993), and is caused by problems such as over-parameterisation of models, data limitations and structural faults in the model. As a result, even though the structure of CRR models is based on a conceptual representation of underlying physical processes, how well these processes are represented by calibrated models is generally unknown, as a good match to total streamflow does not necessarily mean that the component processes are being modelled accurately. For example, similar total streamflow time series can be obtained with very different combinations of baseflow and quickflow.

While there have been many studies comparing the performance of CRR models (Ferket et al., 2010; Knapp et al., 1991; Post et al., 2007; Ranatunga et al., 2008) using total streamflow time series, very few attempts have been made to use baseflow or quickflow estimates for CRR model internal dynamic performance assessment, due to the difficulty of accurately measuring baseflow or quickflow in the field (Dukic, 2006; McCallum et al., 2010). Recently, Ferket et al. (2010) used baseflow estimated from a physically-based digital filter (Furey and Gupta, 2001) to validate the internal dynamics of two CRR models (HBV and PDM) for a subcatchment of the Dender catchment in Belgium. As part of the study, two optimisation algorithms (SCE-UA and MWARPE) were used to calibrate the models by matching total streamflow to observations. They concluded that no clear picture emerged of which model produced the best results of simulating total streamflow, but that the MWARPE calibration algorithm and the HBV model led to the best baseflow estimates, giving the best internal model dynamics, at least when compared with the results obtained using the Furey and Gupta filter.

This study builds on the research by Ferket et al. (2010) by assessing (i) how well the Australian Water Balance Model, which is a commonly used CRR, is able to represent total-, base- and quick-flow for 66 synthetic catchments with different catchment characteristics and hydrological inputs and (ii) the impact of seven different calibration regimes that take internal model dynamics into account in different ways on the accuracy of total-, base- and quick-flow hydrograph prediction. While the methodology is illustrated for this particular case study, its generic nature means it could easily be adapted and applied to other CRR models around the world. The remainder of this paper is organized as follows. The methodology is given in Section 4.2, followed by the results and discussion in Section 4.3 and summary and conclusions in Section 4.4.

4.2 Methodology

The underlying premise of the proposed method for assessing the internal dynamic performance of AWBM under a range of calibration approaches is that a fully integrated SW/GW model can simulate all of the hydrological processes within a catchment, such as the partitioning of rainfall into different components, including overland flow, streamflow, evaporation, infiltration and recharge, as well as subsurface discharge to surface water features (e.g. lakes and streams), in a physically realistic fashion (Therrien et al., 2009). This is a generally accepted assumption, as these models typically represent 3D variably saturated subsurface flow with the Richards' equations, and 1D and 2D surface flow with the diffusion wave approximation to the St. Venant equations. All of the governing flow equations implemented by the fully integrated SW/GW model are solved simultaneously to obtain reasonably accurate estimates of total streamflow, which can be used to calibrate AWBM, and baseflow and quickflow, which can be used to assess and improve the performance of the internal dynamics of AWBM (e.g. whether flow components that make up total streamflow are predicted accurately).

The steps in the methodology adopted for assessing the internal dynamic performance of AWBM are given in Figure 4.1. As shown, initially synthetic total streamflow (q_T^{obs}), baseflow (q_B^{obs}) and quickflow (q_Q^{obs}) hydrographs are generated using a fully integrated SW/GW model for a number of catchments with different physical properties and hydrological inputs in order to ensure the results are as generic as possible. Next, AWBMs are developed for the same catchments by using the same hydrological inputs, but different calibration methods. Finally, the performance of the AWBMs calibrated using the different methods is compared in terms of their ability to predict total-, base- and quick-flow hydrographs accurately. Details of each step in the methodology are given in subsequent sections.

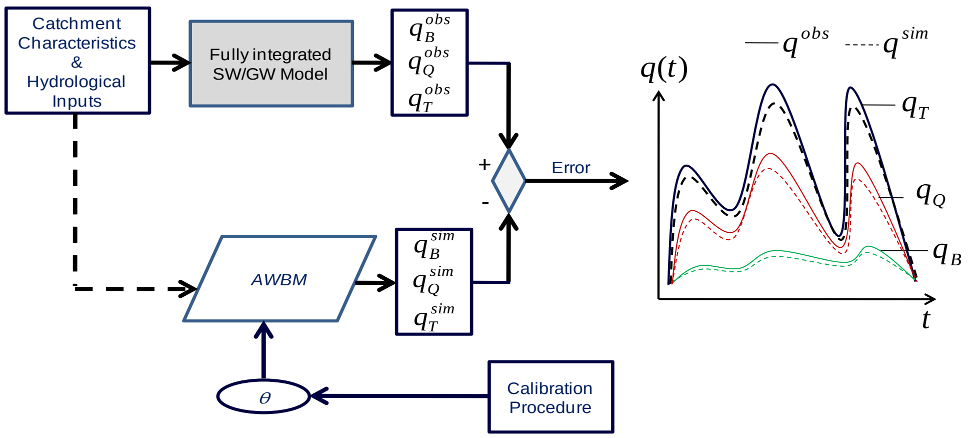

Figure 4.1 Schematic representation of steps in the proposed methodology

4.2.1 Catchment characteristics and hydrological inputs

In this study, the 66 synthetic catchments with different physical characteristics and hydrological inputs developed by (Li et al., 2013a) are used. These catchments have drainage areas ranging from 6 to 192 km^2 and are loosely based on a benchmarked integrated surface-subsurface hydrology problem, the V-catchment test case as shown in Figure 4.2 (Panday and Huyakorn, 2004). A detailed description of these catchments can be found in Li et al. (2013b), thus only a brief overview is provided here. Different physical catchment characteristics are represented using seven variables: catchment area (A), catchment hill slope (S1, which is perpendicular to the channel), catchment channel slope (S2, which is parallel to the channel), catchment aspect ratio (AR), and soil type, which includes K_s and van Genuchten parameters α and β. The hydrological inputs are represented using the ratio of daily rainfall to ET from five Australian cities (Li et al., 2013b), which are obtained from the Australian Bureau of Meteorology National Climate Centre. Details of the different values of the physical catchment characteristics considered are given in Table 4.1 and the characteristics of the hydrological inputs used are given in Table 4.2. Li et al. (2013b) used Latin Hypercube Sampling (LHS) to generate the 66 catchments with different physical catchment characteristics and hydrological inputs used in this study by sampling from these catchment characteristics and hydrological inputs.

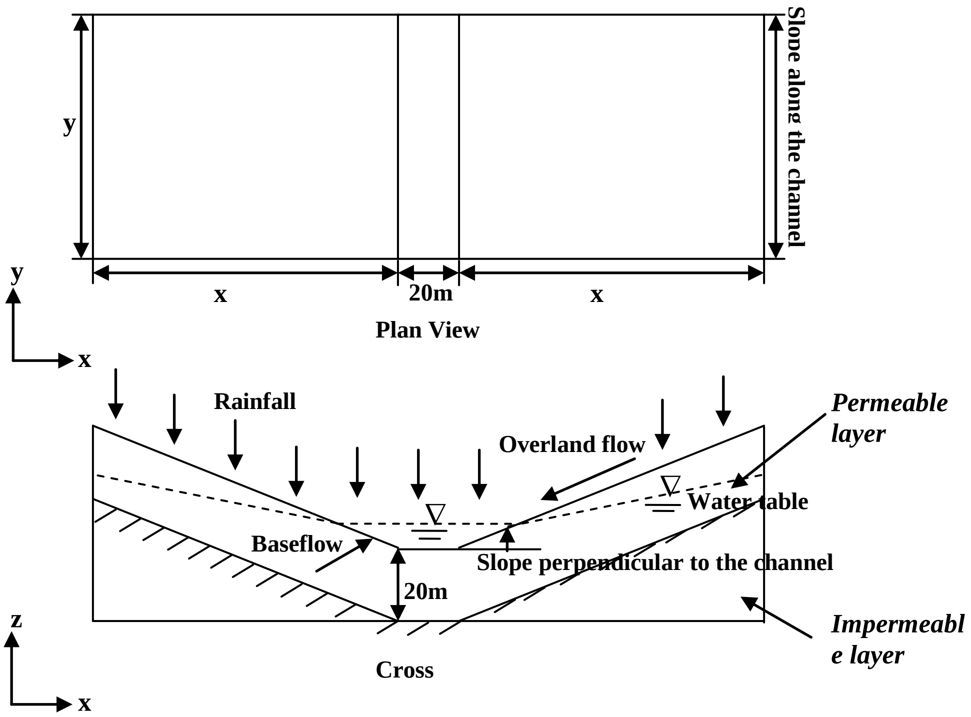

Figure 4.2 Schematic representation of tilted V-catchment flow problem (adopted from Panday and Huyakorn (2004))

Table 4.1 Catchment characteristics considered (adopted from (Li et al., 2013b))

Catchment Characteristic	Unit	Explanation	Values Considered
K_s	m/s	Saturated hydraulic conductivity	2.44E-05, 3.99E-05, 1.12E-04, 2.11E-04, 9.66E-04
α	-	van Genuchten parameter	0.572, 3.366, 6.161, 8.955, 11.75
β	-	van Genuchten parameter	1.32, 1.556, 1.793, 2.029, 2.266
A	km^2	Catchment area	6, 48, 80, 120, 192
S1	-	Hill slope (perpendicular to the channel)	0.005, 0.008, 0.012, 0.016, 0.02
S2	-	Channel slope (along the channel)	0.0025, 0.004, 0.006, 0.008, 0.01
AR	-	Ratio of catchment width to length (x/y)	0.5, 0.75, 1.0, 1.25, 1.5

Table 4.2 Hydrological inputs considered (adopted from (Li et al., 2013b))

City	Gauge No.	Average annual rainfall (mm/a)	Average annual potential ET (mm/a)	R/ET (average annual rainfall/average annual potential ET)
Adelaide	023011	510.16	1470.97	0.347
Melbourne	086071	525.33	911.33	0.576
Sydney	070062	1095.85	920.90	1.190
Brisbane	031011	2238.22	2077	1.078
Darwin	014015	1707.16	2056.37	0.811

4.2.2 Fully integrated SW/GW model

Hydrogeosphere (HGS) is used as the fully integrated SW/GW model to model the 66 synthetic catchments' response to rainfall and ET inputs under different catchment characteristics and hydrological regimes. This is because HGS can be used to simulate hydrological processes within catchments in a physically based manner (Therrien et al., 2009). HGS has been applied successfully to various studies, such as the comparison of baseflow estimation methods (Li et al., 2013b; Partington et al., 2011; Partington et al., 2012), SW/GW disconnection problems (Banks et al., 2011; Brunner et al., 2009), bank storage dynamic processes analysis (Doble et al., 2012) and the study of dual permeability systems (Schwartz et al., 2010). Further description of the code and its numerical formulation can be found in Therrien et al. (2009) and Brunner and Simmons (2012).

As shown in Figure 4.2, the catchment used in this study is symmetrical. As a result, all simulations are conducted for only half of the catchment, as shown for one example of the catchment configurations considered in Figure 4.3, and the reported fluxes are correspondingly half of those expected when accounting for both sides of the stream. Detailed information of the catchment model with the selected values of the HGS parameters can be found in Li et al. (2013b).

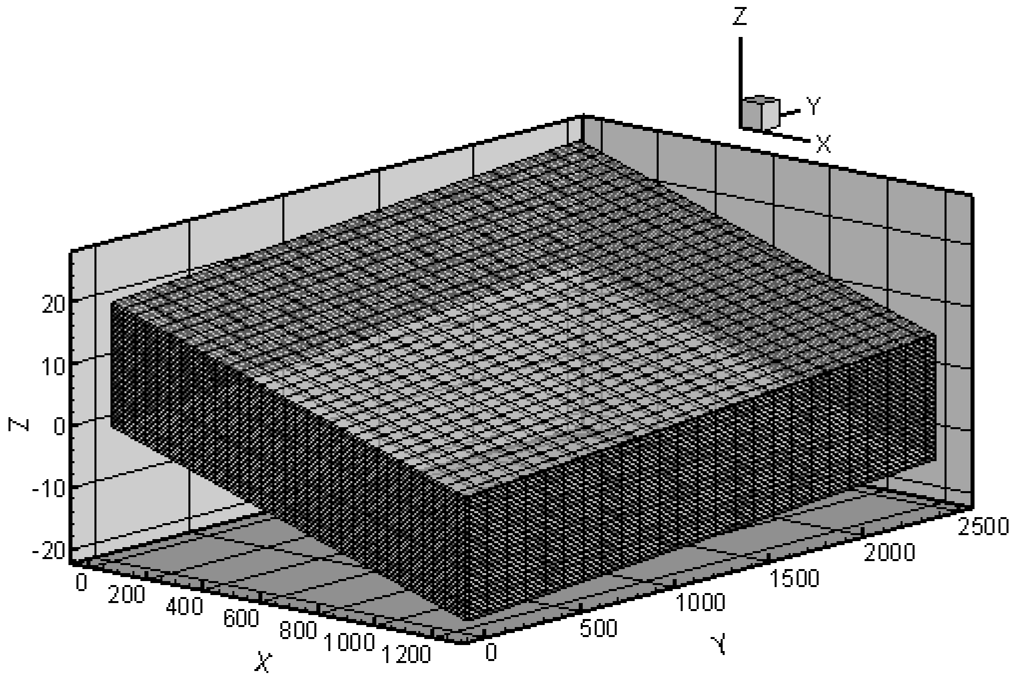

Figure 4.3 An example of 3D catchment model for case study (adopted from Li et al. (2013b))

As mentioned previously, the HGS models are used to obtain the 'observed' streamflow (q_T^{obs}), baseflow (q_B^{obs}) and quickflow (q_Q^{obs}) hydrographs for the 66 catchments. The baseflow hydrograph (q_B^{obs}) is extracted from the model using the HMC method (Partington et al., 2011), based on the nodal fluid mass balance obtained from the model simulations. The HMC method is able to capture the storage effects and time lags within catchments, which provides a means of estimating baseflow from fully integrated SW/GW models. Details of the HMC method can be found in Partington et al. (2011). The quickflow (q_Q^{obs}) is taken as the difference between the total streamflow (q_T^{obs}) and baseflow (q_B^{obs}).

4.2.3 Australian Water Balance Model (AWBM)

AWBM is a saturation overland flow model developed by Boughton (1993, 2004) and is now one of the most widely used CRR models in Australia (Marshall et al., 2004; Ranatunga et al., 2008). AWBM is available in two versions. The first version uses a daily time step and is used for modelling catchment runoff yield, while the second version uses an hourly time step and is used for flood management (Boughton, 2004). The first version is used for this study.

As can be seen in Figure 4.4, AWBM uses rainfall and actual evapotranspiration as inputs and principally consists of a configuration of three different surface storages. The depths of these storages correspond to the parameters C1, C2 and C3. A fraction of the total area is associated with each surface storage, as represented by the parameters A1, A2 and A3. Moisture capacity variation over the catchment is described by the combination of the surface storages and the related fractional areas. An important feature of AWBM is the ability to account for baseflow when predicting streamflow by using a baseflow index (BFI), which is the ratio of the amount of baseflow to the total amount of streamflow and determines the proportion of excess moisture at each time step that is returned to the baseflow. The daily baseflow recession constant (KBase) and daily routed surface runoff recession constant (KSurf) are used to describe the daily discharge from baseflow and surface runoff (quickflow) storage. A summary of the AWBM parameters and their ranges used is given in Table 4.3. In this study, AWBM is implemented using the Rainfall Runoff Library (RRL) developed by the Cooperative Research Centre on Catchment Hydrology (www.toolkit.net.au/rrl).

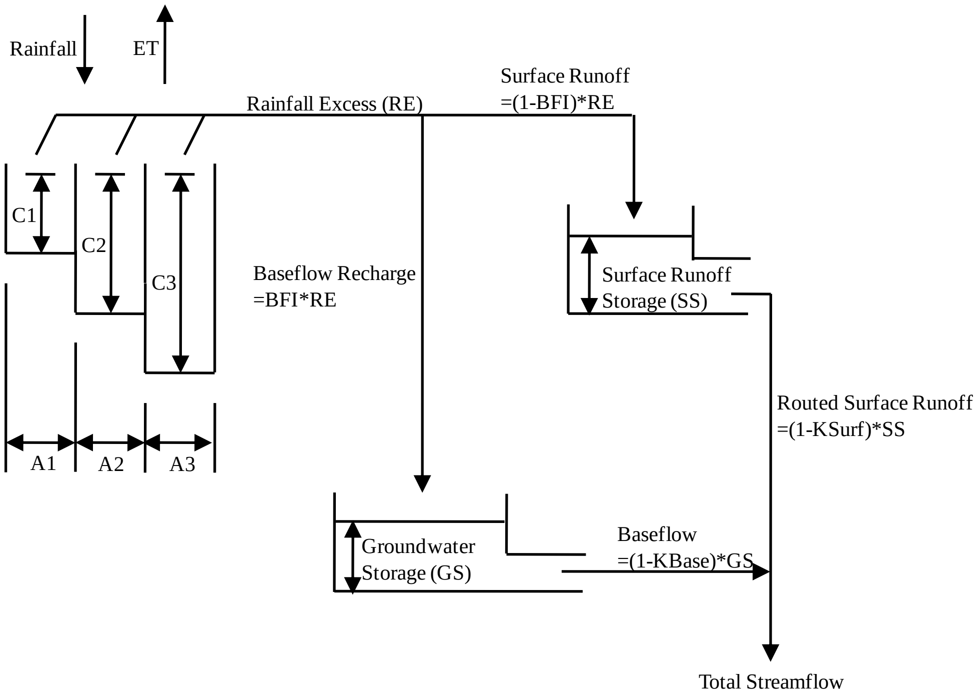

Figure 4.4 Structure of AWBM

Table 4.3 AWBM parameter description and ranges

Parameter	Description	Parameter range
A1	Partial Area	0-1
A2	Partial Area	0-1
BFI	Baseflow Index	0-1
C1	Surface Storage Capacity	0-50
C2	Surface Storage Capacity	0-200
C3	Surface Storage Capacity	0-500
KBase	Daily Baseflow Recession Constant	0-1
KSurf	Daily Surface Flow Recession Constant	0-1

4.2.4 Calibration of Australian Water Balance Model (AWBM)

As stated previously, the effectiveness of calibration methods that take internal model dynamics into account in different ways is investigated in this study. The calibration methods are summarised in Table 4.4 and detailed below. It should be noted that details of the optimisation method and error measure used in the calibration methods are given Sections 4.2.4.2 and 4.2.4.3, respectively.

4.2.4.1 Calibration methods

Values of all of the eight parameters listed in Table 4.3 are obtained as part of the different calibration methods investigated. Five of these parameters (A1, A2, C1, C2 and C3) are related to the moisture capacity of the catchment, two (BFI and KBase) affect baseflow generation and one (KSurf) affects the routed surface runoff, which is referred to as quickflow in this study. In order to be able to assess the impact of calibration methods that take internal model dynamics into account in different ways on the ability to predict total-, base- and quick-flow hydrographs, a calibration approach that does not take internal model dynamics explicitly into account is used to provide a basis of comparison (Method 1). In Method 1, all parameters are calibrated simultaneously so as to minimise the selected error measure between the total streamflow obtained using AWBM (q_T^{sim}) and that obtained using HGS (q_T^{obs}) using the selected optimisation method. The aim of this calibration method is to provide the best possible fit to total streamflow, without any consideration of internal model dynamics.

In order to take internal model dynamics into account explicitly during calibration, six different methods (Methods 2 to 7) are used. In each of these methods, a two-step process is adopted as follows:

In the first step, values of two of the model parameters, BFI and KBase, are estimated. BFI and KBase are selected for this step as they control the separation of rainfall excess into quickflow/baseflow storage and the baseflow component of total streamflow, respectively, and are therefore the two parameters that have a direct effect on the baseflow hydrograph produced by AWBM. Consequently, by estimating values of these parameters first, an attempt is made to obtain the best possible match to the baseflow hydrograph.

In the second step, BFI and KBase are fixed at the values obtained in the first step and the remaining parameters are calibrated simultaneously so as to minimise the selected error measure between the total streamflow obtained using AWBM (q_T^{sim}) and that obtained using HGS (q_T^{obs}) using the selected optimisation method.

The methods used for obtaining values of BFI and KBase for Methods 2 – 7 can be divided into three broad categories. Methods 2 to 4 belong to the first category, in which BFI and KBase are calibrated to baseflow extracted using recursive digital filters (RDFs). In order to do this, KSurf, which determines the magnitude of the quickflow component within total streamflow (Figure 4.4), is set as 1.0, so that the total streamflow produced by AWBM is comprised solely of baseflow. Method 5 belongs to the second category, in which BFI and KBase are estimated using regression relationships with catchment characteristics and hydrological inputs. Methods 6 and 7 belong to the third category, in which BFI and KBase are either estimated by calibration to baseflow extracted using RDFs, as in Methods 2 to 4, or by regression, as in Method 5, based on the predicted accuracy of the RDF. Details of the different methods for estimating BFI and KBase in the first step of the two-step process described above are given below.

Method 2:

In Method 2, BFI and KBase are calibrated simultaneously so as to minimise the selected error measure between the baseflow obtained using AWBM (q_B^{sim}) and that obtained using the Lyne and Hollick (LH) as RDF (Nathan and McMahon, 1990), with the filter parameter set to its default value of 0.925 ($q_B^{obs\_LH(0.925)}$), using the selected optimisation method. The LH filter is used to obtain the baseflow hydrograph as it is one of the most widely used RDFs and has been found to give good results in a number of case studies (Arnold and Allen, 1999; Li et al., 2013b; Murphy et al., 2009). During this calibration process, the remaining parameters are set to the optimal values obtained using Method 1.

Method 3:

Method 3 is identical to Method 2, except that the LH filter parameter is estimated using the regression relationship developed by Li et al (2013b), which provides an estimate of the optimal filter parameter as a function of catchment characteristics and hydrological inputs, rather than using the default value of 0.925. Consequently, the "observed" baseflow is given by ($q_B^{obs\_LH(opt)}$).

Method 4:

Method 4 is identical to Method 3, except that the Eckhart filter (Eckhardt, 2005) is used to obtain the hydrograph of "observed" baseflow ($q_B^{obs\_Eck(opt)}$), rather than the LH filter. The Eckhart filter is used as it is mathematically identical to the Boughton filter (Boughton, 1993), which has been recommended for the purposes of estimating BFI for AWBM by Boughton (2004), but has a filter parameter (BFI_{max}) that can be estimated more easily from catchment characteristics and hydrological inputs than the corresponding filter parameter in the Boughton filter (Li et al., 2013b).

Method 5:

In Method 5, values of BFI and KBase are obtained directly (i.e. without calibration) by developing regression models predicting KBase and BFI as a function of the catchment characteristics (Table 4.1) and hydrologic inputs (Table 4.2) investigated, similar to the regression relationships for predicting filter performance and optimal filter parameters developed by Li et al. (2013b) used in Methods 6 and 7. Values of BFI are calculated as the ratio of the volume of baseflow to the volume of total streamflow obtained from HGS and KBase is obtained by performing recession analysis on the total streamflow hydrographs obtained from HGS. The resulting regression equations and scatter plots are shown in Figure 4.5. As can be seen, BFI can be predicted very well and KBase can be predicted reasonably well. These results also indicate that BFI and KBase are closely related to catchment characteristics and hydrological inputs.

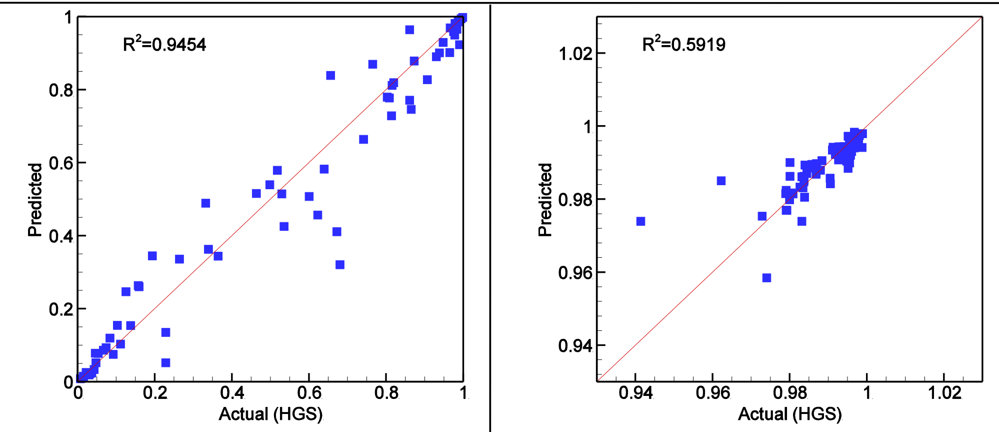

$BFI=1.551\ln(K_s)-0.076\ln(\alpha)-0.839\ln(\beta)-0.513\ln(A)+1.206\ln(S1)+0.574\ln(S2)-0.472\ln(AS)-2.773\ln(rainfall)+1.203\ln(ET)+35.84$

(a) BFI

$Kbase=0.213\ln(K_s)+0.451\ln(\alpha)+1.038\ln(\beta)+0.104\ln(A)+0.373\ln(S1)+0.217\ln(S2)+0.497\ln(AS)+0.836\ln(rainfall)-1.727\ln(ET)+14.48$

(b) KBase

Figure 4.5 Nonlinear regression models for the prediction of BFI and KBase

Method 6:

In Method 6, a modified version of the procedure for improving baseflow estimation using RDFs suggested by Li et al (2013b) is used in order to improve the baseflow estimates obtained using the LH filter in Method 5. First, the regression relationship developed by Li et al. (2013b) is used to determine whether the LH filter can provide satisfactory estimates of baseflow for a particular catchment based on catchment properties and hydrological inputs. If the performance of the LH filter is predicted to be acceptable, Method 3 is used to obtain estimates of BFI and KBase. However, if this is not the case, Method 5 is used.

Method 7:

Method 7 is identical to Method 6, except that Method 4 (Eckhart filter) is used instead of Method 3 (LH Filter).

In order to be able to assess the absolute performance of the different calibration methods in terms of their ability to predict base- and quick-flow hydrographs accurately, and to be able to assess the degree to which the structure of AWBM is able to represent base- and quick-flow processes, two benchmarks are developed. As part of the benchmark development process, the parameters that affect baseflow and quickflow are calibrated to the “observed” base-and quick-flow hydrographs produced by HGS, which are also used to assess the performance of the different calibration methods. A two-step calibration process similar to that used for Methods 2-4 is used in order to obtain the benchmark base- and quick-flow hydrographs. The only difference is in the way the parameters affecting baseflow (i.e. BFI and KBase) are estimated in step 1 of the procedure for obtaining the baseflow benchmark (Benchmark 1) and the way the parameters affecting quickflow (BFI and KSurf) are estimated in step 1 of the procedure for obtaining the quickflow benchmark (Benchmark 2), as detailed below:

Benchmark 1 (Baseflow):

BFI and KBase are calibrated simultaneously so as to minimise the selected error measure between the baseflow obtained using AWBM (q_B^{sim}) and that obtained HGS ($q_B^{obs\_HGS}$), using the selected optimisation method.

Benchmark 2 (Quickflow):

BFI and KSurf are calibrated simultaneously so as to minimise the selected error measure between the quickflow obtained using AWBM (q_Q^{sim}) and that obtained using HGS ($q_q^{obs\_HGS}$), using the selected optimisation method. In order to do this, KBase, which determines the magnitude of the baseflow component within total streamflow (Figure 4.4), is set as 1.0, so that the total streamflow produced by AWBM is comprised solely of quickflow.

Table 4.4 Summary of calibration methods

Calibration method	Details
1	Calibrate all parameters simultaneously to total streamflow.
2	First calibrate BFI and KBase to baseflow obtained using LH filter with default filter parameter (0.925) and then calibrate remaining parameters to total streamflow.
3	First calibrate BFI and KBase to baseflow obtained using LH filter with optimal filter parameters and then calibrate remaining parameters to total streamflow.
4	First calibrate BFI and KBase to baseflow obtained using Eckhart filter with optimal filter parameters and then calibrate remaining parameters to total streamflow.
5	Estimate BFI and KBase based on regression relationships with catchment characteristics and hydrological inputs and then calibrate remaining parameters to total streamflow.
6	Use the regression relationship developed by Li et al. (2013b) to determine whether the LH filter can provide satisfactory estimates of baseflow. If so, use Method 3. If not, use calibration Method 5.
7	Identical to Method 6, except that Method 4 is used instead of Method 3.

4.2.4.2 Optimisation method

Model calibration is conducted using the shuffled complex evolution (SCE-UA) algorithm, because it has been proven to be both accurate and efficient in previous studies (Hapuarachchi et al., 2001). In addition, SCE-UA is widely recognized as being one of the best search procedures for use in CRR modelling applications (Ajami et al., 2004; Franchini et al., 1998). The SCE-UA algorithm is based on the strengths of several existing search procedures, including genetic algorithms (GAs) (Goldberg, 1989) and the Nelder& Mead Simplex downhill search scheme (Nelder and Mead, 1965), but also introduces the concept of complex shuffling (Duan et al., 1992). A detailed description of this method can be found in Duan et al. (1992).

In this study, SCE-UA is implemented using the Rainfall Runoff Library (www.toolkit.net.au/rrl). The number of complexes is set equal to the number of calibration parameters to reduce the chance of premature termination of the search algorithm, as suggested by Kuczera (1997). All of the other parameters are set to the recommended values in Duan et al. (1994). In order to check whether parameter equifinality is a potential problem and to ensure near globally optimal solutions are obtained, each calibration run is repeated ten times. Another important aspect in the application of SCE-UA is that a parameter space needs to be defined, in which the algorithm searches for the optimal parameter combination. The ranges of all of the eight AWBM parameters used are based on the suggestions in the Rainfall Runoff Library (www.toolkit.net.au/rrl) and are listed in Table 4.3.

The length of streamflow data available for AWBM calibration is 10 years (Li et al., 2013b). AWBM runs on a daily time step, and therefore, is calibrated against daily streamflow. The calibration period requires a warm up period to account for the residual soil moisture present in the catchments. This allows the models to account for residual water in the catchment by partially filling their storages, which primes the models for the calibration period. Initial testing demonstrates that a 1 year warm up period is sufficient for model calibration. Chronologically, the warm up period directly proceeds the calibration period.

4.2.4.3 Error measure

The Nash-Sutcliffe coefficient (Ef) (Nash and Sutcliffe, 1970) is chosen as the performance criterion, as it is one of the most highly used performance measures in hydrology. Ef values are calculated by comparing the difference between the 'observed' (e.g. outputs from HGS simulations) and simulated time series for each time step for total streamflow, baseflow and quickflow from AWBM. As suggested by Moriasi et al. (2007), Ef values between 0.5 and 1.0 correspond to 'good' model performance; Ef values between 0.0 and 0.5 show 'acceptable' model performance and 'poor' model performance is represented by negative values of Ef. However, Gupta and Kling (2011) indicated that high values of Ef can give poor model performance. Consequently, although more subjective than the use of statistical measures of goodness-of-fit, plots of simulated and observed hydrographs are also inspected following optimisation.

4.2.5 Evaluation of model performance

As mentioned previously, the performance of AWBM models calibrated using the different methods outlined in Section 4.2.4.1 is compared in terms of overall model predictive performance (i.e. how well the total streamflow generated using AWBM (q_T^{sim}) matches the corresponding streamflow generated using HGS (q_T^{obs})) and the accuracy of the resulting internal model dynamics (i.e. how well the AWBM generated baseflow (q_B^{sim}) and quickflow (q_Q^{sim}) hydrographs match the corresponding hydrographs obtained using HGS (i.e. (q_B^{obs} and q_Q^{obs})) (Figure 4.1). The performance of models developed using the different calibration methods is assessed using Ef and by visual inspection.

4.3 Results and discussion

The performance of the AWBMs calibrated with the seven different methods investigated, as well as that of the two benchmarks, is summarised in Figure 4.6. As can be seen, the results are presented in terms of the percentage of models developed for the 66 catchments resulting in "good" (Ef≥ 0.5), "acceptable" (0≤Ef<0.5) and "poor" (Ef<0) performance, for each of the total-, base- and quick-flow hydrographs. It can also be seen that two sets of results are presented for Method 1. This is because there are two distinct sets of model parameters that result in similar model performance in terms of total streamflow during the 10 calibration trials conducted for some of the 66 catchments. This is because when Method 1 is used, there is no control on internal model dynamics and the only objective is to find a set of model parameters that provides the best match to the "observed" total streamflow hydrograph, as discussed previously. However, as shown in Figure 4.4, the AWBM total streamflow is the sum of routed surface runoff and baseflow, both of which are modelled in an identical fashion, each with a single parameter (KBase for baseflow and KSurf for routed surface runoff). Consequently, similar total streamflow can be obtained by exchanging parameter values for KBase and KSurf, resulting in model equifinality, as observed in the calibration results for Method 1.

An example of this is given in Figure 4.7. As can be seen in Figure 4.7 (a) and (b), good overall model performance is obtained for both parameter sets in terms of matching total streamflow. However, the internal network dynamics are much better when parameter set 1 is used, as indicated by significantly better matches to the base-and quick- flow hydrographs. It is clearly evident that the baseflow and quickflow patterns are reversed for the models with the different parameter sets (e.g. the pattern of baseflow obtained with parameter set 1 is very similar to the pattern of quickflow obtained with parameter set 2). In Figure 4.6, all of the results with parameters that result in better internal model dynamics (e.g. as in Figure 4.7(a)) are represented by Set 1, whereas the results with parameters that result in poorer internal model dynamics (e.g. as in Figure 4.7(b)) are represented by Set 2.

Overall, the results show that total streamflow is predicted well using all calibration methods investigated, with “poor” model performance for fewer than 10% of the catchments, except when Method 5 (Regression) is used, in which case 15% of catchments result in poor model performance (Figure 4.6a). For most of the catchments (54%-68%) “good” performance is obtained. However, the internal model dynamics are not presented as well, especially for baseflow, where “poor” performance is obtained for more than half (58%-74% (ignoring Method 1 with parameter set 2)) of the catchments and “good” performance for fewer than 20% of the catchments (Figure 4.6b). The ability of AWBM to represent quickflow is slightly better, with good performance for 32%-41% of the catchments when the calibration methods that consider internal model dynamics explicitly (i.e. Methods 2 to 7) are used and poor performance for fewer than 30% of the catchments (12%-29%) (Figure 4.6c). It should be noted that when Method 1 is used, “good” performance is only obtained for 12% of catchments, but “acceptable” performance is achieved for the vast majority of the remaining catchments (71%), with poor performance for only 17% of the catchments.

Method 1 is the best-performing calibration approach in terms of matching total streamflow (Figure 4.6a). This is not surprising, as the method calibrates all of the model parameters simultaneously in order to obtain the best match to total streamflow. However, this is at the expense of internal model dynamics. As discussed above, there is a potential problem with equifinality as a result of the structure of AWBM. However, even if the results for Set 1 are considered, the method results in the second highest percentage of catchments with "poor" model performance for baseflow estimation and the lowest percentage of catchments with "good" model performance for quickflow estimation. Nevertheless, the performance of Method 1 is comparable with that of the other methods in terms of baseflow estimation, as baseflow is estimated poorly, irrespective of the method used. In relation to quickflow estimation, even though Method 1 results in significantly lower catchments with "good" performance compared with the other calibration methods, as mentioned above, there is only a small percentage of catchments with "poor" model performance. Consequently, the overall performance of the method is best in terms of total streamflow prediction and reasonable compared with that of the other methods in terms of baseflow and quickflow prediction. However, the equifinality problem requires careful attention, as very poor internal model dynamics can be obtained (e.g. "poor" performance for 100% of the catchments in terms of baseflow prediction and for 50% of the catchments in terms of quickflow prediction) if the "wrong" parameter set (Method 1 (Set 2)) is used.

The methods as part of which BFI and KBase are calibrated to baseflow extracted using RDFs (i.e. Methods 2-4) result in the best match to baseflow. This indicates that the RDFs are able to produce reasonably accurate estimates of baseflow, which is evidenced by the fact that the performance of Methods 2-4 is only slightly worse than that of Benchmark 1 (i.e. where BFI and KBase are calibrated to the baseflow produced by HGS, which is the same baseflow used for performance assessment). It also indicates that there is some benefit in terms of improving internal model dynamics by constraining

BFI and KBase to ensure that baseflow is matched as well as possible. However, the poor performance for Benchmark 1 (i.e. "poor" performance for 57% of the catchments) tends to suggest that the improvement that is possible by adopting this approach is rather limited, possibly due to problems with the conceptual representation of the underlying physical processes associated with baseflow in AWBM.

Of the three methods considered, Method 2, which uses the LH filter with its default filter parameter value of 0.925, performs worst, while the performance of the other two methods (i.e. LH and Eckhart filters with optimal filter parameters) is very similar. The Eckhart filter performs slightly better, with a slightly larger percentage of catchments with "good" performance and a slightly smaller percentage with "poor" model performance. This supports the suggestion by Boughton (2004) that the Boughton filter, which is mathematically identical to the Eckhart filter, as mentioned previously, is well suited to use with AWBM.

While use of Methods 2-4 is able to produce the best results in terms of baseflow estimation, there are some trade-offs in terms of the ability to match total streamflow and quickflow. Even though use of Methods 2-4 results in a significant increase in the percentage of catchments with "good" performance in terms of quickflow prediction compared with Method 1, there is also a slight increase in the percentage of catchments with "bad" performance. In relation to total streamflow, use of Methods 2-4 also results in a slight reduction in performance compared with Method 1. Overall, the LH method with optimal filter parameter values produces the best trade-offs in performance between matching total-, base- and quick-flow among Methods 2-4. However, a disadvantage of this method compared with Method 2 is that information on catchment properties and hydrological inputs is needed in order to apply the regression equations used to obtain optimal filter parameter values, making it more difficult to apply.

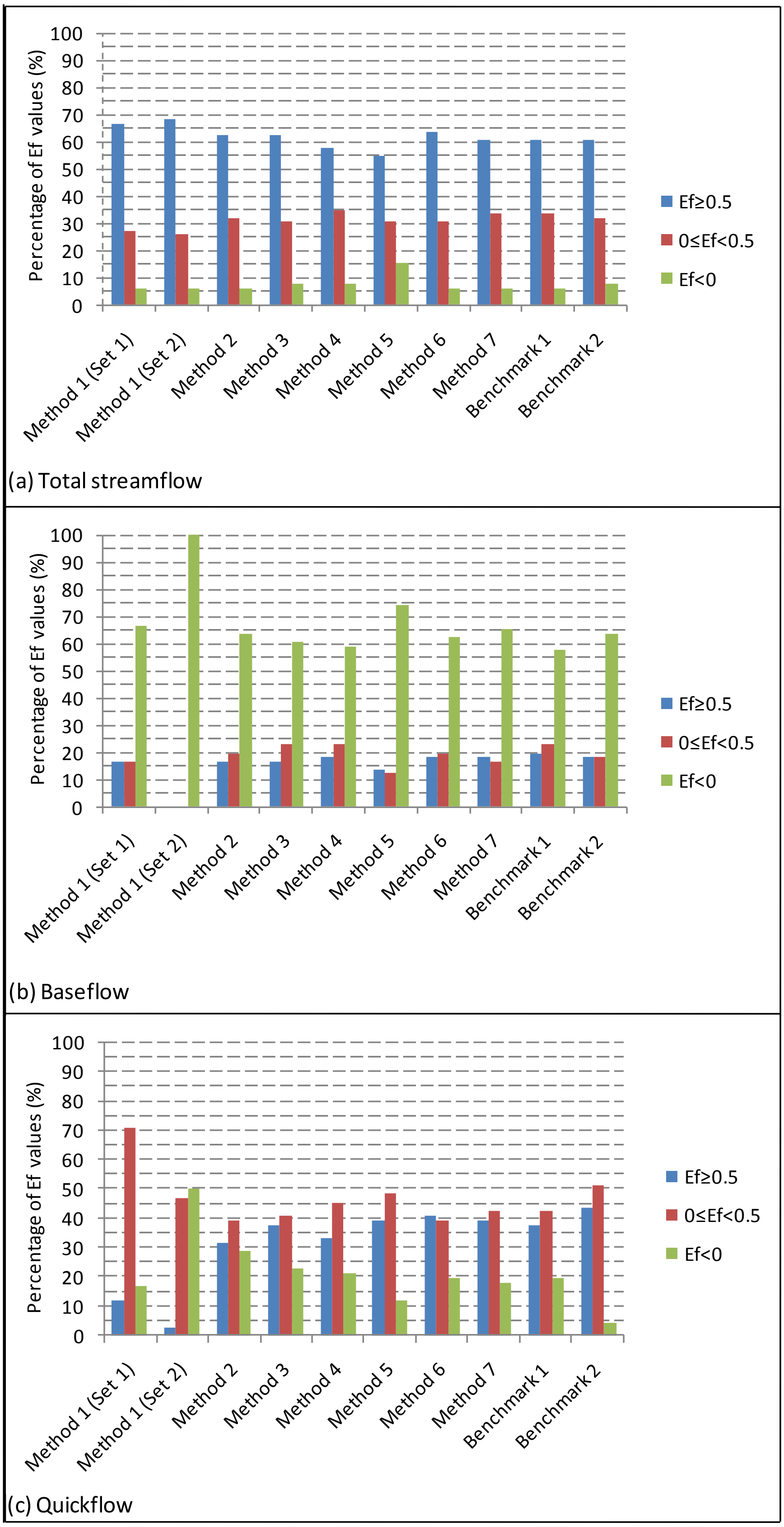

Figure 4.6 Performance of AWBMs for the different calibration methods investigated

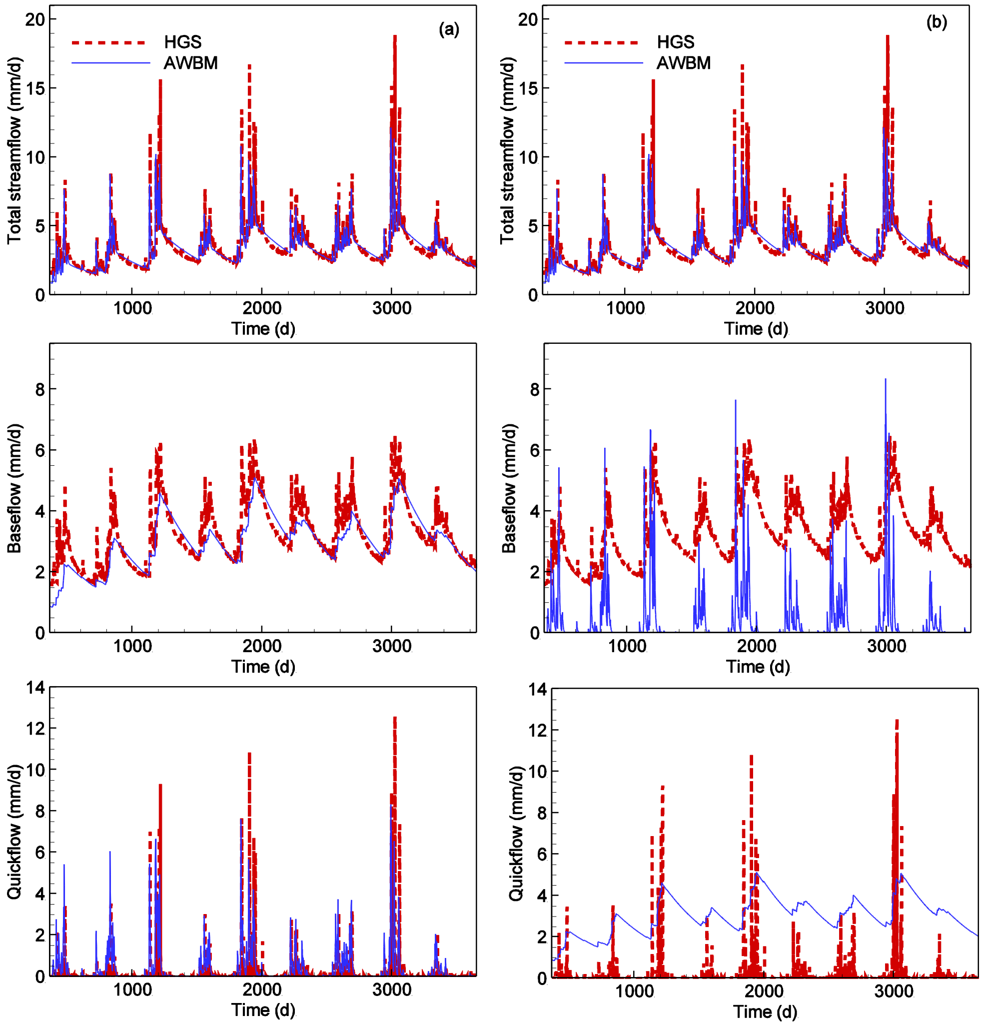

Figure 4.7 Example of total-, base- and quick- flow hydrographs obtained for two distinct parameter sets obtained using Method 1 for one of the 66 catchments investigated

The regression method (Method 5) results in the best performance in terms of matching quickflow, performing only slightly worse than the quickflow benchmark (Benchmark 2). The method results in the smallest percentage of catchments with "poor" performance and second highest percentage of catchments with "good" performance. However, it is also the worst-performing method in terms of matching total- and quick-flow. An advantage of the method is that it does not require estimates of baseflow hydrographs (only total streamflow hydrographs are needed), but a disadvantage is that information on catchment properties and hydrological inputs is needed in order to apply the regression equations used to obtain values of BFI and KBase as part of the calibration process.

The two methods combining aspects of the filter (Methods 2-4) and regression (Method 5) methods (Methods 6-7) provide a good compromise in terms of performing reasonably well on all three hydrographs (i.e. total-, base- and quick-flow). While they are not the best-performing methods for any of the three hydrographs, their performance is more consistent than that of any of the other methods and not far from that of the best-performing method in each case. Of the two methods, the method using the LH filter (Method 6) performs better than the method using the Eckhart filter (Method 7) overall. A disadvantage of these methods is that they are more complex to apply than the other methods, as they require baseflow extraction using a RDF, as well as data on catchment characteristics and hydrological inputs in order to apply the regression equations for predicting filter performance, obtaining the optimal filter parameters and obtaining direct estimates of BFI and KBase in the case where predicted filter performance is poor.

Overall, the results suggest that while total streamflow can be predicted very well over a wide range of catchment characteristics and hydrological inputs using AWBM, the component hydrographs are not modeled very well, particularly baseflow. This raises questions about the way the processes associated with these streamflow components are conceptualized in AWBM.

Of the methods investigated, Methods 3 and 4, as part of which BFI and KBase are calibrated to the baseflow obtained using the LH and Eckhart filters with optimal filter parameters, provide the best performance in terms of baseflow hydrograph prediction. The regression method (Method 5) provides the best match to the quickflow hydrographs and the hybrid method using the LH filter with optimal filter parameters and the regression approach (Method 6) provides the best overall trade-offs in terms of matching all three hydrographs.

4.4 Summary and conclusions

In this paper, the impact of seven different calibration methods on the ability of AWBM to predict total-, base- and quick-flow hydrographs is assessed for 66 catchments with different physical properties and hydrological inputs. The results indicate that total streamflow can generally be predicted to an acceptable level for more than 90% of the 66 catchments. In contrast, baseflow is predicted poorly, with acceptable performance levels ranging from 26% to 41% for the different calibration methods investigated. However, prediction of quickflow is much better, with acceptable performance levels ranging from 71% to 88%. This disparity in performance between baseflow and quickflow prediction is despite the fact that the hydrographs for the 66 catchments consist of approximately equal contributions both ($0.006<BFI<0.997$, Median $BFI=0.53$), suggesting that the way AWBM represents baseflow processes could be improved.

Use of the calibration methods that take internal model dynamics into account explicitly (Methods 2 – 7) results in improved prediction of the component hydrographs. This improvement is particularly significant in terms of producing "good" estimates of quickflow, with the percentage of catchments for which good performance is obtained increasing from ~10% to ~40% for most methods. However, as AWBM is unable to provide good predictions of baseflow in general, as discussed above, the improvements obtained by using Methods 2 – 7 is only small (generally < 5%).

Which calibration method should be used is a function of which components of the hydrograph are most important for the study under consideration.

If total streamflow prediction is most important, Method 1 (i.e. simultaneously calibrating all parameters to total streamflow) should be used. However, in order to obtain reasonable internal model dynamics, the problem of equifinality needs to be addressed.

If baseflow is most important, the methods that calibrate BFI and KBase to baseflow extracted using recursive digial filters (RDFs) (Methods 2 – 4) should be used. Of these methods, the methods that use the optimal filter parameters obtained using the regression equations developed by Li et al. (2013b) (Methods 3 and 4) perform best.

If quickflow prediction is the primary objective, the regression method (Method 5) should be used.

If performance on all three hydrographs is important, the hybrid method using the Lyne and Hollick (LH) filter with optimal filter parameters and the regression method (Method 6) is likely to perform best.

However, it should be noted that most of the methods that perform best require information on catchment characteristics and hydrological inputs in order to apply the regression equations for obtaining optimal filter parameters (Methods 3, 4 and 6), predicting BFI and KBase directly (Methods 5 and 6) and estimating the level of performance of the LH filter with optimal filter parameters (Method 6), which makes them difficult to apply if the required information is not readily available. However, use of Method 2 (LH filter with default filter parameter of 0.925) can be used in order to achieve reasonable improvements in internal model dynamics in such cases.

Finally, it is important to highlight a number of limitations of this study that provide avenues for future studies. Firstly, it is worth pursuing other calibration methods that aim to take the internal model dynamics into account explicitly. For example, changes could be made to the objective function to ensure known features of the total streamflow hydrograph are captured, or different transformations could be applied to the data. Secondly, the fact that synthetic data are used in this study limits its complexity and realism. However, there is a trade-off between realism and the ability to assess model dynamics accurately. For real catchments, the actual base- and quick- flow hydrographs are generally unknown and have to be estimated using a variety of methods. However, the approach adopted in this study enables the base- and quick- flow hydrographs to be known with certainty, enabling an accurate assessment of the internal dynamics of AWBM to be obtained in a simplified setting. Lastly, while the computational experiments are conducted for a range of catchment characteristics and hydrological inputs, these values are also represented in a simplified manner (e.g. uniform rainfall, homogeneous soils, uniform slopes etc.) and the effect of additional complexity on the results obtained should be investigated in future studies.

4.5 Acknowledgement

This research was supported by the Chinese Scholarship Council (CSC) and the University of Adelaide.

Chapter 5

5 Conclusions

Hydrologic models are becoming increasingly important for the planning, design, operation and management of natural and engineered systems. However, due to the complexity of the underlying physical processes, it is difficult to develop such models. Consequently, simplified models are generally used in practice for purposes such as baseflow estimation and rainfall-runoff prediction. However, it is difficult to provide a rigorous assessment of the performance of such simplified models under a range of catchment characteristics (e.g. catchment area, soil type, slope) and hydrological inputs (e.g. rainfall, evaporation) and further improve the models' predictive capability and the way they represent underlying physical processes. Therefore, generic frameworks for i) evaluating and improving recursive digital filters (RDFs) for baseflow estimation and (ii) evaluating the internal dynamic performance of conceptual rainfall runoff (CRR) models are developed and applied.

5.1 Research contributions

The overall contribution of this research is the development of methods for evaluating and improving the predictive performance of simplified hydrologic models, including RDFs for baseflow estimation and CRR models for rainfall runoff prediction, under the premise that fully integrated surface water/groundwater (SW/GW) models are able to provide the best possible approximation to the physical processes of water flow within catchments and can therefore be used as a benchmark against which the performance of these simplified models can be assessed for a variety of physical catchment characteristics and hydrological inputs. The details of specific contributions of this research are as follows:

1. A generic framework is developed for evaluating and improving the performance of RDFs for baseflow estimation by taking different catchment characteristics and hydrological inputs into account. It is then applied to a commonly used RDF (the Lyne and Hollick filter) for a synthetic catchment with different soil properties (saturated hydraulic conductivity (K_s), porosity, residual water content (θ_r), and van Genuchten parameters α and $N(\beta)$). The results show that the performance of the Lyne and Hollick filter is sensitive to soil properties and that performance can be improved by optimising values of the filter parameter based on soil properties (particularly K_s), rather than using the default value of 0.925. This research provides the first step towards being able to assess the performance of RDFs and investigate the improvement of RDFs by finding optimal values of filter parameters under a range of catchment characteristics and hydrological inputs.

2. Continuing from the above research, the framework developed is further applied to three commonly used RDFs (the Lyne and Hollick, Boughton 2-parameter and Eckhart filters) for the same synthetic catchment but with a larger range of catchment characteristics (catchment area, hill

slope, channel slope, aspect ratio, K_s, and van Genuchten parameters α and β) and hydrological inputs (rainfall and evapotranspiration for Adelaide, Brisbane, Darwin, Melbourne and Sydney). The outputs from the RDF calibration and performance assessment procedures over these catchment characteristics and hydrological inputs show that the commonly used RDF parameter values cannot provide satisfactory baseflow estimates. Therefore, nonlinear regression equations are developed for predicting RDF performance and optimal RDF parameters based on these catchment characteristics and hydrological inputs for the three RDFs investigated, in order to help with providing guidance on checking RDF suitability for a particular catchment and estimation of the value of the optimal RDF parameter for practical applications.

3. A framework is developed for assessing and improving the predictive ability and internal model dynamics of CRR models. This framework is developed for the Australian Water Balance Model (AWBM), a commonly used CRR model. Through using this framework, how well AWBM is able to predict total-, base- and quick-flow is assessed under a wide range of catchment characteristics and hydrological inputs. In addition, the impact of a number of calibration regimes that take internal model dynamics into account in different ways on the accuracy of total-, base- and quick-flow hydrograph prediction is evaluated for AWBM under the same range of catchment characteristics and hydrological inputs. The results obtained show that consideration of the internal model dynamics during the calibration processes is able to result in improvements in model internal dynamics with representation of baseflow and quickflow. While the methodology is illustrated for this particular case study, its generic nature means it could easily be adapted and applied to other conceptual rainfall runoff (CRR) models around the world.

5.2 Publications

Apart from the three journal articles which form the main body of this thesis, one conference papers has also resulted from this research. A list of all of the publications arising from this research is presented below.

Journal articles:

1. Li, L., Maier, H.R., Lambert, M.F., Simmons, C.T., and Partington, D. (2013). "Framework for assessing and improving the performance of recursive digital filters for baseflow estimation with application to the Lyne and Hollick filter." Environmental Modelling & Software, 41, 163-175.

2. Li, L., Maier, H.R., Partington, D., Lambert, M.F., and Simmons, C.T. (2013). "Prediction of accuracy and optimal parameter values of recursive digital baseflow filters based on physical catchment characteristics and hydrological inputs." Environmental Modelling & Software (submitted).

3. Li, L., Lambert, M.F., Maier, H.R., Partington, D., and Simmons, C.T. (2013). “Assessment of the internal dynamics of the Australian Water Balance Model under different calibration regimes.” Environmental Modelling & Software (submitted).

Conference article:

1. Li, L., Maier, H.R., Lambert, M.F., Simmons, C.T., and Partington, D. (2011). "Sensitivity of optimal baseflow filter parameter to catchment soil characteristics." Proceedings of the 34th IAHR World Congress, Engineers Australia, Brisbane, Australia.

5.3 Research limitations

The limitations of this research are discussed below:

1. A main limitation of this research is that the frameworks developed in this research are under the premise that fully integrated SW/GW models are able to provide the best possible approximation to the physical processes of water flow within catchments and can therefore be used as a benchmark against which the performance of RDFs for baseflow estimation and CRR models for rainfall runoff prediction can be assessed for a variety of physical catchment characteristics and hydrological inputs. In addition, this study is only conducted for a synthetic catchment with uniform catchment characteristics and hydrological inputs. Consequently, the results obtained from this research cannot be validated using field data.

2. Development of the predictive nonlinear regression relationships for determining whether use of a particular filter is appropriate and for determining optimal RDF parameter values for a synthetic catchment case study provides a first step towards maximising RDF performance and increasing confidence in the accuracy of the baseflow obtained using RDFs. However, firstly, the impacts of spatial variability in catchment characteristics (e.g. heterogeneous soil type, slopes and vegetations, convergent and divergent catchment shapes) and hydrological inputs (e.g. spatially different rainfall and evapotranspiration (ET)) on the performance of the regression relationships developed in this research are not considered. In addition, these regression equations require data on a number of catchment characteristics and rainfall and evapotranspiration (ET), some of which are spatially heterogeneous and difficult to obtain in practice. Furthermore, due to the lengthy model run-times that result from solving the highly nonlinear differential equations describing flow, only 70 samples are generated for developing these regression equations. Lastly, only three RDFs are considered, and it would be useful to develop

such relationships for other RDFs. All of these limitations need to be addressed in future work.

3. Similar to the limitations stated above, most of the calibration methods adopted for assessing the internal dynamic performance of AWBM are based on the regression equations, which require information of catchment characteristics and hydrological inputs. This makes them difficult to apply in practice if the required information is not available. In addition, it is worth pursuing other calibration methods that aim to take the internal model dynamics into account explicitly, e.g. different data transformation, or different objective functions to ensure known features of the total streamflow hydrograph are captured. Furthermore, no validation procedure has been performed for AWBM after being calibrated using different methods. Lastly, only AWBM is considered, and it would be useful to assess and validate other CRR models using the approach presented in this thesis.

5.4 Recommendations for future work

A number of the limitations of the current research presented in the previous section also represent opportunities for future research, including:

1. There is no doubt that the consideration of actual catchment conditions, rather than just a hypothetical catchment for numerical experimentation using fully integrated SW/GW models, will enable the results obtained to be validated using field data. Fully integrated SW/GW models have been used for real catchments with different applications (Pérez et al., 2011; Partington et al., 2012; Thompson et al., 2004). Future work should consider using data generated from case studies developed for real catchments for validating the results obtained from this research.

2. The catchment characteristics and hydrological inputs used for all of the simulations carried out in this research are spatially and temporally uniform. Further studies should aim to investigate the impacts of

variations in geology, topography and vegetation on the current results. This can be done by incrementally by adding layers of complexity to similar models.

3. The determination of relationships between optimal values of hydrologic model parameters and catchment characteristics and hydrological inputs rely on a large number of samples. 70 samples based on a synthetic catchment with different catchment characteristics and hydrological inputs have been generated and used in this thesis. Such work should continue to obtain a larger number of samples with different catchment characteristics and hydrological inputs, which can help with the development of more flexible predictive models, such as artificial neural networks (ANN) or genetic programming, rather than the regression relationships developed here.

4. Future work is required to consider additional RDFs and CRR models. In addition, deeper investigations should be conducted for these simplified models, e.g. whether the performance of simplified models can be improved by modifying their structures.

References

Abbott, M.B., Bathurst, J.C., Cunge, J.A., O'Connell, P.E., Rasmussen, J., 1986. An introduction to the European Hydrological System — Systeme Hydrologique Europeen, "SHE", 1: History and philosophy of a physically-based, distributed modelling system. Journal of Hydrology 87(1–2) 45-59.

Ajami, N.K., Gupta, V.K., Wagener, T., Sorooshian, S., 2004. Calibration of a semi-distributed hydrologic model for streamflow estimation along a river system. Journal of Hydrology 298 112-135.

Arnold, J.G., Allen, P.M., 1999. Automated Methods for Estimating Baseflow and Ground water Recharge from Streamflow Records. Journal of the American Water Resources Association 35(2) 411-424.

Arnold, J.G., Allen, P.M., Muttiah, R., Bernhardt, G., 1995. Automated Baseflow Separation and Recession Analysis Techniques. Ground Water 33(6) 1010-1018.

Bako, M.D., Hunt, D.N., 1988. Derivation of baseflow recession constant using computer and numerical analysis. Hydrological Sciences 33(4) 357-367.

Banks, E.W., Brunner, P., Simmons, C.T., 2011. Vegetation controls on variably saturated processes between surface water and groundwater and their impact on the state of connection. Water Resources Research 47(11) W11517.

Beven, K., 1993. Prophecy, reality and uncertainty in distributed hydrological modelling. Advances in Water Resources 16(1) 41-51.

Beven, K.J., 2005. Rainfall-runoff Modeling: Introduction, In: Anderson, M.G. (Ed.), Encyclopedia of Hydrological Sciences. Wiley and Sons, pp. 1-12.

Blessent, D., Therrien, R., MacQuarrie, K., 2009. Coupling geological and numerical models to simulate groundwater flow and contaminant transport in fractured media. Computers & Geosciences 35(9) 1897-1906.

Boughton, W.C., 1993. A hydrograph-based model for estimating the water yield of ungauged catchments, Hydrology and Water Resources Symposium: Institution of Engineers Australia, Newcastle, NSW, pp. 317-324.

Boughton, W.C., 2004. The Australian water balance model. Environmental Modelling & Software 19(10) 943-956.

Boughton, W.C., 2009. Selecting Parameter Values for the AWBM Daily Rainfall-Runoff Model for Use on Ungauged Catchments. Journal of Hydrologic Engineering 1343-1350.

Bowden, G.J., Maier, H.R., Dandy, G.C., 2005. Input determination for neural network models in water resources applications. Part 2: Case study: forecasting salinity in a river. Journal of Hydrology 301(1-4) 93-107.

Brodie, R., Hostetler, S., 2005. A Review of Techniques for Analysing Baseflow from Stream Hydrographs, Proceedings of the NZHS-NZSSS 2005 Conference: Auckland, p. 5.

Brookfield, A.E., Sudicky, E.A., Park, Y.-J., Jr., B.C., 2009. Thermal transport modelling in a fully integrated surface/subsurface framework. Hydrological Processes 23(15) 2150-2164.

Brunner, P., Cook, P.G., Simmons, C.T., 2009. Hydrogeologic controls on disconnection between surface water and groundwater. Water Resources Research 45(1) W01422.

Brunner, P., Simmons, C.T., 2012. HydroGeoSphere: A Fully Integrated, Physically Based Hydrological Model. Ground Water 50(2) 170-176.

Chapman, T., 1999. A comparison of algorithms for stream flow recession and baseflow separation. Hydrological Processes 13(5) 701-714.

Chapman, T.G., 1991. Comment on evaluation of automated techniques for baseflow and recession analysis by Nathan, R.J., McMahon, T.A. Water Resources Research 27(7) 1783-1784.

Chapman, T.G., Maxwell, A.I., 1996. Baseflow separation-Comparison of numerical methods with tracer experiments, Proceedings of the 23rd hydrology and water resources symposium: Hobart Australia.

Chiew, F.H.S., Peel, M.C., Western, A.W., 2002. Application and testing of the simple rainfall-runoff model SIMHYD, In: Singh, V.P., Frevert, D. (Eds.), Mathematical Models of Small Watershed Hydrology and

Applications. Water Resources Publications: Littleton, Colorado, pp. 335-367.

D'Odorico, P., Laio, F., Ridolfi, L., 2005. Noise-induced stability in dryland plant ecosystems, Proceedings of the National Academy of Sciences of the United States of Amrica, pp. 10819-10822.

Delleur, J.W., 1982. Introduction to urban hydrology and stormwater management, Urban Stormwater Hydrology. AGU: Washington, DC, pp. 1-34.

diGiammarco, P., Todini, E., Lamberti, P., 1996. A conservative finite elements approach to overland flow: the control volume finite element formulation. Journal of Hydrology 175(1–4) 267-291.

Doble, R., Brunner, P., McCallum, J., Cook, P.G., 2012. An Analysis of River Bank Slope and Unsaturated Flow Effects on Bank Storage. Ground Water 50(1) 77-86.

Duan, Q., Sorooshian, S., Gupta, V., 1992. Effective and Efficient Global Optimization for Conceptual Rainfall-Runoff Models. Water Resources Research 28(4) 1015-1031.

Duan, Q.Y., Sorooshian, S., Gupta, V.K., 1994. Optimal use of the SCE-UA global optimization method for calibrating watershed models. Journal of Hydrology 158 265-284.

Dukic, V., 2006. Modeling of base flow of the Basin of Kloubara River in Serbia. Journal of Hydrology 327(1-2) 1-12.

Dunkerley, D.L., 2008. Bank permeability in an Australian ephemeral dry-land stream variation with stage resulting from mud deposition and sediment clogging. Earth Sruface Processes and Landforms 33 226-243.

Eckhardt, K., 2005. How to construct recursive digital filters for baseflow separation. Hydrological Processes 19(2) 507-515.

Eckhardt, K., 2008. A Comparison of Baseflow indices, which were calculated with seven different baseflow separation methods. Journal of Hydrology 352(1-2) 168-173.

Evans, R., Neal, B., 2005. Baseflow analysis as a tool for groundwater-surface water interaction assessment, International Water Conference: Auckland, New Zealand.

Ferket, B.V.A., Samain, B., Pauwels, V.R.N., 2010. Internal validation of conceptual rainfall–runoff models using baseflow separation. Journal of Hydrology 381 158-173.

Franchini, M., Galeati, G., Berra, S., 1998. Global optimization techniques for the calibration of conceptual rainfall-runoff models. Hydrological Sciences 43(3) 443-458.

Freeze, R.A., 1972. Role of Subsurface Flow in Generating Surface Runoff 1. Base Flow Contributions to Channel Flow. Water Resources Research 8(3) 609-623.

Freeze, R.A., Harlan, R.L., 1969. Blueprint for a physically-based, digitally-simmulated hydrologic response model. Journal of Hydrology 9(3) 237-258.

Furey, P.R., Gupta, V.K., 2001. A physically based filter for separating base flow from streamflow time series. Water Resources Research 37(11) 2709-2722.

Furey, P.R., Gupta, V.K., 2003. Tests of two physically based filters for base flow separation. Water Resources Research 39(10) 1297.

Furman, A., 2008. Modelling coupled surface-subsurface flow processes: a review. Vadose Zone Journal 7(2) 741-756.

Gaukroger, A.M., Werner, A.D., 2011. On the Panday and Huyakorn surface-subsurface hydrology test case: analysis of internal flow dynamics. Hydrological Processes.

Gibbs, M.S., Maier, H.R., Dandy, G.C., 2012. A generic framework for regression regionalization in ungauged catchments. Environmental Modelling & Software 27–28(0) 1-14.

Gilfedder, M., Walker, G.R., Dawes, W.R., Stenson, M.P., 2009. Prioritisation approach for estimating the biophysical impacts of land-use change on stream flow and salt export at a catchment scale. Environmental Modelling & Software 24(2) 262-269.

Goderniaux, P., Brouyère, S., Fowler, H.J., Blenkinsop, S., Therrien, R., Orban, P., Dassargues, A., 2009. Large scale surface-subsurface hydrological model to assess climate change impacts on groundwater reserves. Journal of Hydrology 373(1-2) 122-138.

Goldberg, D.E., 1989. Genetic algorithms in search, optimization, and machine learning. Addison-Wesley Longman Publishing co., Inc. , Boson, MA, USA.

Gupta, H., Sorooshian, S., Yapo, P., 1999. Status of Automatic Calibration for Hydrologic Models: Comparison with Multilevel Expert Calibration. Journal of Hydrologic Engineering 4(2) 135-143.

Gupta, H.V., Kling, H., 2011. On typical range, sensitivity, and normalization of Mean Squared Error and Nash-Sutcliffe Efficiency type metrics. Water Resour. Res. 47(10) W10601.

Gupta, H.V., Kling, H., Yilmaz, K.K., Martinez, G.F., 2009. Decomposition of the mean squared error and NSE performance criteria: Implications for improving hydrological modelling. Journal of Hydrology 377 80-91.

Gupta, V.K., Sorooshian, S., 1985. The automatic calibration of conceptual catchment models using derivative-based optimization algorithms. Water Resources Research 21(4) 473-486.

Guttal, V., Jayaprakash, C., 2007. Impact of noise on bistable ecological systems. Ecological Modelling 201(3–4) 420-428.

Guttal, V., Jayaprakash, C., 2009. Spatial variance and spatial skewness: leading indicators of regime shifts in spatial ecological systems. Theoretical Ecology 2(1) 3-12.

Hall, F.R., 1968. Base-Flow Recession-A Review. Water Resour. Res. 4.

Hansen, N., 2009. Benchmarking the Nelder-Mead Downhill Simplex Algorithm With Many Local Restarts, ACM-GECCO Genetic and Evolutionary Computation Conference: Montreal, Canada.

Hapuarachchi, H., Li, Z., Wang, S., 2001. Application of SCE-UA Method for Calibrating the Xinanjiang Watershed Model. Journal of Lake Sciences 12(4) 304-314.

Helton, J.C., Johnson, J.D., Sallaberry, C.J., Storlie, C.B., 2006. Survey of sampling-based methods for uncertainty and sensitivity analysis. Reliability Engineering & System Safety 91(10-11) 1175-1209.

Herron, N., Croke, B., 2009. Including the influence of groundwater exchanges in a lumped rainfall-runoff model. Mathematics and computers in simulation 79(9) 2689-2700.

HydroGeoLogic, 2000. MODHMS: a comprehensive MODFLOW-based hydrologic modelling system, Code documentation and user's guide. HydroGeoLogic Inc.: Herndon, VA.

Iman, R.L., Helton, J.C., 1985. Comparison of uncertainty and sensitivity analysis techniques for computer models. Sandia National Labs., Albuquerque, NM (USA).

Iman, R.L., Shortencarier, M.J., 1984. A FORTRAN 77 program and user's guide for the generation of latin hypercube and random samples for use with computer models. The Division : Available from GPO Sales Program, Division of Technical Information and Document Control, U.S. Nuclear Regulatory Commission ; National Technical Information Service, Washington, DC; Springfield, Va.

Isukapalli, S.S., Georgopoulos, P.G., 1999. Computational methods for efficient sensitivity and uncertainty analysis of models for environmental and biological systems, Technical Report CCL/EDMAS-03. Rutgers, State University of New Jersey.

Janssen, P., Heuberger, P., Sanders, R., 1992. UNCSAM 1.1: A Software Package for Sensitivity and Uncertainty Analysis: Manual. National Institute of Public Health and Environmental Protection, Bilthoven, The Netherlands.

Jayatilaka, C.J., Storm, B., Mudgway, L.B., 1998. Simulation of water flow on irrigation bay scale with MIKE-SHE. Journal of Hydrology 208 108-130.

Jones, J.P., Sudicky, E.A., Brookfield, A.E., Park, Y.-J., 2006. An assessment of the tracer-based approach to quantifying groundwater contributions to streamflow. Water Resources Research 42(2) W02407.

Khan, S., Yufeng, L., Ahmad, A., 2009. Analysing complex behaviour of hydrological systems through a system dynamics approach. Environmental Modelling & Software 24(12) 1363-1372.

Knapp, H.V., Durgunoglu, A., Ortel, T.W., 1991. A review of rainfall-runoff modeling for stormwater management, U.S. Geologic Survey, Illinois District, p. 96.

Kollet, S.J., Maxwell, R.M., 2006. Integrated surface-groundwater flow modeling: A free-surface overland flow boundary condition in a parallel groundwater flow model. Advances in Water Resources 29(7) 945-958.

Kuczera, G., 1997. Efficient subspace probabilistic parameter optimization for catchment models. Water Resources Research 33(1) 177-185.

Lacey, G.C., Grayson, R.B., 1998. Relating Baseflow to Catchment Properties in South-Eastern Australia. Journal of Hydrology 204(1-4) 231-250.

Legates, D.R., McCabe, G.J., 1999. Evaluating the use of "goodness-of-fit" Measures in hydrologic and hydroclimatic model validation. Water Resources Research 35(1) 233-241.

Li, L., Lambert, M.F., Maier, H.R., Partingtion, D.P., Simmons, C.T., 2013c. Assessment of the Internal Dynamics of the Australian Water Balance Model under Different Calibration Regimes. Enviromental Modelling & Software Submitted.

Li, L., Maier, H.R., Lambert, M.F., Simmons, C.T., Partington, D., 2011. Sensitivity of optimal baseflow filter parameters to catchment soil characteristics, Proceedings of the 34th IAHR World COngress: Brisbane, Australia, pp. 1643-4650.

Li, L., Maier, H.R., Lambert, M.F., Simmons, C.T., Partington, D., 2013a. Framework for assessing and improving the performance of recursive digital filters for baseflow estimation with application to the Lyne and Hollick filter. Environmental Modelling & Software 41(0) 163-175.

Li, L., Marier, H.R., Partington, D., Lambert, M.F., Simmons, C.T., 2013b. Performance Assessment and Improvement of Recursive Digital Baseflow Filters for Catchments with Different Physical Characteristics and Hydrological Inputs. Environmental Modelling & Software Submitted.

Linsley, R.K., Kohler, M.A., Paulhus, J.L.H., Wallace, J.S., 1988. Hydrology for Engineers. McGraw-Hill Book Co., Singapore.

Longobardi, A., Villani, P., 2008. Baseflow index regionalization analysis in a mediterranean area and data scarcity context: Role of the catchment permeability index. Journal of Hydrology 355(1-4) 63-75.

Lyne, V., Hollick, M., 1979. Stochastic Time-Variable Rainfall-Runoff Modelling, I.E. Aust. Natl. Conf. Publ. Inst. of Eng.: Canberra, Australia, pp. 89-93.

Maier, H.R., Jain, A., Dandy, G.C., Sudheer, K.P., 2010. Methods used for the development of neural networks for the prediction of water resource variables in river system: Current status and future directions. Environmental Modelling & Software 25(8) 891-909.

Manache, G., Melching, C.S., 2008. Identification of reliable regression-and correlation-based sensitivity measures for importance ranking of water-quality model parameters. Environmental Modelling & Software 23(5) 549-562.

Marsh, T.J., Hannaford, J., 2008. Hydrological data UK. UK Hydrometric Register. Center for Ecology & Hydrology: Wallingford, p. 210.

Marshall, L., Nott, D., Sharma, A., 2004. A comparative study of Markov chain Monte Carlo methods for conceptual rainfall-runoff modeling. Water Resources Research 40(2) W02501.

Mau, D.P., Winter, T.C., 1997. Estimating Groundwater Recharge from Streamflow Hydrographs for a Small Mountain Watershed in a Temperate Humid Climate. Groundwater 35(2) 291-304.

May, R.J., Dandy, G.C., Maier, H.R., Nixon, J.B., 2008a. Application of partial mutual information variable selection to ANN forecasting of water quality in water distribution systems. Environmental Modelling & Software 23(10-11) 1289-1299.

May, R.J., Maier, H.R., Dandy, G.C., Fernando, T.M.K.G., 2008b. Non-linear variable selection for artificial neural networks using partial mutual information. Environmental Modelling & Software 23(10-11) 1312-1326.

Mazvimavi, D., Meijerink, A.M.J., Savenije, H.H.G., Stein, A., 2005. Prediction of flow characteristics using multiple regression and neural networks: A case study in Zimbabwe. Physics and Chemistry of the Earth, Parts A/B/C 30(11–16) 639-647.

McCallum, J.L., Cook, P.G., Brunner, P., Berhane, D., 2010. Solute dynamics during bank storage flows and implications for chemical base flow separation. Water Resour. Res. 46(7) W07541.

McCuen, R.H., 2005. Hydrologic Analysis and Design, third ed, New Jersey.

McCuen, R.H., Knight, Z., Cutter, A.G., 2006. Evaluation of the Nash-Sutcliffe Efficinecy Index. Journal of Hydrology Engineering 11(6) 597-602.

McKay, M.D., Beckman, R.J., Conover, W.J., 1979. A Comparison of Three Methods for Selecting Values of Input Variables in the Analysis of Output from a Computer Code. Technometrics 21(2) 239-245.

Moriasi, D.N., Arnold, J.G., Liew, M.W.V., Bingner, R.L., Harmel, R.D., Veith, T.L., 2007. Model evaluation guidelines for systematic quantification of accuracy in watershed simulations. American Society of Agriculture and Biological Engineers 50(3) 885-900.

Morris, M.D., 1991. Factorial Sampling Plants for Perliminary Computational Experiments Technometrics 33(2) 161-174.

Muleta, M.K., Nicklow, J.W., 2005. Sensitivity and uncertainty analysis coupled with automatic calibration for a distributed watershed model. Journal of Hydrology 306(1–4) 127-145.

Murphy, R., Graszkiewicz, Z., Hill, P., Neal, B., Nathan, R.J., Ladson, T., 2009. Project 7: Baseflow for catchment simulation (Phase 1-Selection of baseflow separation approach). Australian Rainfall and Runoff Technical Committee: Australia.

Mwakalila, S., Feyen, J., Wyseure, G., 2002. The Influence of Physical Catchment Properties on Baseflow in Semi-Arid Environments. Journal of Arid Environments 52 245-258.

Nash, J.E., Sutcliffe, J.V., 1970. River flow forecasting through conceptual models: Part 1. A discussion of principles. Journal of Hydrology 10(3) 282-290.

Nathan, R.J., McMahon, T.A., 1990. Evaluation of Automated Techniques for Base Flow and Recession Analysis. Water Resources Research 26(7) 1465-1473.

Nathan, R.J., McMahon, T.A., 1992. Estimating Low Flow Characteristics in Ungauged Catchments. Water Resources Management 6 85-100.

Nejadhashemi, A.P., Shirmohammadi, A., Montas, H.J., 2003. Evaluation of Streamflow Partitioning Methods, ASAE Annual International Meeting. American Society of Agricultural Engineers: Las Vegas, Nevada, USA, p. 13.

Nejadhashemi, A.P., Shirmohammadi, A., Montas, H.J., Sheridan, J.M., Bosch, D.D., 2007. Analysis of watershed physical and hydrological effects on baseflow separation, 2007 ASABE Annual International Meeting, Technical Papers. American Society of Agricultural and Biological Engineers: Minneapolis, MN, United states.

Nejadhashemi, A.P., Shirmohammadi, A., Sheridan, J.M., Montas, H.J., Mankin, K.R., 2009. Case Study: Evaluation of Streamflow Partitioning Methods. Journal of Irrigation & Drainage Engineering 135(6) 791-801.

Nelder, J., Mead, R., 1965. The downhill simplex method. Computer Journal 7 308-313.

Oudin, L., Hervieu, F., Michel, C., Perrin, C., Andréassian, V., Anctil, F., Loumagne, C., 2005. Which potential evapotranspiration input for a lumped rainfall–runoff model Part 2—Towards a simple and efficient potential evapotranspiration model for rainfall–runoff modelling. Journal of Hydrology 303(1–4) 290-306.

Pérez, A.J., Abrahão, R., Causapé, J., Cirpka, O.A., Bürger, C.M., 2011. Simulating the transition of a semi-arid rainfed catchment towards irrigation agriculture. Journal of Hydrology 409(3–4) 663-681.

Panday, S., Huyakorn, P.S., 2004. A fully coupled physically-based spatially-distributed model for evaluating surface/subsurface flow. Advances in Water Resources 27(4) 361-382.

Parker, G., 2006. Automated Baseflow Separation for Canadian Datasets (ABSCAN): User's Manual, Thinknew Analytics: Ottawa, Canada.

Partington, D., Brunner, P., Simmons, C.T., Therrien, R., Werner, A.D., Dandy, G.C., Maier, H.R., 2011. A hydraulic mixing-cell method to quantify the groundwater component of streamflow within spatially distributed fully integrated surface water-groundwater flow models. Environmental Modelling & Software 26(7) 886-898.

Partington, D., Brunner, P., Simmons, C.T., Werner, A.D., Therrien, R., Maier, H.R., Dandy, G.C., 2012. Evaluation of outputs from automated baseflow separation methods against simulated baseflow from a physically based, surface water-groundwater flow model. Journal of Hydrology 458–459 28-39.

Partington, D., Werner, A.D., Brunner, P., Simmons, C.T., Dandy, G.C., Maier, H.R., 2009. Using a fully coupled surface water-groundwater model to quantify streamflow components, World IMACS/MODSIM Congress: Cairns, Australia.

Pitt, R., Chen, S.-E., Clark, S.E., Swenson, J., Ong, C.K., 2008. Compaction's Impacts on Urban Storm-Water Infiltration. Journal of Irrigation and Drainage Engineering 134(5) 652-658.

Post, D., Vaze, J., Viney, N., Chiew, F., 2007. Regionalising the hydrologic response of ungauged catchments using the SIMHYD, IHACRES, and Sacramento rainfall-runoff models, MODSIM 2007 International Congress on Modelling and Simulation. Modelling and Simulation Society of Australian and New Zealand, Christchurch: Christchurch, New Zealand, pp. 2534-2540.

Post, D.A., Jakeman, A.J., 1996. RELATIONSHIPS BETWEEN CATCHMENT ATTRIBUTES AND HYDROLOGICAL RESPONSE CHARACTERISTICS IN SMALL AUSTRALIAN MOUNTAIN ASH CATCHMENTS. Hydrological Processes 10(6) 877-892.

Press, W.H., Teukolsky, S.A., Vetterling, W.T., Flannery, B.P., 1992. Numerical recipes in FORTRAN 77: the art of scientific computing. Cambridge University Press, Cambridge.

Price, K., 2011. Effects of watershed topography, soils, land use, and climate on baseflow hydrology in humid regions: A review. Progress in Physical Geography 35(4) 465-492.

Puhlmann, H., Von Wilpert, K., Lukes, M., Droge, W., 2009. Multistep outflow experiments to derive a soil hydraulic database for forest soils. European Journal of Soil Science 60(5) 792-806.

Ranatunga, K., Nation, E.R., Barratt, D.G., 2008. Review of soil water models and their applications in Australia. Environmental Modelling & Software 23(9) 1182-1206.

Ravazzani, G., Rametta, D., Mancini, M., 2011. Macroscopic cellular automata for groundwater modelling: A first approach. Environmental Modelling & Software 26(5) 634-643.

Schwartz, F.W., Sudicky, E.A., Mclaren, R.G., Park, Y.-J., Huber, M., Apted, M., 2010. Ambiguous hydaulic head and 14C activities in transient regional flow. Ground Water 48(3) 366-379.

Schwartz, S.S., 2007. Automated Algorithms for Heuristic Base-Flow Separation. Journal of the American Water Resources Association 43(6) 1583-1594.

Seibert, J., 1999. Conceptual runoff models - fiction or representation of reality?, Department of Earth Sciences, Hydrology. Uppsala University: Uppsala, Sweden, p. 52.

Sharma, A., 2000. Seasonal to interannual rainfall probabilistic forcasts for improved water supply management: part 1-a strategy for system predictor identification. Journal of Hydrology 239 232-239.

Sieber, A., Uhlenbrook, S., 2005. Sensitivity analyses of a distributed catchment model to verify the model structure. Journal of Hydrology 310(1–4) 216-235.

SIMLAB, 2010. Simlab version 2.2, free software for uncertainty and sensitivity analysis. Joint Research Center of the European Commission.

Sloto, R.A., Crouse, M.Y., 1996. HYSEP: A Computer Program for Streamflow Hydrograph Separation and Analysis. U.S. Geological Survey: Pennsylvania.

Smakhtin, V.U., 2001. Estimating continuous monthly baseflow time series and their possible applications in the context of the ecological reserve. Water SA 27(2) 213-217.

Sobol, I.M., 1993. Sensitivity estimates for non-linear mathematical models. mathematical modeling and computational experiment 1(4) 407-414.

Spongberg, M.E., 2000. Spectral analysis of base flow separation with digital filters. Water Resour. Res. 36(3) 745-752.

Stein, M., 1987. Large Sample Properties of Simulations Using Latin Hypercube Sampling. Technometrics 29(2) 143-151.

Stigler, S.M., 1986. The history of Statistics: The Measurement of Uncertainty Before 1900. MA: Belknap Press of Harvard University Press.

Sulis, M., Meyerhoff, S.B., Paniconi, C., Maxwell, R.M., Putti, M., Kollet, S.J., 2010. A comparison of two physics-based numerical models for simulating surface water-groundwater interactions. Advances in Water Resources 33(4) 456-467.

Szilagyi, J., 2004. Heuristic Continuous Base Flow Separation. Journal of Hydrologic Engineering 9(4) 311-318.

Tallaksen, M.L., 1995. A Review of Baseflow Recession Analysis. Journal of Hydrology 165 349-370.

Tan, S.B.K., Lo, E.Y.-M., Shuy, E.B., Chua, L.H.C., Lim, W.H., 2009a. Generation of Total Runoff Hydrographs Using a Method Derived from a Digital Filter Algorithm. Journal of Hydrologic Engineering 14(1) 101-106.

Tan, S.B.K., Lo, E.Y.-M., Shuy, E.B., Chua, L.H.C., Lim, W.H., 2009b. Hydrograph Separation and Development of Empirical Relationships Using Single-Parameter Digital Filters. Journal of Hydrologic Engineering 14(3) 271-279.

Therrien, R., McLaren, R.G., Sudicky, E.A., Panday, S.M., 2009. HydroGeoSphere: A Three-dimensional Numerical Model Describing Fully-integrated Subsurface and Surface Flow and Solute Transport: Waterloo.

Therrien, R., Sudicky, E.A., 1996. Three-dimensional analysis of variably-saturated flow and solute transport in discretely-fractured porous media. Journal of Contaminant Hydrology 23(1-2) 1-44.

Thompson, J.R., Sørenson, H.R., Gavin, H., Refsgaard, A., 2004. Application of the coupled MIKE SHE/MIKE 11 modelling system to a lowland wet grassland in southeast England. Journal of Hydrology 293(1-4) 151-179.

Troutman, B.M., 1985. Errors and Parameter Estimation in Precipitation-Runoff Modeling: 1. Theory. Water Resources Research 21(8) 1195-1213.

Tuteja, N.K., Cunnane, C., 1999. A quasi physical snowmelt run-off modelling system for small catchments. Hydrological Processes 13(12/13) 1961-1975.

van Genuchten, M.T., 1980. A closed-form Equation for Predicting the Hydraulic Conductivity of Unsaturated Soils. Soil Science Society of America Journal 44(5) 892-898.

VanderKwaak, J., 1999. Numerical Simulation of Flow and Chemical Transport in Integrated Surface-Subsurface Hydrologic Systems, Earth Sciences. University of Waterloo: Waterloo, Ontario, p. 217.

VanderKwaak, J.E., Loague, K., 2001. Hydrologic-response simulations for the R-5 catchment with a comprehensive physics-based model. Water Resources Research 37(4) 999-1013.

Vogel, R.M., Fennessey, N.M., 1994. Flow-duration curves--New interpretation and confinence intervals. Journal of Water Resources Planning and Management 120(4) 485-504.

Vugrin, K.W., Swiler, L.P., Roberts, R.M., Stucky-Mack, N.J., Sullivan, S.P., 2005. Confidence Region Estimation Techniques for Nonlinear Regression: Three Case Studies. Sandia National Laboratories: New Mexico and California, p. 31.

Wagener, T., Kollat, J., 2007. Numerical and visual evaluation of hydrological and environmental models using the Monte Carlo analysis toolbox. Environmental Modelling & Software 22(7) 1021-1033.

Weatherill, D., Graf, T., Simmons, C.T., Cook, P.G., Therrien, R., Reynolds, D.A., 2008. Discretizing the Fracture-Matrix Interface to Simulate Solute Transport. Ground Water 46(4) 606-615.

Werner, A.D., Wood, M., Simmons, C.T., Lockington, D.A., 2008. Salinograph trends as indicators of the recession characteristics of stream components. Hydrological Processes 22 3020-3028.

Yu, P.-S., Yang, T.-C., Chen, S.-J., 2001. Comparison of uncertainty analysis methods for a distributed rainfall–runoff model. Journal of Hydrology 244(1–2) 43-59.

Appendix A

Copy of Paper from Chapter 2

Li, L., Maier, H.R., Lambert, M.F., Simmons, C.T., Partington, D., 2013. Framework for assessing and improving the performance of recursive digital filters for baseflow estimation with application to the Lyne and Hollick filter. Environmental Modelling & Software 41 163-175.

Li, L., Maier, H.R., Lambert, M.F., Simmons, C.T. & Partington, D. (2013) Framework for assessing and improving the performance of recursive digital filters for baseflow estimation with application to the Lyne and Hollick filter.
Environmental Modelling and Software, v. 41(March), pp. 163-175